Addis Ababa University
College of Natural Science
School of Earth Sciences

Geology, geochemistry and genesis of tantalite deposit of the primary ore zone of Kenticha rare metal pegmatite field, Adola Belt, Southern Ethiopia

By

Mohammed Seid Mohammedyasin

Id. No.: GSR/2072/05

Stream: Mineral exploration

Advisor: Dr. Zerihun Desta (EMDSC)

Co-advisor: Dr. Worash Getaneh (AAU)

A thesis submitted to the School of Earth Sciences of Addis Ababa University in partial fulfilment of the requirements for a Master Degree (MSc) in Mineral Exploration

Submission date: May 31, 2016

Declaration

I hereby declare that this thesis represents my own work and is submitted in partial fulfilment of the requirements for a Master Degree (MSc) in Mineral Exploration. This work has not been previously submitted to Addis Ababa University, or any other institution, for any degree, diploma or other qualification, and all sources of material used in this thesis have been duly acknowledged.

Mohammed Seid _____ Date: _____

(Student)

Approved by

1. Dr. Zerihun Desta_____Date:_____
   (Advisor)
2. Dr. Worash Getaneh_____Date:_____
   (Co-advisor)
3. Dr. Mulugeta Alene_____Date:_____
   (Examinor)
4. Prof. Gezahagn Yirgu_____Date:_____
   (Examinor)
5. Dr. Balemwal Atinafu_____Date:_____
   (Head department)

Acknowledgement

I would like to acknowledge my advisor Dr. Zerihun Desta (EMDSC) and co-advisor Dr. Worash Getaneh for their guidance, constructive criticisms and discussions. I would like to say thanks for your continueddialogue maintained throughout the year. Special thanks to Mrs Aselefech, Mr. Abdellah, Mr. Sadik, Mr. Yidnekachew, Mr. Tsegaye, Mr. Ashenafi, Mr. Seid, Mr. Retaand all who helped me in the course of my thesis work at Ethiopian Mineral Development Share Company (EMDSC) for their benevolent helps. Specially, I am indebted to Sadik and Yidnekachew deserve utmost thanks for their consistent help during this work.

My study was sponsored byDebre Markos University, I am grateful for givingme such an invaluable opportunity to study at Addis Ababa University (AAU).

My profound gratitude for data provider (EMDSC), which make it possible to continue researchon my interest, and without the license provider of Petrograph, ArcGIS, CorelDrawand GEOrient softwares, thiswork would have not been easy to handle. EMDSC is also highly acknowledge for one-way trips for field work (Addis Ababa to Kenticha) and drill core sample selection (Addis Ababa to Shakiso), and for their facilities during these time. Further, I am glad to EMDSC and also personally to Dr. Zerihun Desta (CEO of EMDSC) for sharing me an invaluable literature resources, knowledge and XRF result of eleven samples.

The most incredible efforts of my beloved sister Mushra Seid and her husband Sheik Awol Urbera, and allmy families which have played a great role from my elementary school and throughout myjourney to the AAU have a most valuable place in my life. I have no words to appreciatetheir roles to shape my life, simply thank you. My wife Kubra Seid, your support and patience during the thesis work is appreciated. I love you all! Today your dream is partially achieved!

To my friends Leta and Gashaw at AAU thank you for yourencouragement and help. I enjoyed the co-existencewith you during my thesis work.

Abstract

Tantalum is the most important valuable raw-material in electronic, medical and chemical industries.The Kenticha rare-element granite pegmatite in the Neoproterozoic Adola Belt of southern Ethiopia, is a subhorizontal sheet-like structurally controlled intrusive body, is an important source of tantalite, niobite and beryl where tantalite is currently mined and exported globally. A little is known about the mineralogy, content of trace elements, ore forming and interplay processes, and mechanisms leading to tantalite-columbite mineralization in granite pegmatites. The aim of this work is to evaluate the geology and geochemistry of tantalite deposit in the primary ore zone of the Kenticha granite pegmatite to further elucidate the genesis of the tantalite deposit. An integrated approach of geological field work, rock and ore petrography, and whole-rock analysis by ICP-MS and ICP-AES using drill core data was used to achieve this aim. The Kenticha rare metal pegmatite deposit is controlled by major deep-seated normal faults striking in a N–S direction that allow the emplacement of the deposit bounded by the serpentinite to the hangingwall and granite to the footwall. The Kenticha peraluminous pegmatite deposit show zonal variations in mineralogical assemblage, tantalite concentration, and trace and rare earth elements content. Six distinct mineral assemblages and three main zones: border, intermediate and core zones were identified from literature analysis,field observation, petrographic study and whole-rock analysis. The tantalum and niobium concentration increase towards the core zone while the niobium concentration increase to border zone. The columbite group minerals (CGM) variation diagram shows progressive fractionation from ferroniobite to manganotantalite of primary magmatic fractionation with later hydrothermal-metasomatic alteration. It is strongly differentiated granitepegmatite enriched with Rb,Be, Nb, Ta and Csand depleted in V, Ba and Sr contents for whole–rock analyses of the Kenticha drill core samples. The rare earth element (REE) patterns of the primary ore zone shows slight enrichment in LREE with strong negative Eu-anomaly. From mineralogical assemblage, tectonic setting and geochemical signatures the genesis of Kenticha tantalite deposit is by partial melting of metasedimentary rocks predated the granite and pegmatite with later hydrothermal-metasomatic enrichment of tantalite in the area. Its formation and emplacement is related to the collision and felsic magmatism during post-Gondwana assembly.

Preface

This thesis is submitted for the partial fulfilment of a Master Degree (MSc) in Mineral Exploration during the spring semester of 2016 at Addis Ababa University. It mainly addresses the geology, geochemistry and genesis of tantalite deposit in the primary ore zone of Kenticha rare metal field, Adola Belt, southern Ethiopia.

Mohammed Seid

Dedication

To my sister Mushra Seid, “the second mom” for her invaluable life time support!!

Contents

List of Figures

List of Tables

List of abbreviations

AAS: Atomic Absorption Spectrometry

ALS: Australia Laboratories Service

ANS: Arabian Nubian Shield

CGM: Columbite Group Mineral

COLG: Collisional Granite

EAO: East African Orogeny

EMA: Ethiopian Mapping/Meteorological Agency

EMDSC: Ethiopian Mineral Development Share Company

EMPA: Electron microprobe analysis

GSE: Geological Survey of Ethiopia

HFSE: high field strength element

HREE: heavy rare earth element

ICP-MS: Inductively Coupled Plasma-Mass Spectrometry

ICP-AES: Inductively Coupled Plasma-Atomic Emission Spectrometry

ICP-OES: Inductively Coupled Plasma-Optical Emission Spectrometry

LCT: lithium-cesium-tantalum family

LILE: large ion lithophile element

LREE: light rare earth element

NYF: niobium-yttrium-fluorine family

ORG: Orogenic Granites

PPL: plane polarized light

REE: rare earth elements

TNO: tantalum-niobium oxide

VAG: Volcanic Arc Granites

WPG: Within Plate Granites

XPL: cross polarized light

XRF: X-ray fluorescence

Chapter 1 Introduction

1.1 Rationale

Tantalum is one of the most valuable mineral used in electronic industries, super alloys, metal carbides, and in chemical and medical industries. Tantalum is one of the five refractory metals which is dark in colour, very hard, ductile, and highly conductive of heat and electricity. It has high melting (3020 °C) and boiling (5560 °C) points, next to tungsten and rhenium. Currently, Ethiopia is one of the top ten tantalum producing country which supplies closely 10% of the world's consumption. Columbite-tantalite group minerals (CGM) are the major sources of tantalum recovered from rare metal granites and granitic pegmatites (Černý, 2005). CGMs have a general formula of AxByCz, where position of A can be occupied by Na, Ca, Ba, Th, Pb, REE, Mn^{2+}, and Fe^{2+}, position of B by Nb, Ta, Ti, Fe^{3+}, Sn, Hf and Al, and position of C by O, OH, and F. Tantalum and niobium are common constituent in pegmatites and granitic pegmatites (Dill, 2015). They also exist in their oxide forms.

Despite considerable researches on the petrogenesis and chemistry of Ta-Nb oxides (TNO) from well-known individual deposits and regional studies (Abdalla et al., 1998; Baumgartner et al., 2006; Belkasmi et al., 2000; Cèrny and Ercit, 1985; Galliski and Černý, 2006; Küster, 2009; Partington et al., 1995; Van Lichtervelde et al., 2007), but a little is known about their mineralogy and the content of trace elements (Melcher et al., 2015), the ore forming processes leading to Ta-Nb mineralization (Badanina et al., 2015), and the interplay ore forming processes from primary magmatic fractionation to secondary replacement by hydrothermal-metasomatic fluids (Badanina et al., 2015; Van Lichtervelde et al., 2007). Besides, the mechanism of ore forming processes through anatexis and the role of chemical quenching in deep-seated pegmatites are poorly understood (Simmons, 2007). Furthermore, there is still unresolved puzzle of how and when pegmatites are separated from their source granites and how comagmatic dikes acquire an increasing chemical fractionation from their distant source (London and Morgan, 2012).

In 1920s, different models explaining the internal evolution of granitic pegmatites had been proposed; of which (1) fractional crystallization of the melt from the margin of the pegmatite body towards the centre (Cameron, 1949) and (2) segregation of aqueous fluids from the silicate melt are the two well know models (Jahns and Burnham, 1969). Two styles of mineralizations i.e., magmatic origin and metasomatic-hydrothermal alteration, has suggested by Černý

(2005)and Van Lichtervelde et al. (2007). For example,experimental results on fluid melt partition coefficient of mica indicate that Ta does not transported by fluids (Chevychelov et al., 2004), hence alteration of mica contain high concentration of Ta.

Advances in modern microbeam analytical techniques such as electron microprobe analysis (EMPA), Laser Ablation-Inductively Coupled Plasma-Mass Spectrometry (LA-ICP-MS), ion microprobe, infrared microthermometer, fluid inclusion thermometry, new dating techniques (e.g., Ar-Ar) and new isotope systematics (e.g., Ge, B, etc.) provides more information on the genesis of mineral deposits. These techniques help to trace the origin of the melt forming the pegmatites and associated mineral deposits, stages of paragenesis, zoning, fractionation and the chemical evolution of the mineral-forming environment from a melt to a hydrothermal–metasomatic fluid (Badanina et al., 2015).

The Kenticha tantalite deposit in the southern Ethiopia is an important source of economic tantalum concentrate (mined 120 t tantalum concentrate annually, 55% Ta_2O_5) of the country. The Kenticha granitic pegmatite was discovered by the Ethio-Soviet exploration program during the 1980s (Kozyrev et al., 1982). The mining has been focused on the weathered ore (upto 60m depth) of the deposit. Few scientific studies (Desta, 1996, 1991; Desta et al., 1995; Küster et al., 2009; Tadesse and Desta, 1996; Tadesse, 2001) had been conducted on the Kenticha tantalite deposit and most of them were focused on the weathered ore zone. The Ethiopian Mineral Development Share Company (EMDSC) drilled deep boreholes for exploration of primary ore zone (below 60 m depth) which needs detail scientific studies to understand the chemical evolution and genesis of tantalite deposit in the area.

This study uses petrographic studies (thin and polished sections) and whole-rock analysis using drill core samples from the deep boreholes to understand the geology, geochemistry and genesis of the tantalite deposit. Trace element analysis was carried out using lithium borate fusion and Inductively Coupled Plasma Mass Spectrometry (ICP-MS) and the major oxides by lithium borate fusion and Inductively Coupled Plasma Atomic Emission Spectrometry (ICP-AES).

1.2 Statement of the problem

Most of the previous works are limited to the weathering ore zone, which is currently becoming depleted(e.g., Desta, 1991; Desta et al., 1995; Küster, 2009; Tadesse and Desta, 1996; Tadesse, 2001). Küster et al.(2009) has done a comprehensive and detail work on the geochemistry and age dating of the main Kenticha, Bupo, Kilkele and Shuni Hill pegmatites using borehole data. However, still more works are needed for both exploration of the deeper horizons of the primary ore zone and for scientific wonders. Most of these previous works also gave emphasis on the mineralogical composition, zoning, fractionation and age determination of granite pegmatites and associated ore minerals on the weathered zone. The primary ore deposit in the area was confirmed from deep drilling by Ethiopian Mineral Development Share Company (EMDSC) which needs detailed geological, mineralogical and geochemical characterization of the ore body. This study would help to understand the origin of granite pegmatite and associated ore minerals and their geological and chemical evolution. Besides, it is the best way to study mineral alterations from the primary ore. So, the possible changes of the weathered ore from its parent primary ore were clearly traced. Results of deep level primary ore exploration shows the primary ore is the subsurface extension of the weathered ore. Detailed geological, mineralogical and geochemical analyses of the primary ore also gave a valuable information on the genesis of the ore deposit and the parent rock for both the pegmatites and granites. Furthermore, the ore forming environment was inferred from the analysis and interpretation of this work.

1.3 Objectives

1.3.1 General objective

The main objective of this study is to better understand the genesis of the tantalite deposit of the primary ore zone of the Kenticha rare metal field, southern Ethiopia.

1.3.2 Specific objectives

- To examine the fractionation, regional and compositional zonings and identify paragenetic stages so as to understand the chemical evolution of the Kenticha tantalite deposit.
- To explore the origin of the melt controlling the rare element mineralogy of Kenticha rare metal pegmatites.
- To understand the genesis of the Kenticha tantalite deposit, rare metal mineralization, with respect to the pegmatites and the host-rocks.

1.4 Data and Methods

1.4.1 Pre-field work

The work is divide into three phases: the pre-field, field and post-field phases. During the pre-field phase further literature analysis were done. Replanning for field workand laboratory analysis also were done. Arranging for field work and collecting necessary field instruments from EMDSC were done in advance to the field work.

1.4.2 Field work and sampling methods

The field work was conducted for 15 days for geological mapping of the area in a scale of 1:5000 finalized by using ArcGIS and CorelDraw softwares, field observation, and to take some on-site measurements such as attitude of faults and joints. The dominant lithological unit that can be mapped on this scale has been considered as a unit. Based on this, three mappeable unites have been identified i.e. the granite, pegmatite and serpentinite units. The outcropped lithologies and minerals, and relative timing of the emplacement of the Kenticha rare metal pegmatite was clearly recognized in the field. Some of the mineralogical variations, zonal differences in mineral assemblage and alterations was also recognized during the field work in the open-pit mine site, trenches, pits and hand-dug wells. The dip and strike of the major geologic structures controlling the ore deposit i.e., deep-seated major faults, and some minor faults were measured and graphically analysed by equal area stereonet and rose diagrams using GEOrient software. This structural analysis was also compared with measured strike and dip of the joint sets (Tadesse, 1998).

Samples were collected from all localities in the open-pit mine for hand specimen mineralogical identification. Moreover, three tantalite crystal samples were used for polished section which were used as a reference for tantalite characterization under ore microscopy. The drill core and powder samples from deep boreholes were used for the petrographic and geochemical analyses, respectively. The samples were first crushed in jaw crusher and then pulverized in an agate mill for chemical analysis.

1.4.3 Petrography

Besides the field work, petrographical and analytical techniques were used to understand the detail mineral assemblages, zoning, alteration and paragenetic relationships, and the genesis of the tantalite deposit. Thin- and polished sections were prepared at Geological Survey of Ethiopia (GSE). Three granite, ten pegmatite and two serpentinite drill core samples, of totally fifteen thin section, were prepared for rock petrography. Seven drill core pegmatite samples and three tantalite crystal samples from the open-pit mine were polished for ore petrography. Both the thin and polished sections were analysed at Mineralogy and Petrography, and Ore Microscopy Laboratories of Addis Ababa University (AAU) School of Earth Sciences. Mineralogical zoning, mineral assemblages and alteration were examined using both microscopies.

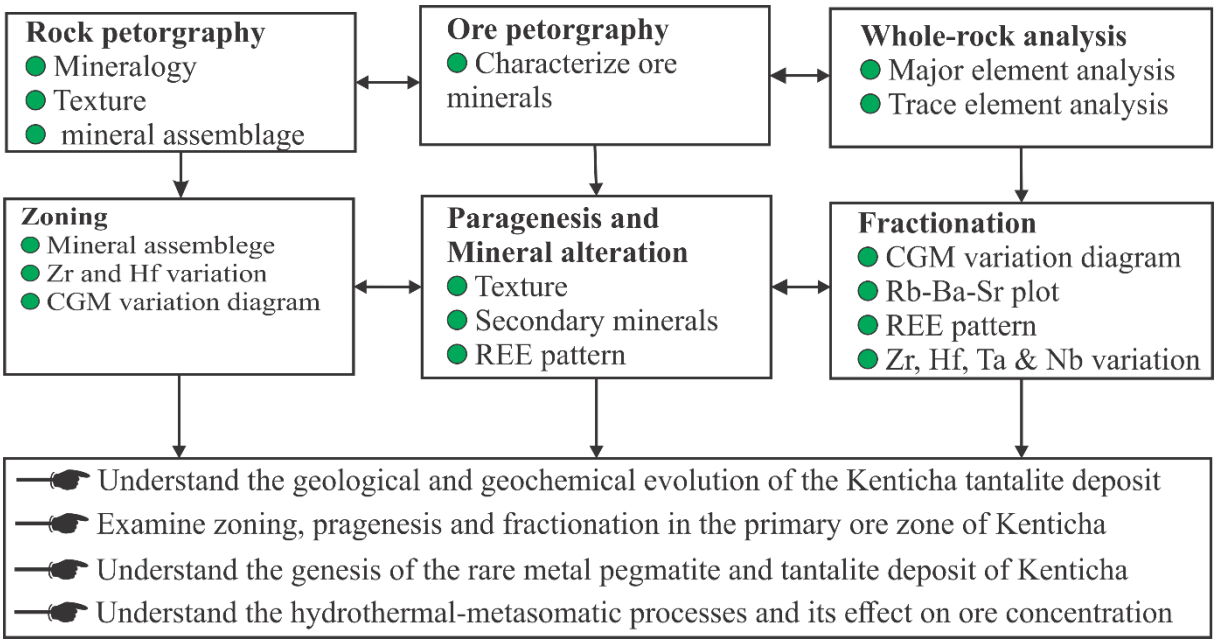

Figure 1.1: Work flow of the study. Mineral assemblage, texture and zoning were characterized petrographically. Paragenesis and fractionation were studies by using different plots of the whole-rock data; such as general classification diagrams, columbite group mineral (CGM) variation diagrams, and other important binary and triangular plots of trace and rare earth (REE) elements.

Table 1.1: Samples description used for thin and polished sections. Where Msc: muscovite; Mic: microcline; Spd: spodumene; Alb: Albite, and Qtz: Quartz.

Sample name	Sampling depth (m)	location	Analytical method	Description
K-1-16A-14	128.5-130	X = 4860.5, Y = 4778	Thin section only	Mic – Alb – Spd Pegmatite
K-1-16A-37	167.5-169	X = 4860.5, Y = 4778	Thin section only	Mic – Spd – Alb Pegmatite
K-1-16A-43	176-178	X = 4860.5, Y = 4778	Thin- & polished-section	Mic – Spd – Alb Pegmatite
K-1-16A-57	197.5-199	X = 4860.5, Y = 4778	Thin section only	Mic – Spd – Alb Pegmatite
K-1-24B-18	103-106	No location information	Thin section only	Pegmatite
K-1-24B-44	143-145	No location information	Thin- & polished-section	Pegmatite
K-1-24B-39	133-136	No location information	Thin- & polished-section	Pegmatite
K-1-24B-grt	163-165	No location information	Thin section only	Albite granite
K-1-221-srp	168-168	X = 4955.7, Y = 4992.4	Thinsection only	Serpentinite
K-1-221-chl	138-141	X = 4955.7, Y = 4992.4	Thin section only	Chlorite schist
K-1-221-tlc	69-72	X = 4955.7, Y =4 992.4	Thin section only	Talc schsit
K-1-221-5	105-107	X = 4955.7, Y = 4992.4	Polished section only	Qtz core pegranite
K-1-221-26	144-147	X = 4955.7, Y =4 992.4	Thin- & polished-section	Msc – Alb – Spd Pegmatite
K-1-221-50	210-213	X = 4955.7, Y = 4992.4	Thin- & plolished-section	Mic block + (Msc + Alb) Pegmatite
K-1-221-59	225-228	X = 4955.7, Y = 4992.4	Thin- & polished-section	Msc – Alb Pegmatite
K-1-221-grt	234-237	X = 4955.7, Y =4 992.4	Thin section only	Albite granite
SS1	~ 50-60	From the open-pit mine	Polished section only	Tantalite crystal in quartz core
SS2	~ 40-50	From the open-pit mine	Polished section only	Tantalite crystal in pegmatite
SS3	~ 30-40	From the open-pit mine	Polished section only	Tantalite crystal in pegmatite

1.4.4 Analytical methods

Ten drill core granite and one granite and one talc samples were crushed and pulverized into 75 µm size. The twelve powder samples from deep boreholes were used for whole-rock analysis, from duplicate samples taken for grade definition and reserve calculation by EMDSC. These boreholes were selected from all localities at different depths for the representation of the lateral and vertical variations of major and trace elements in the deposit to show the zoning pattern. The samples also systematically assigned from the border to the core pegmatite zones based on the drill core logging. i.e., macroscopic identification of texture, mineral assemblage and concentration of major oxides and trace elements.

The concentration of major and selected trace elements in pegmatite and granites were determined by a combination method (code: ME-MS81d) Inductively Coupled Plasma-Mass Spectrometry (ICP-MS; code: ME-MS81) and Atomic Emission Spectrometry (ICP-AES; code: ME-ICP06) both by decomposing the sample by lithium metaborate fusion (code: FUS-LIO1) at the laboratory of Australian Laboratory Services (ALS), Ireland. In brief, a prepared sample (0.200 g) is added to lithium metaborate ($LiBO_2$) flux (0.90 g), mixed well and fused in a furnace at 1000°C. The resulting melt is then cooled and dissolved in 100 mL of 4% HNO_3/2% HCl solution. Ions are extracted from the plasma through a pinhole-sized orifice into a pumped vacuum system and focused with an ion lens into a mass spectrometer. This solution is then analysed by Inductively Coupled Plasma-Mass Spectrometry for 31 trace elements including the rare earth elements (REE). Additionally, the same solution is then analysed by ICP-AES and the results are corrected for spectral inter-element interferences. The concentration of thirteen oxides is calculated from the determined elemental concentration and the result is reported in that format (ALS, 2016). Calibration was done by an in-house CGM reference material and standard.

Moreover, secondary data from the weathered ore zone from Desta et al. (1995) were also selectively utilized for comparison, with the primary data from the primary ore zone. It includes whole-rock analysis of the granite and pegmatite samples, analytical results of some rock forming minerals (oxides and trace elements concentration including REE) using ICP-MS, XRF and AAS (c*f.*(Desta et al., 1995; Küster et al., 2009) for the details). Furthermore, electron microprobe analysis (EMPA) of some rock forming and columbotantalite group (CGM) minerals were also part of this data set for comparison. Totally more than 62 samples, 28

samples of primary data and more than 34 samples of secondary data from main Kenticha rare metal pegmatite were utilized for the geochemical interpretation.

Table 1.2: Kenticha rare metal pegmatite samples used for whole-rock analysis. Where Msc: muscovite; Mic: microcline; Spd: spodumene; Peg: pegmatite; Alb: Albite and Qtz: Quartz. The samples were analysed by ICP-AES and ICP-MSfor oxides and trace elements, respectively.

Sample name	Sampling depth (m)	Location (conventional)	Mineral assemblage
K-1-249-59	110.4 – 112.1	X = 6048.3, Y = 5251.3	Msc-Qtz-Alb-Mic peg
K-1-28A-28	198.0 – 199.5	X = 5071.6, Y = 5021.4	Msc-Spd-Alb Peg
K-1-27-42	105.5 – 106.5	X = 4652.0, Y = 4606.0	Mic-Alb-Spd Peg
K-1-24B-41	150.0 – 151-5	No location information	Mic-Alb-Spd-Qtz
K-1-32A-25	117.0 – 118.5	X = 4895.6, Y = 4864.8	Msc-Alb-Spd Peg
K-1-219-36	142.0 – 143.8	No location information	Msc-Qtz-Spd-Alb Peg
K-1-225-28	140.5 – 142.7	X = 4967.3, Y = 5175.7	Qtz-Msc-Alb-spd Peg
K-1-85A-2	89.0 – 90.5	X = 5361.5, Y = 5035.2	Talc
K-1-245-50	189.5 – 191.5	X = 6068.9, Y = 5381.8	Msc-Qtz-Alb Peg
K-1-69A-32	130.5 – 132.0	X = 5632.7, Y = 5245.2	Msc-Alb gnt + Msc-Alb pPg
K-1-245-42	189.5 – 191.5	X = 6068.9, Y = 5381.8	Msc-Qtz-Alb peg
K-1-224-31	206.1 – 207.7	X = 5033.5, Y = 5037	Msc-Qtz-Alb-granite

The analysis and interpretation of the whole-rock datawas done using different plots such as tectonic discrimination and columbite variation diagrams, REE patterns and other important plots. The petrographical and geochemical results were finally integrated to understand the geology, geochemistry and genesis of the Kenticha tantalite deposit. Most sensitive elements for igneous fractionation were used to elucidate the magma fractionation.

1.5 Literature review on the rare metal granitic pegmatites

1.5.1 Classification of granite pegmatites

The classification of granitic pegmatite has been attempted since then by Ginsburg et al. (1979) and frequent attempts were also done by Černý and his co-workers (e.g., Černý and Ercit, 2005; Černý, 1991; Černý et al., 2012). The current classes of pegmatite are defined based on the metamorphic environment of their host-rocks, mineralogy, elemental composition, and texture. On these basis five classes of pegmatites has been defined: (1) abyssal, (2) muscovite, (3) muscovite rare-element, (4) rare-element, and (5) miarolitic pegmatites (Figure 1.3). Most of

these classes subdivided into different subclasses based on their geochemical, in part geological, characteristics and further subdivision into types and subtypes leading to subtle differences in geochemical signatures or pressure-temperature conditions of solidification (Černý and Ercit, 2005). The rare element pegmatite generated in large plutons are emplaced largely at intermediate to relatively shallow depths. This class is divided into two subclasses: (1) the rare element rare earth element (REL-REE) subclass derived from post- to anorogonic metaluminous to peraluminous mostly of extensional settings granite, and (2) rare element Lithium (REL-Li) subclass are the most differentiated of the whole spectrum classification and aredominantly from syn- to late-orogenic peraluminous granites, largely compressional orogenic regimes. The REL-Li subclass is further divided into types and subtypes. The types are beryl, complex albite-spodumene (include spodumene, lepidolite, elbaite, amblygonite subtypes) and albite types *(cf.* Černý and Ercit, 2005 for the detail).

Further petrogenic families, LCT (Li-Cs-Ta) and NYF (Nb-Y-F), of pegmatites derived from igneous differentiation of plutonic parents has been also identified. The LCT families are predominant than other types of pegmatites (Černý et al., 2012). They contains mostly high concentrations of Cs, Ta, Nb, Rb, Be and Sn and elevated amounts of fluxing components such as Li, P, B and F. However, the pegmatites derived by other processes cannot be explained in this approach. The origin of the pegmatites and their genetic link with the granites is controlled by the pressure-temperature condition, metamorphic grade and depth. For instance miarolitic pegmatites of shallow-level has no igneous control while the rare-element pegmatites of intermediate-depth are generally linked with the granites and are emplacement along deep-seated fault in tectonically active regimes. According to most authors the Mica-bearing pegmatites are formed both by anatexis (Simmons, 2007) and igneous fractionation (e.g., Černý et al., 1985). The composition of granites leading to rare-metal mineralization mostly lies into the S-type (enriched in B, P and F, which are derived from micas) and the A-type (enriched in F, which are derived amphiboles and biotites) granites, but the I-type sources are devoid of fluxing components which are known in base-metal mineralizations.

Most of the LCT pegmatites have compositional affinity with peraluminous S-type granites expressed by mineral assemblages constitute of muscovite, garnet, cordierite, sillimanite or andalusite, tourmaline and gahnite (Chappell and White, 2001). These granites stem from the anatexis of metamorphic schists and aluminous gneisses of sedimentary origin. Most of the

pegmatites that belong to the NYF family are sourced from A-type granites and is generally thought (but not exclusively restricted) to be gneissic granulites deep in the continental crust, but not exclusively restricted.

Class	Subclass	Type	Subtype	Family
Abyssal	HREE			NYF
	LREE			
	U			NYF
	BBe			LCT
Muscovite				
Muscovite–rare element	REE			NYF
	Li			LCT
Rare element	REE	allanite–monazite		NYF
		euxenite		
		gadolinite		
	Li	beryl	beryl–columbite	LCT
			beryl–columbite–phosphate	
		complex	spodumene	
			petalite	
			lepidolite	
			elbaite	
			amblygonite	
		albite–spodumene		
		albite		
Miarolitic	REE	topaz–beryl		NYF
		gadolinite–fergusonite		
	Li	beryl–topaz		LCT
		spodumene		
		petalite		
		lepidolite		

Figure 1.2: Pegmatite classification schemeof Černý and Ercit (2005), modified to show the correlation between pegmatite classes and families. NYF = niobium-yttrium-fluorine family (green); LCT = lithium-cesium-tantalum family (yellow); HREE = heavy rare earth elements; LREE = light rare earth elements.

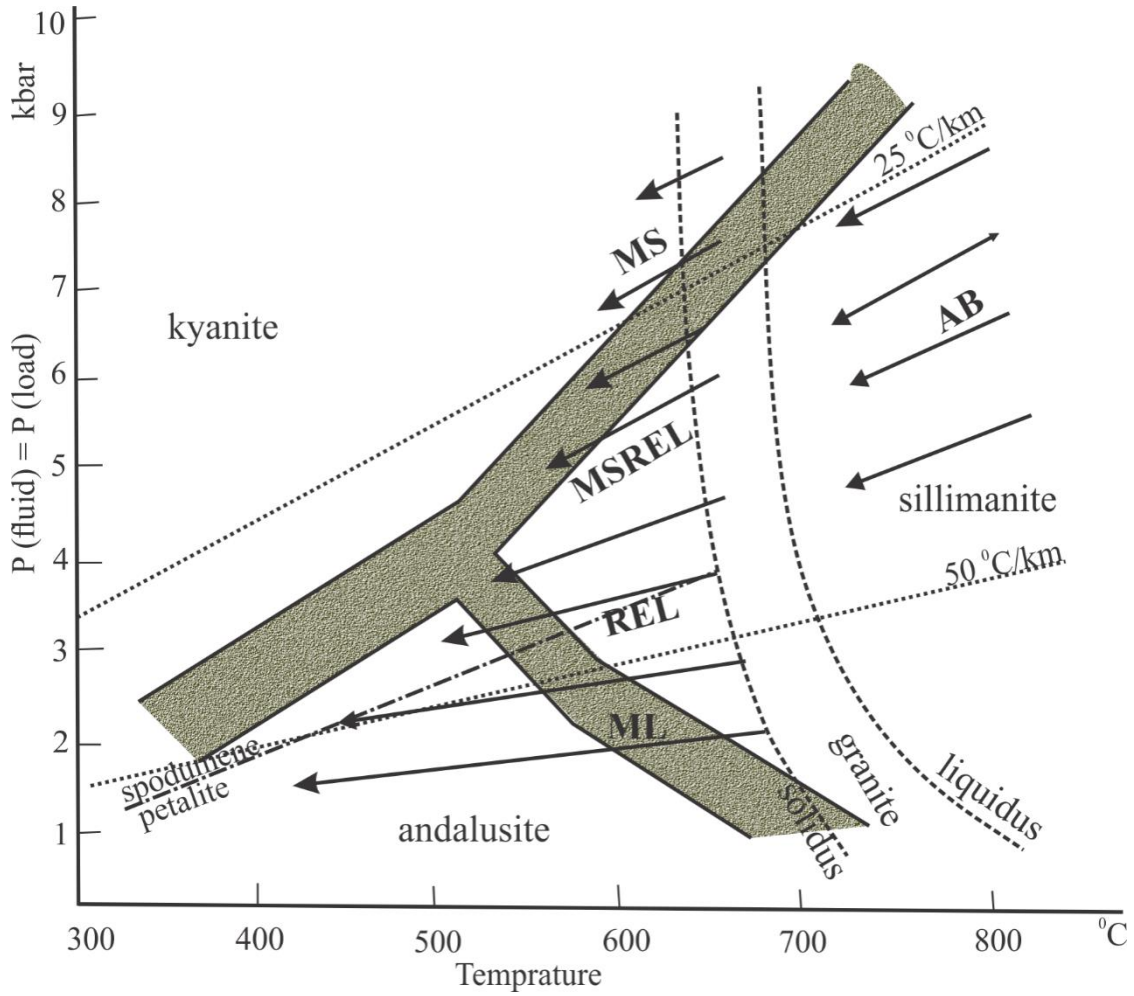

Figure 1.3: Schematic P-T fields of regional host-rocks of granitic pegmatites of abyssal (AB), muscovite (MS), muscovite-rare element (MSREL), rare-element (REL) and miarolitic (ML) classes. Arrows indicate regional trends of fractionation of pegmatites relative to metamorphic grades of the host-rocks. The MS, MSREL, REL and ML are transitional one to the other (modified from Černý and Ercit, 2005) See Robie and Hemingway, 1984 for the Aluminosilicate fields, London, 1984 for spodumene-petalite boundary, Jahns, 1982 for granite liquidus-solidus. The lower and higher geothermal gradient corresponds to average Barrovian and Ahukuma metamorphic facies-series, respectively. CGM crystallization from a melt is possible only at final near solidus stage of both peralkaline and peraluminous magma at high degrees of crystallization of strongly evolved low temperature melts (Chevychelov et al., 2010).

1.5.2 Formation of granite Pegmatites

Among the various proposed models that explain the formation of pegmatites (1) the fractional crystallization of the melt and (2) interaction of aqueous fluid with the melt are the two

competing models (London and Morgan, 2012). The concentration of fluxing components and other incompatible elements increase towards the centre of the magma chamber as crystallization proceeds resulting increasing chemical fractionation from the margin to the centre of the pegmatites (Cameron, 1949). The formation of giant crystals and exotic minerals however can be evidenced for the interaction of fluids and the melt by alkalis incongruent partitioning (Jahns and Burnham, 1969)such as the aqueous fluids enriched in K, and the melt enriched in Na. Later, the model of buoyant ascent, has been proposed by Jahns (1982) in order to explain the chemical fractionation of the pegmatites.

The geochemical signature of rare-element pegmatites display extreme fractionation from leucocratic, high-silica, metaluminous to peraluminous granites and rhyolites. High trace element concentrations, is affected by the style of partial melting and the degree of volatile saturation (Černý et al., 1985). It starts from metamorphic protoliths to the formation of granites generating geochemically specialized fertile pegmatites. Preferential partition (London's model) of rare-elements from granites into smaller volumes of residual melts also used to explain this enrichment in rare-elements (Černý, 1991). Complexing, rare-element mineralization by hydrothermal and metasomatic processes, also plays an important role on the accumulation of some elements (e.g., Nb, Ta, Ga, Zr, Hf and probably also Li, Cs, Tl and Mn).

The provenance of pegmatites need to be traced back from their source granite, and can be mantle or crustal origin. The compatibility of the elements in granitic pegmatites depends on the temperature, pressure and mineral phases in the system,and modified by fractional crystallization and assimilation processes. These incompatible elements in the rock forming minerals further increases until they form their own distinctive minerals such as spodumene, beryl and feldspars(Černý et al., 2012).

The composition of simple granitic pegmatites is similar to granite and commonly contains garnet, tourmaline, apatite, micas, Fe–Ti oxides, and minor amount of few other common minerals. The complex varieties may further include Li, Be, Ta and Nb (Linnen et al., 2012). Besides, pegmatites are also sources of high-quality gem minerals, such as beryl, tourmaline, topaz, spodumene, and spessartine. These gems mostly formed (1) in miarolitic cavities near the centres of pegmatite bodies or (2) in reaction zones between pegmatites and ultramafic host-rocks (Simmons et al., 2012).

Trace element and REE signatures of pegmatites are commonly used to ascribe to a known parent granite. The trace element signature clearly indicate most pegmatite are S- or A-type granite, but rarely I-type granites. LCT granitic pegmatite family of peraluminous to hyperaluminous systems are in general late- to post-tectonic, commonly Band P-enriched, with strong tendency to accumulate substantial Li, Rb, Cs, Ta, Be and Sn in the most evolved pegmatite members. They display moderately to slightly HREE-depleted patterns and low REE abundances and negative Eu anomaly is occasionally well expressed but in most cases absent. Partial melting of metamorphic protoliths leaving REE-rich accessory minerals in the residue, progressive REE-depletion of the differentiating melts by precipitation of monazite, xenotime, apatite, garnet, tourmaline, columbite-tantalite and microlite, and a change in oxidation state of Eu produce these features. In contrast to this, the NYF family subaluminous to metaluminous granitic, mainly A- to locally I-derived, predominantly post-tectonic to anorogenic; the granite-pegmatite suites are commonly B- and P-depleted, poor in Li, Cs, Ta and Sn. Their most evolved pegmatites belong to either the gadolinite subtype enriched in Y, HREE, Be, Nb, F, U, Th, Ti, Zr and Sc, or the allanite-monazite subtype enriched with LREE, U, Th, Be, Nb and F. The parent granites show high HREE. High-percentage melting of previously large ion lithophile element (LILE) depleted) protoliths and possible input from mantle-derived magmas, followed by limited ranges of differentiation, seem to be responsible for these features. The REE patterns of the most evolved granites of these types are closely mimicked by the wall zones of derived pegmatites(Černý, 1997).

1.5.3 Origin of granite pegmatite by partial melting

Two end member models have been proposed for the formation of fertile pegmatites i.e., continuous crystallization and partial melting. Continuous crystallization of pre-existing parental rocks by partial melting which homogenize in a collective reservoir produces variety of granitic magmas depending on the degree of fractional crystallization. The varying degree of partial melting produces wide compositional variation of granite magmas. Partial melting of compositionally distinct protoliths can also produce wide compositional spectrum of granite magmas with the same degree of partial melting. This could be arise from mineralogical, trace element chemistry, mineral stability field of sheet silicates or accessory minerals and their content in the mineral/residuum phase, and metasomatic alteration of the source metasedimentary lithology (Shearer et al., 1992). Simmons et al. (1995) suggested that ghost

and relict textures in the minerals, effect of fracturing in the mineral grains and the pattern of REE in the wall zone can be used as evidence for partial melting.

Partial melting of mica rich pre-existing metamorphic rocks in collisional zones commonly forms LCT granitic pegmatites and gives high concentration of trace and rare earth elements. Muscovite and biotite carry most of the trace elements. Abundant muscovite schistof marine sedimentary origin react extensively at the onset of anatexis (London and Morgan, 2012). Consequently, large fractions of the rare element content transferred to the initial small volume of partial melt. The melting reactionof muscovite and biotite also produce K-feldspar with some amount of alumunosilicate and spinel under low H_2O saturation condition.(e.g., Acosta-Vigil et al., 2003) of rubidium, slightly incompatible in K-feldspar. The ratio of Li and Cs, which are compatible elements in K-feldspar, is elevated as compared to Rb during consecutive crystallization resulting rare-alkali enrichment (Černý et al., 2012).

1.6 Geographic setting

1.6.1 Location and accessibility

The Kenticha rare-metal pegmatite deposit is located in the Guji Zone, Oromia Regional State and situated from 39°01'00" to 39°02'00" E longitude to 5°27'30" and 5°29'00" N latitude. The Kenticha area is 550 km far from Addis Ababa through Addis Ababa-Hawassa-Shakiso-Kenticha partly asphalted and partly all-weather road (Figure 1.4). The Kenticha rare metal pegmatites are situated in the Neoproterozoic Adola Belt within the Precambrian basement of southern Ethiopia, formed during the accretion of ocean arc terranes of southern part of Arabian-Nubian shield (ANS) (Johnson and Woldehaimanot, 2003; Stern, 1994; Stoeser and Camp, 1985). The rare metal bearing pegmatites of Kenticha and Aflata are north-south extended 100 km in the Adola Belt.

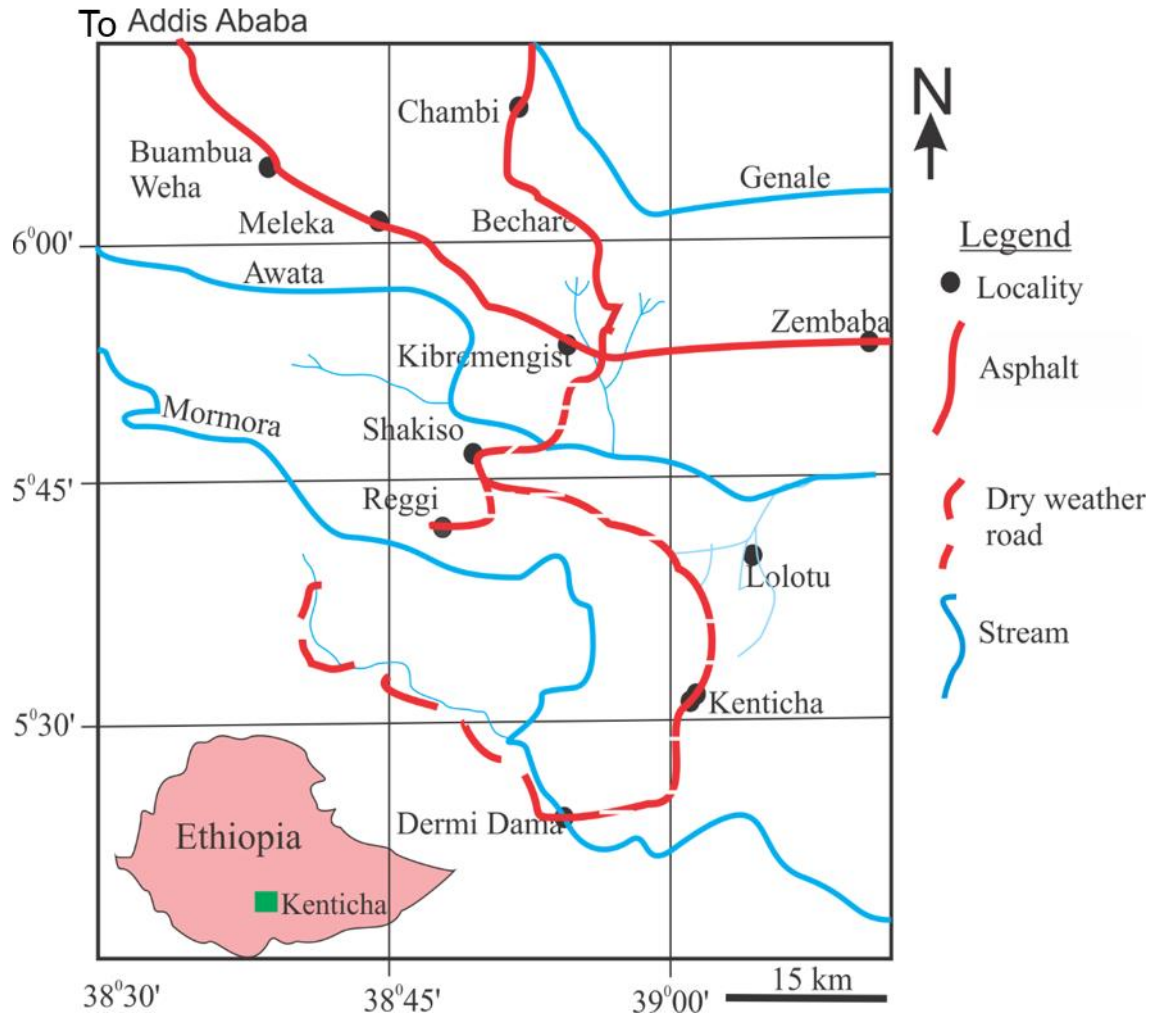

Figure 1.4: Location, accessibility and drainagemap of the Kenticha and Adola area (Modified from Wondafrash, 2010).

1.6.2 Physiography and climate of the study area

The deposit is confined to the central area of the Kenticha range with maximum elevation of 1665 m to 1750 m and topography ranging from 80 m to 130 m. The main waterways are the Awata and Mormora rivers and two water streams draining to the northern and southern parts across the deposit. These streams are fed by the annual rainfall ranging 1100 mm to 1300 mm (EMA, 2015).

The climate of the region is equatorial-monsoon with an abrupt change of dry and rainy seasons. The high amount of precipitation is recorded from March to May and September to November with maximum daily precipitation of 83.6 mm. While the driest season is from the second November through March with maximum daily temperature of greater than 35 °C (EMA, 2015).

Following the mining work in the area, a small town called Chebe has established with a growing population each year. The local language is Oromiffa.

1.7 Chapter scheme

This thesis is divided into five chapters; introduction, regional geological setting, results, discussion, and conclusions and recommendations, respectively. The content of each Chapter is highlighted in Table 1.3.

Table 1.3: The chapter scheme of the thesis and the main contents in each of the Chapters.

	Content
Chapter 1	• This chapter gives a brief overview about the rational and the objectives of the work, and classification and formation of granitic pegmatites. • Introduces the methods adopted and the major outcome of the study. • Presents the work flow and the methods used for this study • Briefs the three phases of field wok and discussed each of the analytical and petrographic techniques employed.
Chapter 2	• Briefly summarizes the geology and tectonic evolution of the ANS and the Precambrian southern Ethiopia and mineralization in the Adola Belt. • Summarizes the geology and mineralization of the study area
Chapter 3	• This chapter is divided into two main parts as it presents the main results from the (1) geology of the area from field observation and petrographic characterization of the samples and (2) the geochemistry tantalite deposit.
Chapter 4	• The main results and findings are discussed by emphasizing the geology of granitic pegmatite and mineralization of culombo-tantalite minerals, chemical evolution and their genesis. • The major phases of paragenesis and mineral alteration, and style of mineralization are identified.
Chapter 5	• Finally, the main conclusions of this work are drawn • Recommendations and future research directions are suggested.

Chapter 2 Regional geological setting

2.1 The geology of Arabian-Nubian Shield

The Arabia-Nubian Shield (ANS), northern part of the East African Orogen (EAO), is developed through horizontal crustal accretion during the closure of the Mozambique Ocean as recognized from the ophiolites and their dismembered fragments, and chemically distinct island-arc volcanic and plutonic complexes (Kusky, 2003). The suture zones of the ophiolite suites further traced in the Mozambique Belt evidenced that they were formed by orogenic mechanism. The N-S trending southern ANS arc-arc sutures (Barsaloi-Tuludimtu-Baraka sutures and Galana-Adola-Moyale-Ghedem-Arag-sutures), flanked by partly migmatic gneiss terranes, might represent either pre-Neoproterozoic crust or roots of Neoproterozoic arcs (Stern et al., 2010). Wrench tectonics in the region concentrated along two shear belts, i.e., western Barka Sinistral Shear Zone which is probably northern extension of Tuludimtu Belt and the Eastern Ghedem-Araq Shear Belt (Asmara-Nakfa Shear Belt) to the east a continuation of the Adola-Moyale Belt (Ghebreab et al., 2009).

Following the amalgamation (680-640 Ma) of Gondwana, the proto-Arabian Nubian Shield is affected by regional exhumation, erosion, and subsidence. From 610 Ma on, granitic magmatism was occurred by increasing the amounts of alkali-feldspar granite and alkali granite (Johnson et al., 2011). Juvenile crust and(or) depleted mantle are magma sources of the late Cryogenian-Ediacaran granitoids, mostly originated in anorogenic, post-collisional, commonly extensional settings. They were derived by melting and fractionation of (1) anhydrous high-grade metamorphosed lower crust, mafic- to intermediate calc-alkaline crust, and(or) (2) subduction-modified mantle wedges associated with slab break-off or delamination (Johnson et al., 2011). Further granitic magmatism was continued until 565-560 Ma and the East African Orogeny ceased by 550 Ma. Most geochemical data came from granitoids in the ANS have indicated the early magmatic calc-alkaline granitoids are formed within evolving arc setting (e.g., Hargrove et al., 2006). The youngest late- to post-collisional alkaline suite granitoids have formed during the decay of the previously consolidated orogon, possibly involving sub-continental lithospheric delamination (e.g., Farahat et al., 2007; Johnson et al., 2011).

2.2 The Precambrian basement of southern Ethiopia

The Precambrian geology of southern Ethiopia consists of two distinct lithotectonic terranes: (1) the granite-gneiss terrane, consisting of high-grade para- and orthogneisses and deformed and metamorphosed granitoids, biotite-hornblende gneiss and amphibolite and (2) the ophiolitic fold and thrust belts, consisting of low-grade, mafic-ultramafic and sedimentary assemblages. The granitoids compositionally ranges from undiformed to foliated diorite to granites (Abdelsalam et al., 2008; Tsige, 2006; Worku and Schandelmeier, 1996; Worku and Yifa, 1992; Yibas et al., 2002; Yihunie et al., 2004). The volcanosedimentary ophiolites suites are composed of mafic and ultramafic metasedimentary rocks, which represent the Cryogenian arc-arc sutures overprinted by Ediacaran deformation (Abdelsalam and Stern, 1996). The low-grade metamorphic volcano-sedimentary unit consists of amphibolite, carbonaceous quartz-mica schist, chlorite-actinolite schist, quartz-feldspar-biotite schist, metaconglomerate, graphitic quartzite and mafic to ultramafic bodies.

The Adola belt (Chater, 1971; Gilboy, 1970) and the surrounding southern Ethiopia later divided into Lower, Middle and Upper Complexes (Kazmin, 1972; Kazmin et al., 1978). The Lower Complex comprises the Archaen cratonic basement of high-grade gneisses and migmatites with subordinate quartz-feldspathic gneisses and schists. The Middle Complex covered by platforms of psammitic and pelitic metasediments with minor marbles and schists of Lower to Middle Proterozoic age and the Upper Complex of Neoproterozoic age consist low grade, predominantely greenschist facies, volcanosedimentary ophiolitic assemblages (Kazmin et al., 1978). However, geochronological and isotopic studies defined the Precambrian basement rocks of southern Ethiopia is dominantly Neoprotrozoic in age(Ayalew et al., 1990; Gerra, 2000; Gichile, 1992; Teklay et al., 1998) and the Archean or pre-Neoproterozoic rocks appreciably are part of pre-Neoproterozoic continental fragments (Tadesse and Allen, 2002).

2.3 The Adola Belt

The Adola Belt is known in its gold mineralization quartz veins and veinlets in lenses of biotite schists and is associated with the low-grade wall-rock alteration (Tsige, 2006; Figure 2.1). Fluid inclusion studies from the Lege Dembi gold deposit (Aster et al., 1988; Bilay et al., 1997; Mechessa, 1996; Tadesse, 1990) implies a broadly similar fluid composition and P-T conditions of trapping are existed for the evolution of the metamorphic fluids. The occurrence of native

Au as inclusions and on the edges of galena in this area exhibits a low temperature environment of precipitation (Tadesse, 2004).

The Adola Belt includes the Aflata and Kenticha Formations, Adola orthometamorphic rock series and early Paleozoic post orogenic granites and pegmatites from older to younger, respectively. The Kenticha Formation in found in a narrow synclinal structure comprising biotite-, muscovite-, garnet amphibolite- and quartz-feldspatic–gneisses, fine grained amphibolite-, staurolite-garnet-biotite-, garnet-staurolite- and two-mica –schists, and marble in the order of older to younger ages (Emelyanov et al., 1986; Kozyrev et al., 1982).

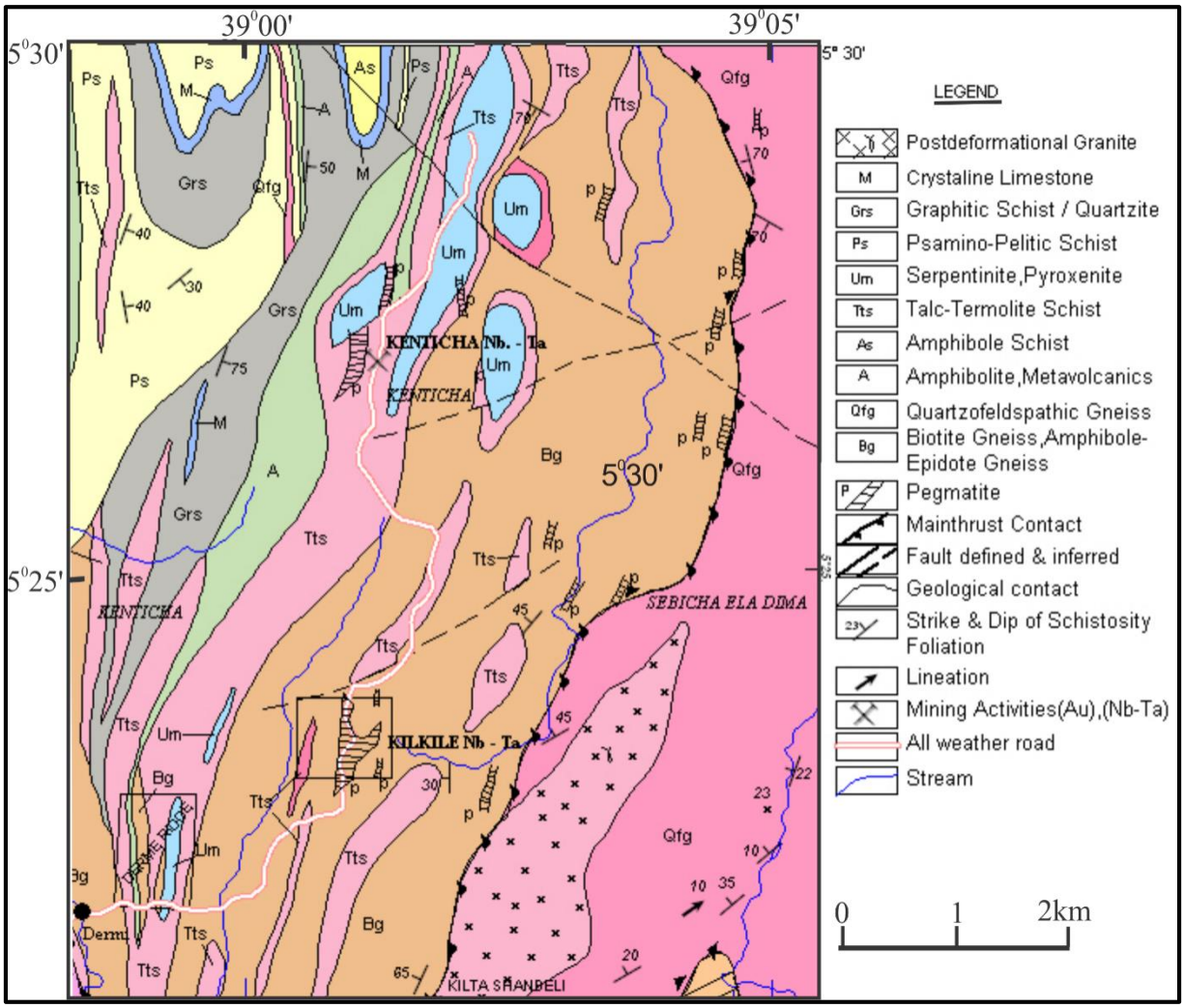

Figure 2.1: The geological map of the Kenticha Pegmatite Belt including the main Kenticha, Kilkele, Derme Dama and Kilta Shambeli Pegmatites (Kozyrev et al., 1988). This map shows the pegmatite distribution in the region.

2.4 The Kenticha rare metal pegmatite

The Kenticha granites are compositionally peraluminous and fertile with varieties of minerals such as biotite, muscovite, tourmaline, spessartine, almandine, corderite and topaz. There are three different types of granites i.e., biotite granite, two mica granite and alaskitic granite. Biotite- and two mica granites are the parent for alaskitic granites and pegmatites. The alaskitic granites and the pegmatite bodies are injected as magmatic dikes into the host-rocks. This granite is characterized by (1) devoid of biotite, (2) replacement of albite by k-feldspar and muscovite, and (3) enriched in quartz, Nb, Ta, Rb, Cs, Li and Sn and depleted in aluminium, titanium, magnesium, calcium, potassium, iron oxides, Sr, Ba, and Zr than the biotite and two-mica granites (Desta, 1996; Desta et al., 1995).

The Kenticha rare metal pegmatite is emplaced as a dome and lenticular shaped biotite, mica and alaskitic post-orogenic granitic intrusions to the ultrabasic rocks of serpentinite, talc and talc-actinolite rocks. The host metamorphic rocks are dominantly gneiss; biotite, biotite-muscovite, garnet-amphibolite and quartzo-feldspatic discontinuous beds of biotite, garnet-staurolite and mica gneisses and schist (Tadesse, 2001). The emplacement of the pegmatite bodies are controlled by the deep-seated N-S trending faults (Desta et al., 1995; Tadesse, 1998). The pegmatites are emplaced in highly faulted and folded zones trending in a N-S direction. Both the granites and pegmatites in the area are affected by the Balkalian orogeny (Tadesse and Desta, 1996). The country/host-rocks are dated ~ 580 ± 50-680 ± 30 Ma (Tadesse and Desta, 1996) and the pegmatites are emplaced during ~530 Ma, over printed by postmagmatic fluids (Küster et al., 2007). The emplacement of Kenticha and Bupo pegmatite is coeval and temporally related to postorogenic granite magmatism (Küster, 2009; Küster et al., 2007; Worku and Schandelmeier, 1996).

The Kenticha rare metal pegmatite belt comprises several groups of pegmatites which shows a fractionation trend. In situ fractionation of subhorizontal pegmatite sheet at Kenticha accounts for chemical and mineralogical zoning. The crystallization was occurred under closed system and contamination with the ultramafic host-rocks from the hangingwall was during postmagmatic hydrothermal stages (Küster et al., 2009). Results of Major and trace element analysis and their trends in ore, accessary and rock forming minerals suggest that these groups of granite-pegmatites are cogenetic in nature (Desta et al., 1995). The zonal distribution of the

groups helps for selection of exploration criteria, to develop 3D model of their distribution for further detailed deep level explorations and volumetric calculations.

Regional zoning of series of N-S trending barren to rare-metal enriched granites in the area can be classified into 5 different types of pegmatites based on their geological and geochemical signatures (Desta et al., 1995; Tadesse and Desta, 1996; Tadesse, 2001). These are (1) barren pegmatites, (2) Ta-poor pegmatites (Kilkele II and III, and Bupo II), (3) Ta-rich beryl-columbite subtype (Kilkele I and Dermidama), (4) complex spodumene type, and (5) albite spodumene type (Bupo I) (Figure 2.2). The regional zoning is also described in similar mineralogy, composition and texture with the above classification. Simple description as spodumene type for Kenticha rare metal pegmatite would not fit since it also consists of Li-silicates accommodated in lepidolite, spodumene, holmquistite, albite and swinfordite and Li-phosphates existed in the form of amblygonite and lithiophyllite (Dill, 2015). Numerous veins and dikes in Kenticha show inward mineralogical and textural changes in an increasing in complexity parallel to the degree of pegmatite fractionation (Tadesse, 2001). Such zoning and mineralogical changes from the rime to the core zones are caused by inward crystallization of hydrous magma (Černý, 1990; Shearer et al., 1987). Consequently, inward changes in mineralogy is recognized from sodic aplite, microcline-quartz-albite zone followed by quartz-muscovite-albite-spodumene zone to lenticular masses of greisen, lepidolite and quartz core units.

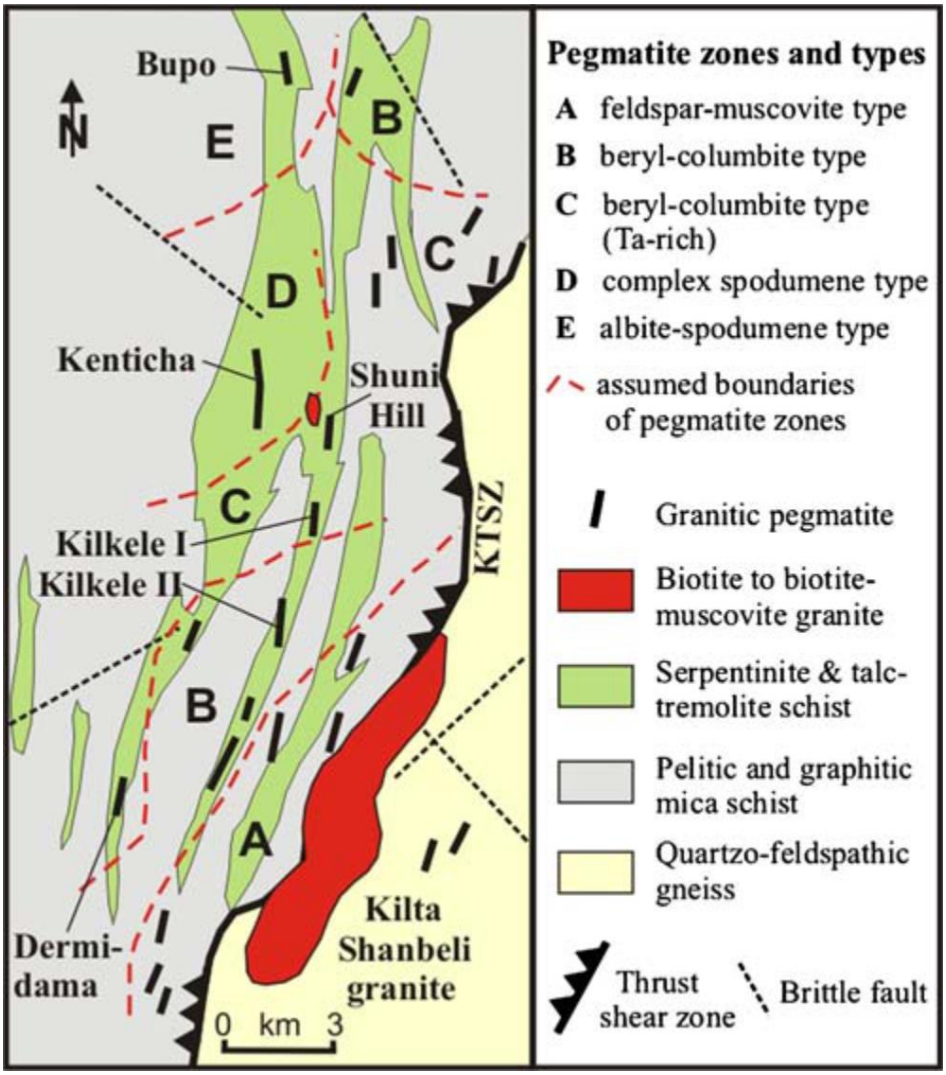

Figure 2.2: Central part of Kenticha rare metal pegmatite field and regional pegmatite zoning (modified from Desta et al., 1995).

Different types of compositional zoning in Kenticha granite pegmatite such as oscillatory, patchy and mixed oscillatory has been identified. The oscillatory zoning is developed as result of repetitive variations related to crystal growth processes, concentration of the major elements, segregation of gas-saturated magma and is consistent with the periodic variation in Ta, Nb, Mn and Fe contents. The texture of this zoning is manifested by relatively homogeneous core, zoned mantle and faceted border zone. The patchy zoning and other replacement textures of columbite-tantalite are formed by late-coming gaseous-rich chemical fluids resorption and replacement processes (Tadesse and Desta, 1996). The late generation by replacement processes are relatively rich in Ta and Mn.

The primary ore deposit shows complex internal structure and variety of alternating paragenetic associations. The bottom of this ore body muscovite two-feldspar granite that grades upward

into albite, muscovite-quartz-microcline and muscovite-quartz-albite-microcline pegmatite zones. The middle zone is dominated by muscovite-spodumene-microcline-albite pegmatite superimposed with albitized and greisenized linear units. The upper zone is the most differentiated pegmatite with spodumene, large quartz cores, microcline and ambigonite montebrasite blocks, and spodumene-quartz zones. The last stage of paragenesis dominated hydrothermally metasomatized mineral associations such as (1) fine to very fine grained and inequigranular tabular albites, (2) cleavalendite, (3) small flaky and coarse-flaky pink coloured Li-bearing muscovites, (4) lepidolite-quartz, and (5) quartz-albite and quartz-albite-muscovite associations (Desta et al., 2003). Segregation of cleavalendite and lepidolite-qaurtz complex zones, and greizenized quartz cores and blocky microcline develop high amount of Ta contents in the metasomatically altered upper zones.

Similarly, the Ta content in the weathering mantle ore is very high in metasomatic mineral associations and characterized by pronounced albitization and greisenization. While the low Ta content is found in ores associated with granite, muscovite-microcline-albite zones, and blocky microcline and quartz cores. The Ta content is also increased upward from bottom to top. Ta is associated with the columbite-tantalite group minerals forming flattened and short prismatic small grain crystals of 5-7 cm length (Ethiopian Mineral Development Enterprise, 1997).

Chapter 3 Geology and Geochemistry of Kenticha tantalite deposit

3.1 The geology of Kenticha tantalite deposit

3.1.1 Field observation

The area is divided into eight localities (sectors) based on geomorphological and structural boundaries. Each of the localities also can be characterized by typical mineral assemblage. Three main mappeable units i.e., pegmatite, serpentinite and granite are clearly observed in the study area (Figure 3.1). There is no much variation in mineralogy between pegmatites and granites but pegmatites are very coarse grain rocks as compared to the granites. The Kenticha rare metal pegmatite is mainly composed of spodumene, quartz, muscovite, albite and microcline with different mineralogical association and order of abundance in different localities (localities 1 to 8). The ore bearing pegmatite is associated with the ultramafic rocks of serpentinite and talc chlorite, and post tectonic granite. Besides the above three lithological unites talc-chlorite and biotite schists also outcrop within the ore body and at the boundary to the serpentinite, respectively. The biotite schist, the so called "glimmerite", outcrops as thin transitional bed between the serpentinite and pegmatite body. This thin layer is formed by metamorphism of serpentine and some of the minerals also changed into chlorite which result chlorite schist. The granite and the serpentinite further surrounded by Precambrian metamorphic rocks of Middle Complex consisting of biotite, biotite amphibolite, mica schist, gneiss and amphibolite rocks (Desta et al., 2003). The post tectonic granite to the footwall and the ultramafic rocks to the hanging wall are bounding the ore-bearing pegmatite (Figure 3.2). The deep-seated faults in the area are trending N-S. Most of the veins in the ore zone are mainly filled by spodumene (Figure 3.4a). This indicates the temporal relationship between the rare metal mineralization and the veins, which are predated the orebody.

The pegmatite rock samples in locality 2 (L2) are composed of mainly quartz + microcline + muscovite + spodumene + albite mineral associations. Besides this black tourmaline, biotite (glimmerite), chlorite and amazonite were observed. The white spodumene variety fills the different sets of veins increasing down to the depth in their density. The quartz and muscovite are sometimes intergrown together with the spodumene.

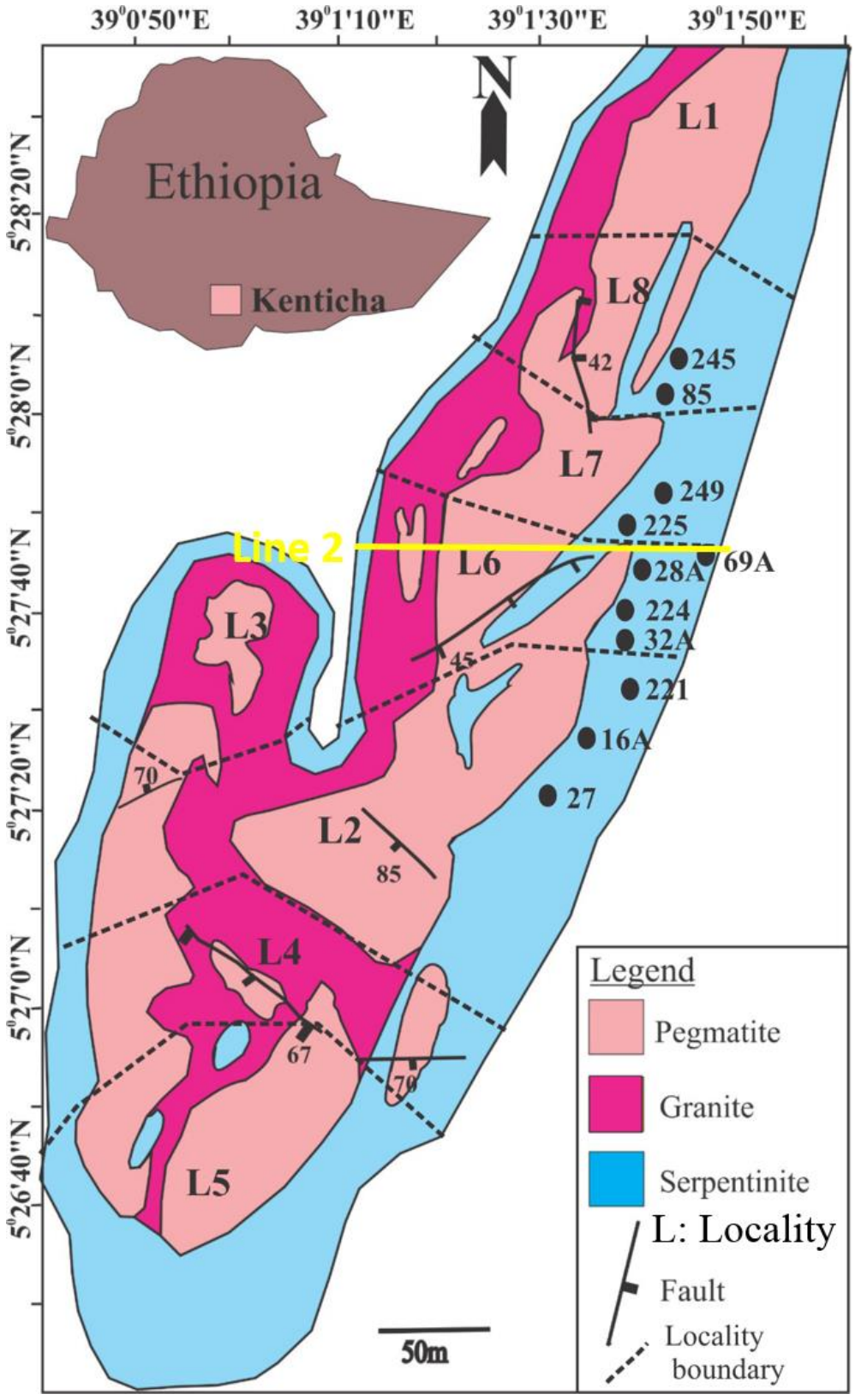

Figure 3.1: Geological map of the main Kenticha rare metal pegmatite. The borehole numbers are indicated with the black circle. Rough estimated boundary for the eight localities (L1 to L8) is outlined by the dotted line.

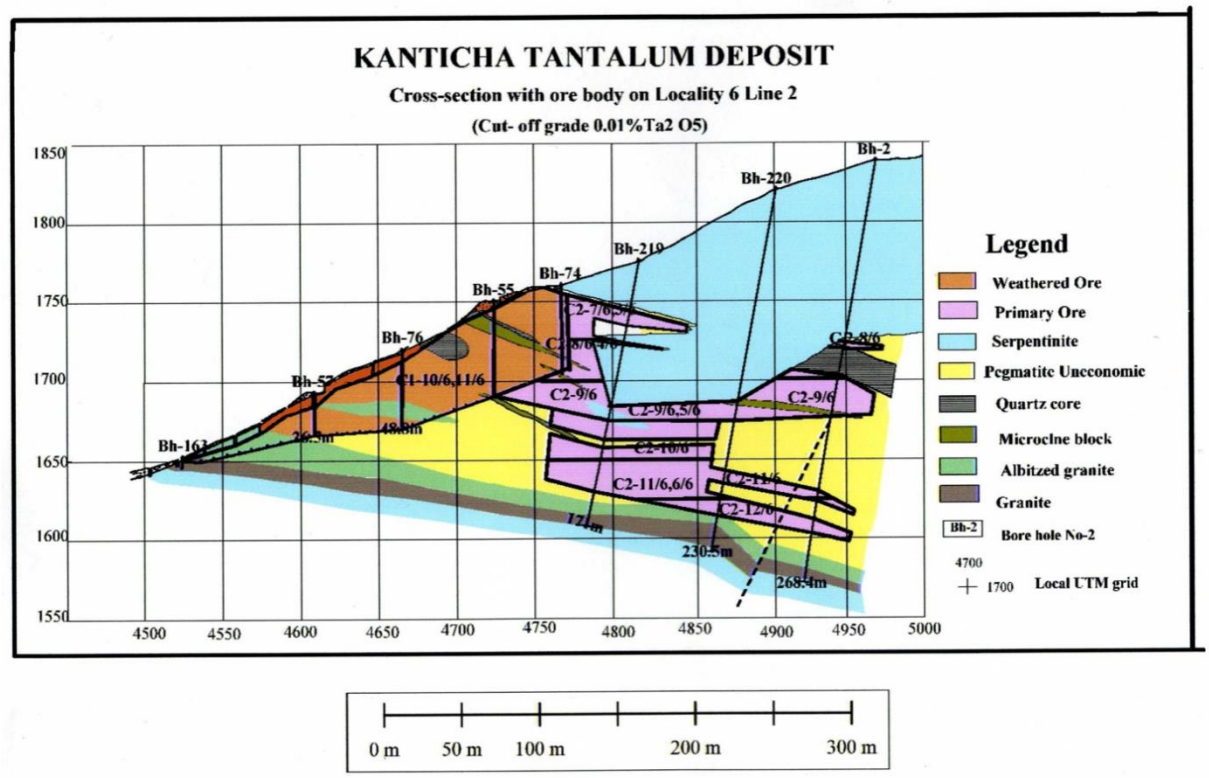

Figure 3.2:Cross-section of Kenticha tantalite deposit including the weathered and the primary zone crossing three deep boreholes (Bh-2, B-220 & Bh-210) and an inferred fault juxtaposing the granites (presented with permission from EMDSC). The position of this section is indicated on Figure 3.3.

In locality 6 (L6) the spodumene changes to pink in colour and relatively harder than the white variety. Microcline, spodumene, quartz and muscovite mineral association become more dominant in this locality.Large crystals of tantalite are commonly visible in the quartz core zone, in localities 2 and 6 (Figure 3.3). Further to the locality 7 (L7) the mineral assemblage is changed to spodumene, quartz, muscovite and microcline. In localities 1 and 8 (L1 & L8) the muscovite and microcline (+ quartz) are dominantly observed in the mine site and hand-dug pits. Eluvial, alluvial and delluvial pegmatites are outcropped in locality 3 (L3) and some extent at localities 4 and 5 (L4 & L5). This mineralogical assemblage indicates the Kenticha rare metal pegmatites are highly zoned. These are the result of weathering and mineral replacement processes (see (Desta et al., 1995).

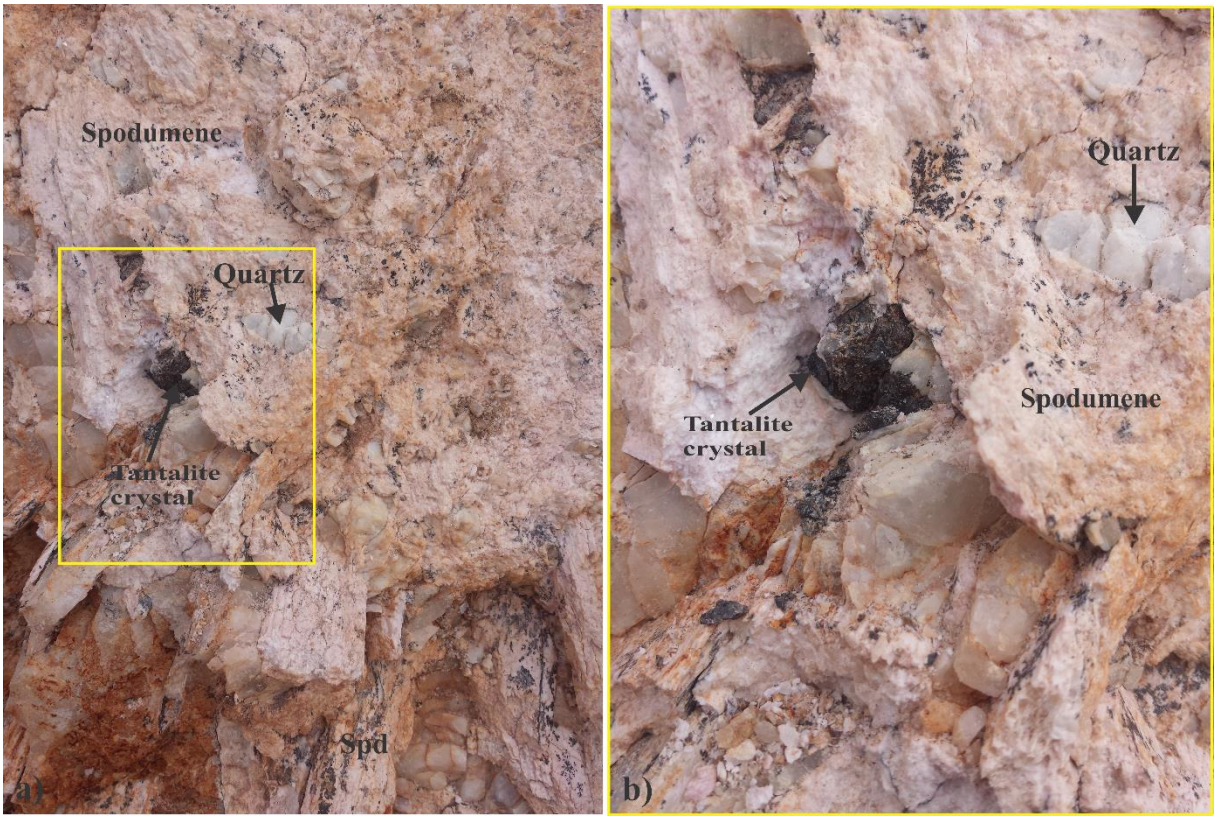

Figure 3.3: Tantalite crystal observed on a hand specimen in the field with spodumene-quartz pegmatites which is clear in the (b) zoomed in (yellow box in a is approximately 1m by 1.5m).

Thin layer of biotite schist is found at the boundary between the pegmatite body and the serpentinite rock (Figure 3.4b). Biotite schist is enriched in biotite and in some parts also contain black tourmaline. Chlorite and talc-chlorite schists on the other hand are commonly found in the faulted and sheared zones.

The serpentinite in the hangingwall is overlying the pegmatite (Figure 3.4b). It is an ultramafic rock enriched in dark coloured minerals. It also contains thin layers of chromite which should have been formed by gravitational settling of chromiterich meltduring the early stage of magmatic crystallization (Figure 3.5a). Serpentinite and talc-chlorite/tremolite rocks are considered to be associated with the formation of the deep-seated faults in the area.

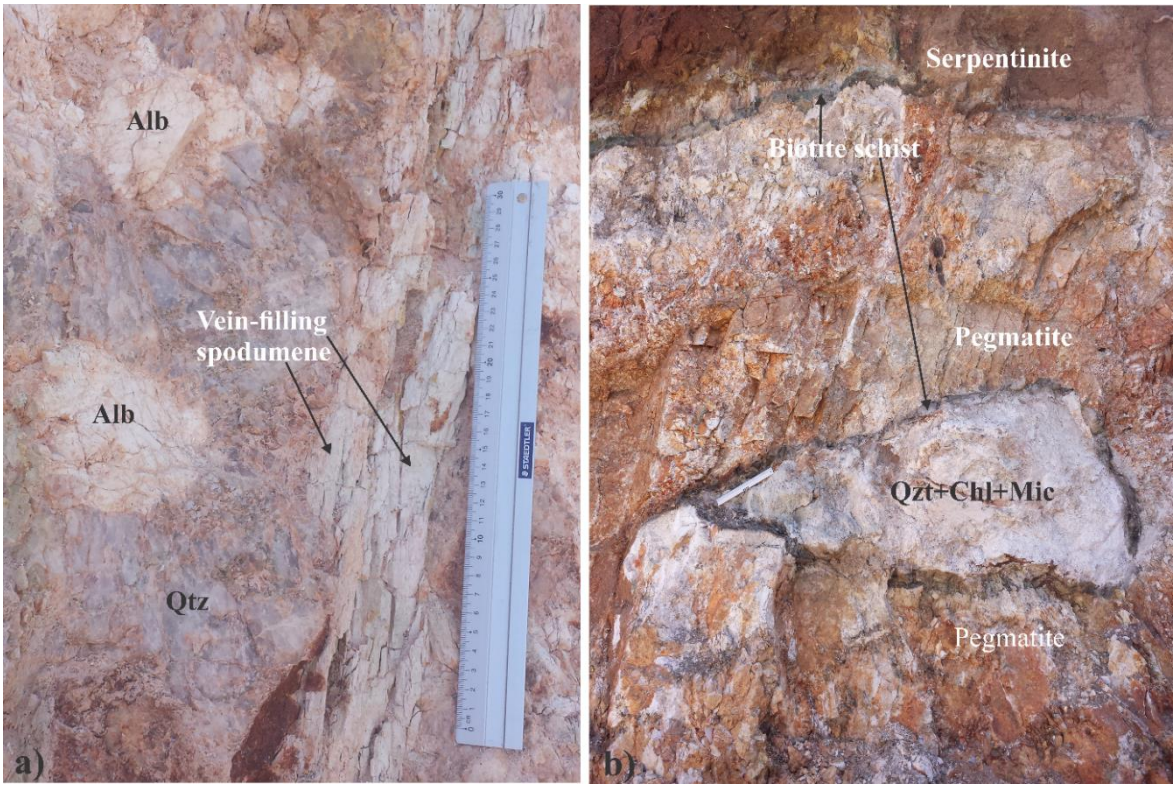

Figure 3.4: a) Spodumene lathand b) biotite schist (glimmerite) at the boundary between the pegmatite body and serpentinite.

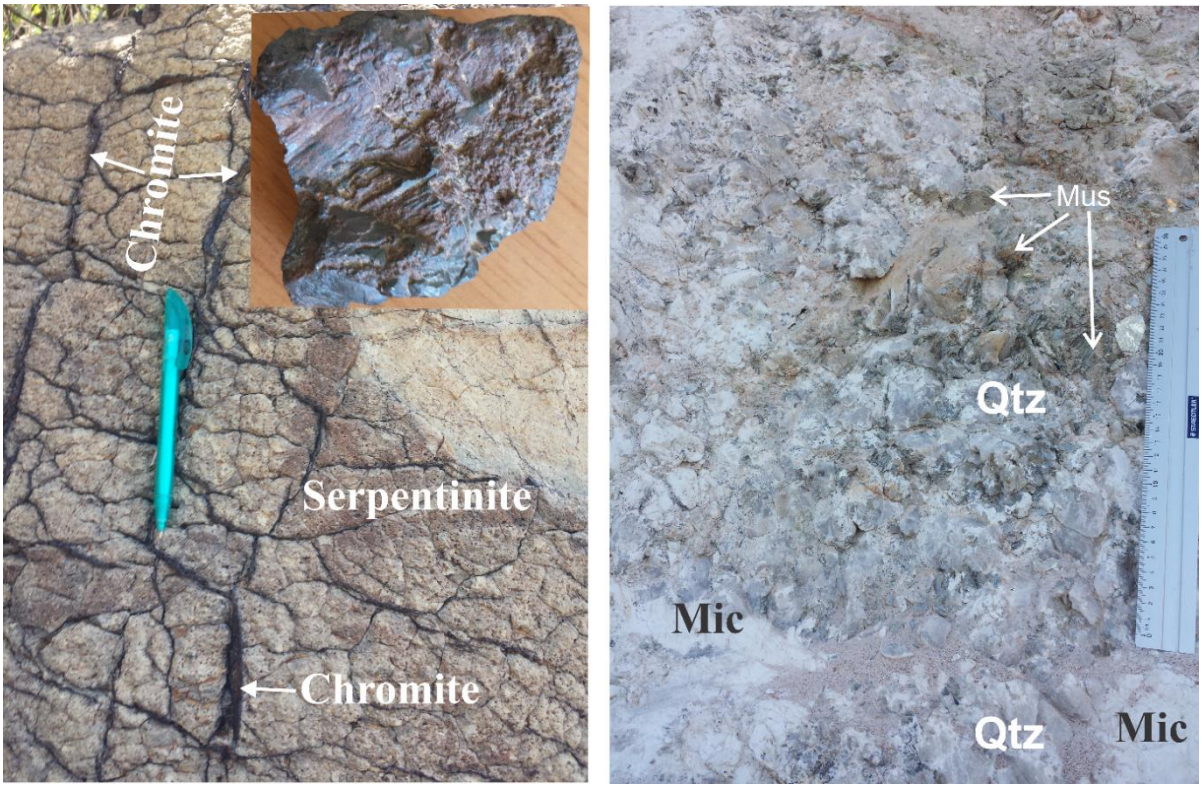

Figure 3.5: (a) Thin layers of chromite within the serpentinite, where the inset is a chromite crystal and (b) muscovite + quartz +microcline pegmatite.

Granite on the other hand is dominantly exposed at the footwall of the ore body, and is considered to be the parent rock for the pegmatite. It mostly composed of quartz, k-feldspar, albite and minor amount of muscovite.

Previous works indicate that the Kenticha rare metal pegmatite shows these types of zoning: (1) quartz + microcline + albite with subordinate muscovite, (2) quartz + albite of aplitic layer, (3) muscovite-quartz-microcline-albite pegmatite, (4) spodumene-microcline -albite pegmatite partly albitized or greisenized, (5) microcline-albite-green and pink spodumene pegmatite with quartz-microcline block which is partly albitized and greisenized, and (6) quartz core (*cf.* Desta, 1996).

3.1.2 Rock forming minerals

1. Serpentine (sample K-1-221-srp)

Serpentine is the most dominant mineral in this rock (K-1-221-srp) with some orthopyroxene (Figure 3.6a). The orthopyroxene crystals show replacement which increases from the ream (brown) to the centre (dark). The opaque minerals under plane- and cross-polarized lights (PPL & XPL) are (1) breakdown of orthopyroxene into iron oxides which are brown at their ream or (2) chromite, formed by gravitational settling during the early stage of magmatic crystallization, which is fully opaque and show vein-like appearance in the field.

2. Talc and chlorite (samples K-1-221-tlc and K-1-221-chl)

It is difficult to discriminate talc and muscovite under microscope though they are distinct in hand specimen. Talc does not show mottled appearance, black dotes, as of micas and is most clearly seen when close to the extinction (sample K-1-221-tlc). In contrast to muscovite, talc shows inelastic property during deformation. It is an elongated pink to light green (XPL) and yellow (PPL) (Figure 3.6b). Besides, minor talc alteration also observed in this sample.

Chlorite is the most dominant mineral in this sample with a noticeable alteration. The colour of chlorite varies from grey (PPL) to light green/blue to pink (XPL) (sample K-1-221-chl). The alteration in this case is greyer colour both under PPL and XPL (Figure 3.6d).

3. Rock forming minerals in granite samples (samples: K-1-24B-grt & K-1-221-grt)

Quartz is the most common mineral showing lack of alteration (PPL) slightly higher interference than feldspar and non-uniform extinction (XPL) (samples: K-1-24B-grt & K-1-221-grt). Albite is abundantly observed in this sample, so as the granite in albite granite (Figure 3.6c, 3.6e and 3.6f).

4. Rock forming minerals in ppegmatite samples

The samples are largely composed of quartz, microcline, albite, muscovite and biotite in a different order of mineralogical assemblage (Figure 3.7). There are six main mineral assemblages identified: (1) alaskitic granite (quartz + microcline + albite with subordinate muscovite), (2) aplitic layer (quartz + albite), (3) muscovite-quartz-microcline-albite pegmatite, (4) spodumene-microcline-albite pegmatite partly albitized or greisenized, (5) microcline-albite-green and pink spodumene pegmatite with quartz-microcline block which is partly albitized and greisenized, and (6) quartz core. The concentration of tantalum increases from the border to the core zones.

From these mineralogical assemblages quartz is dominant to the core zone while albite is more common in the border and wall zones. This is related to mineralogical zonation, in consequences variation inTa ore concentration is occurred in each zone, increasing from the border to the core zones. Secondary muscovitization and further alteration of muscovite to chlorite has been observed during thin section analysis. Muscovite also altered to chlorite and tourmaline to clay and muscovite. Garnet also has been recognize in this sample (K-24B-19) with relict texture, yellowish (PPL) to dark (XPL) in colour. Lepidolite show typical of albite twining and showing biotite appearance was also identified in some other pegmatite samples. It replaced microcline. Microcline on other hand is altered to sericite.These minerals show their own texture such as platy, idioblastic, xenoblastic, relict, flaky, fibrous, and veinlet textures. However some of the minerals may show more than one type of textures such as muscovite, tourmaline and antigorite (see Table 3.1). Secondary muscovite also observed in the samples. i.e., evidence for muscovitization (Figure 3.7d). Fracturing on the ream of spodumene can suggest the tectonic fracturing during the formation of the deposit. This event is even more visible in talc which is showing brittle deformation (Figure 3.6b).

Table 3.1: Texture and alteration/replacement of some of the common minerals in the pegmatite samples.

Mineral	Texture	Replacement/alteration
Muscovite	Platy, flaky	Altered to chlorite
Biotite	platy	Replace chlorite
Quartz	Xenobalstic	
Microcline	Xenobalstic	Altered to sericite
Albite	Xenoblastic	Altered brown Ant
Spodumene	Idioblastic	
Chlorite	Platy	
Talc	platy	
Tourmaline	Idioblastic to Xenobalstic	Altered to clay and Msc
Garnet	relict	
Lepidolite	platy	Replace microcline
Antigorite	Platy, veinlet	
Chrysotile	fibrous	

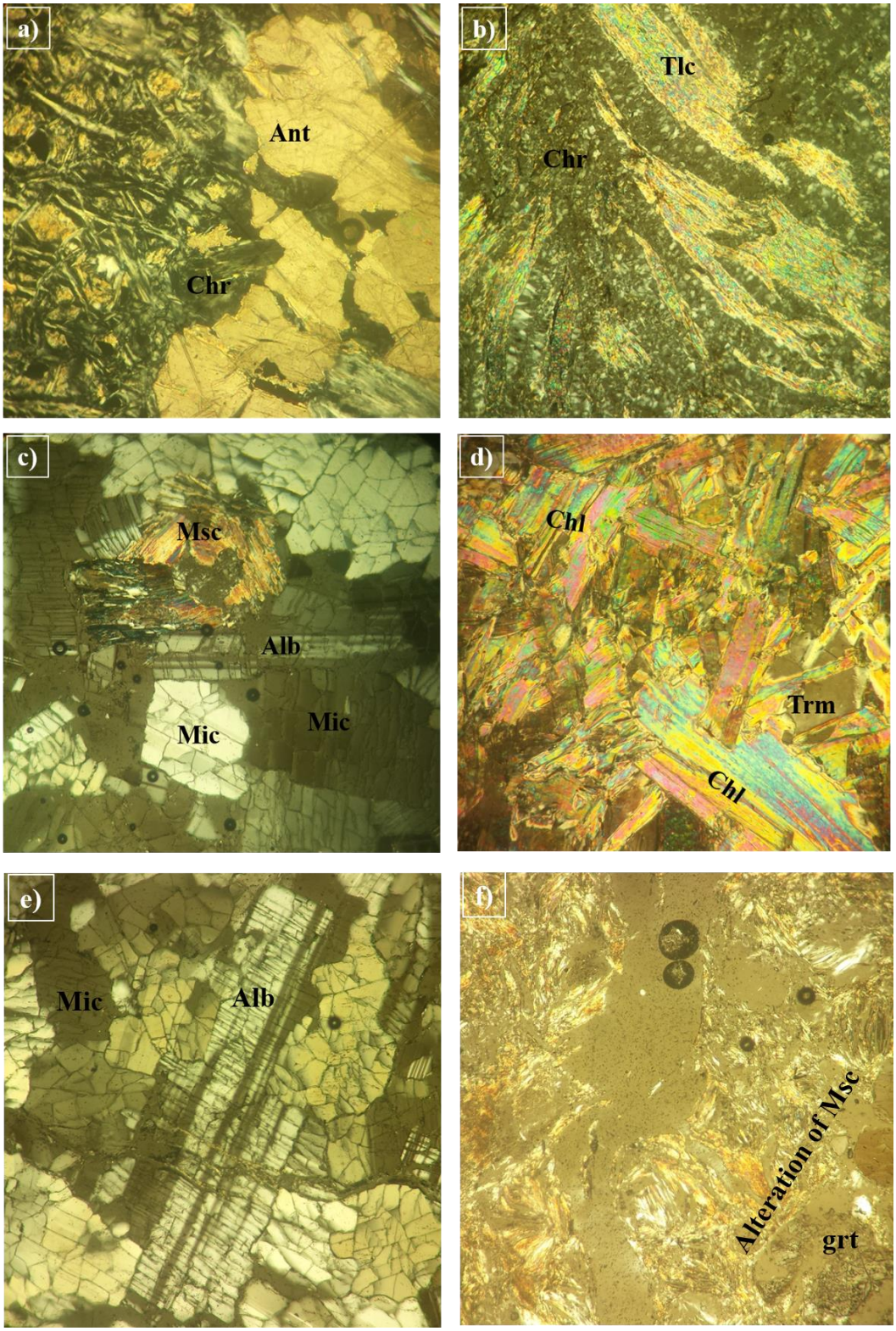

Figure 3.6: Photomicrograph of the host-rocks and granite, e.g., serpentinite (a), talc- & chlorite schists (b and d), albite granite (c, e and f). Note: Ant: Antigorite; Chr: chrysotile; Tlc: talc; Chl: chlorite; Trm: tourmaline; MSc: muscovite; Mic: microcline. Note: all photomicrographs are under XPL with 10x20 magnification.

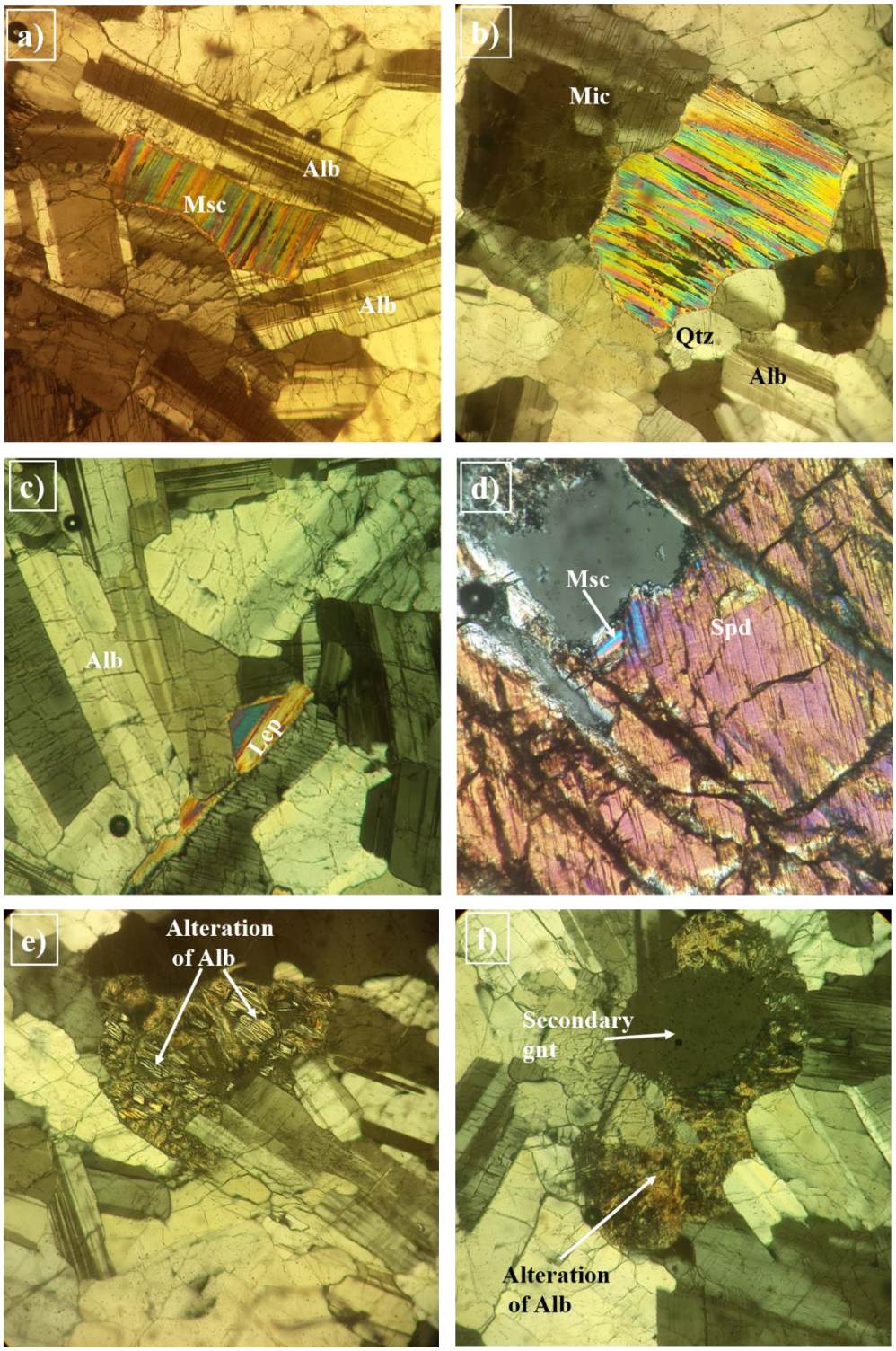

Figure 3.7: Photomicrograph of pegmatite samples. The elements such as Msc, Mic, Alb, Qtz, Spd (spodumene), Lep (lepidolite, showing albite twining) are the major constituent of the Kenticha rare metal pegmatite (a toc). Spodumene with some alteration to apatite which is grey (XPL) colour to yellow (PPL) (d), albite intergrowth with biotite and secondary minerals imbedded on the altered albite also shown (e and f). Note: all photomicrographs are under XPL with 10x10 magnification.

3.1.3 Ore forming minerals

The ore minerals such as tantalite, spodumene and beryl are commonly found in the Kenticha rare metal pegmatite. The accessory minerals include spessartine garnet, pyrite, hematite, magnetite and tantalite under ore microscope is light colour and elongated mineral (Figure 3.8a & 3.8b). Colourful zoned features; within the tantalite ore (Figure 3.8c & 3.8d) and diffused/cloudy green to pink colour features probably be internal reflection of tantalite. It also shows brownish internal reflections.

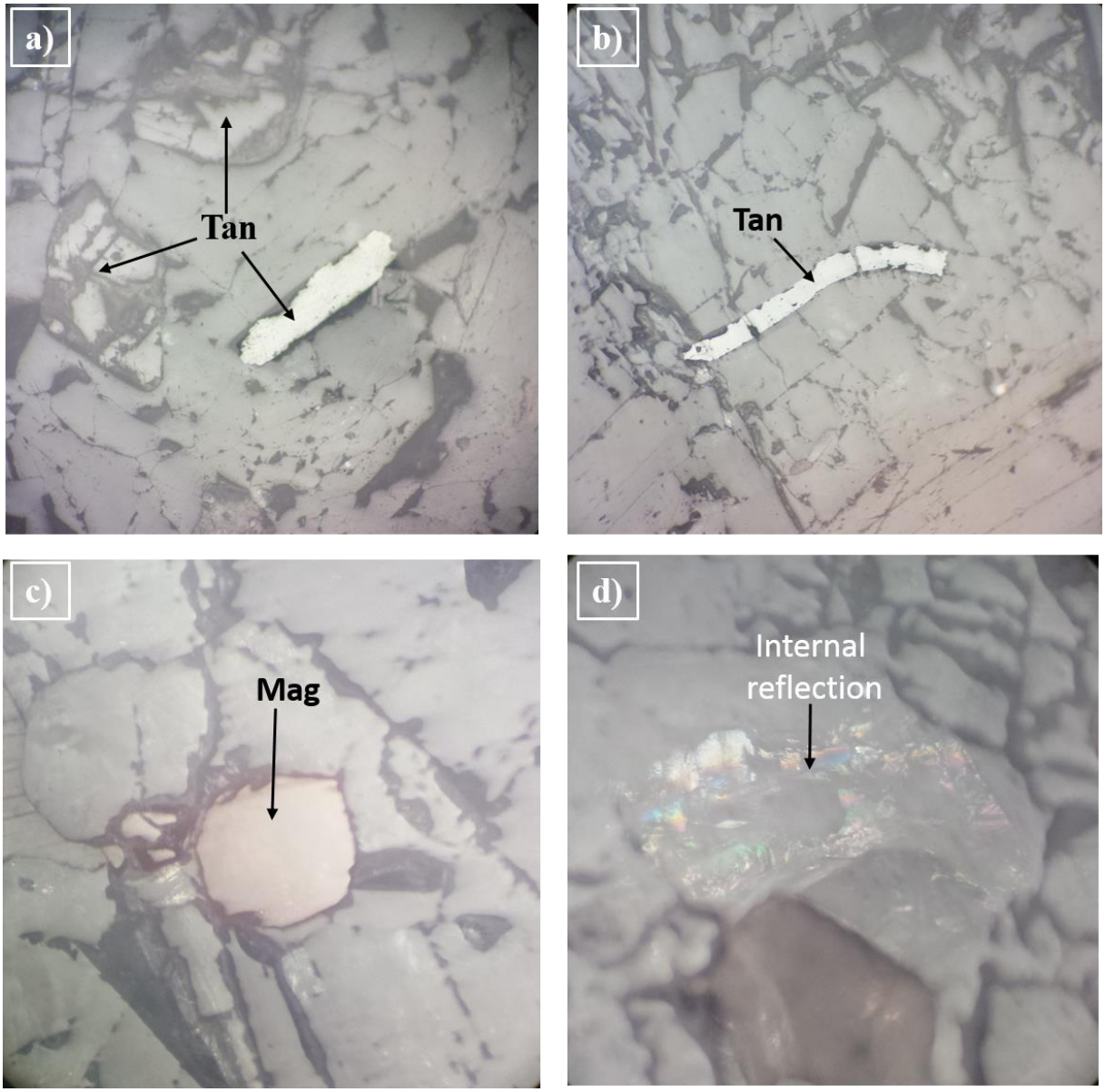

Figure 3.8: (a & b) Tantalite ore, (c) accessory magnetite and (d) internal reflection of a mineral under ore microscopy (10x20 magnification). Tantalite under ore microscope is light colour and elongated mineral. The background to the ore minerals are silicates such as microcline and albite.

Internal reflection in the tantalite crystal has been observed (Figure 3.9a and 3.9b). The most dominant and "rainbow" like reflection were observed within the tantalite crystal. However, this could be related to the fracturing of the tantalite crystal. When the fracture is intense it becomes dark in colour (Figure 3.9c). The brownish coloured is identified shows the characteristic of ferrotantalite (Figure 3.9d).

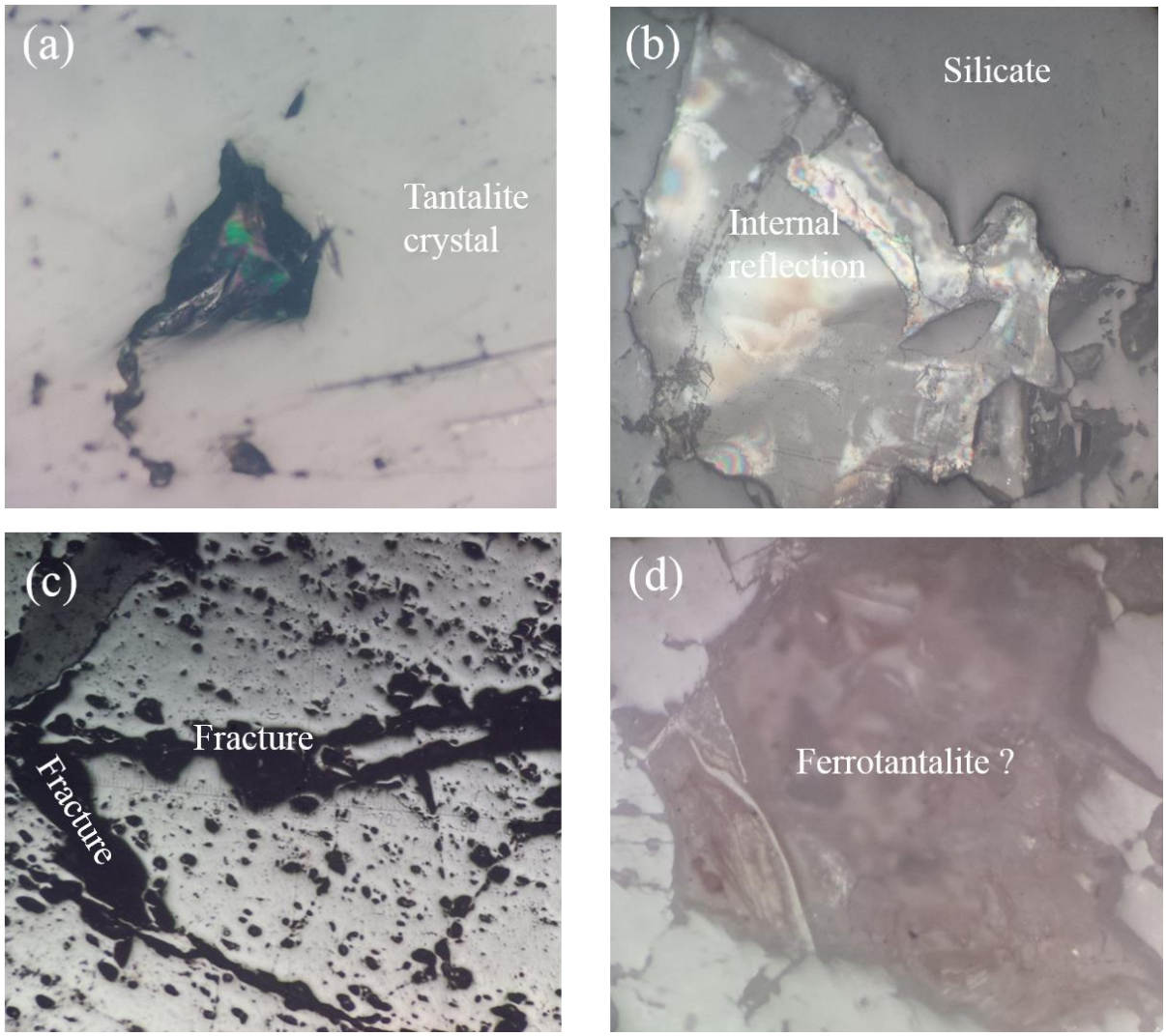

Figure 3.9: Ore micrographs of tantalite crystals showing no internal reflection and some shows a "rainbow" like internal reflections along fractures of the crystal (a and b). The brownish crystal could be ferrotantalite (c). The tantalite crystal also show defused brownish to light green colour internal reflection (d).Note: all the micropraphs are 10 x 20 magnification.

3.1.4 Geologic structures

Deep-seated faults control the mineralization of the study area. The attitude of the faults were measured and analysed by using rose diagram and equal area stereo net. The deep-seated normal faults are mainly striking N-S and dipping to the east. These faults are controlling the rare metal mineralization in the area. The emplacement of the pegmatites fallow these faults. Besides the deep-seated normal faults there are also minor normal faults that are trending NW-SE and NE-SW direction varying in their dip angle and direction. The orientation of the joint sets and the minor faults is similar which imply that the jointing was related with the minor faulting events. They all are striking NNW-SSE and NW-SE and dipping NNE and NE directions, respectively (see Figure 3.10b to 3.10e).

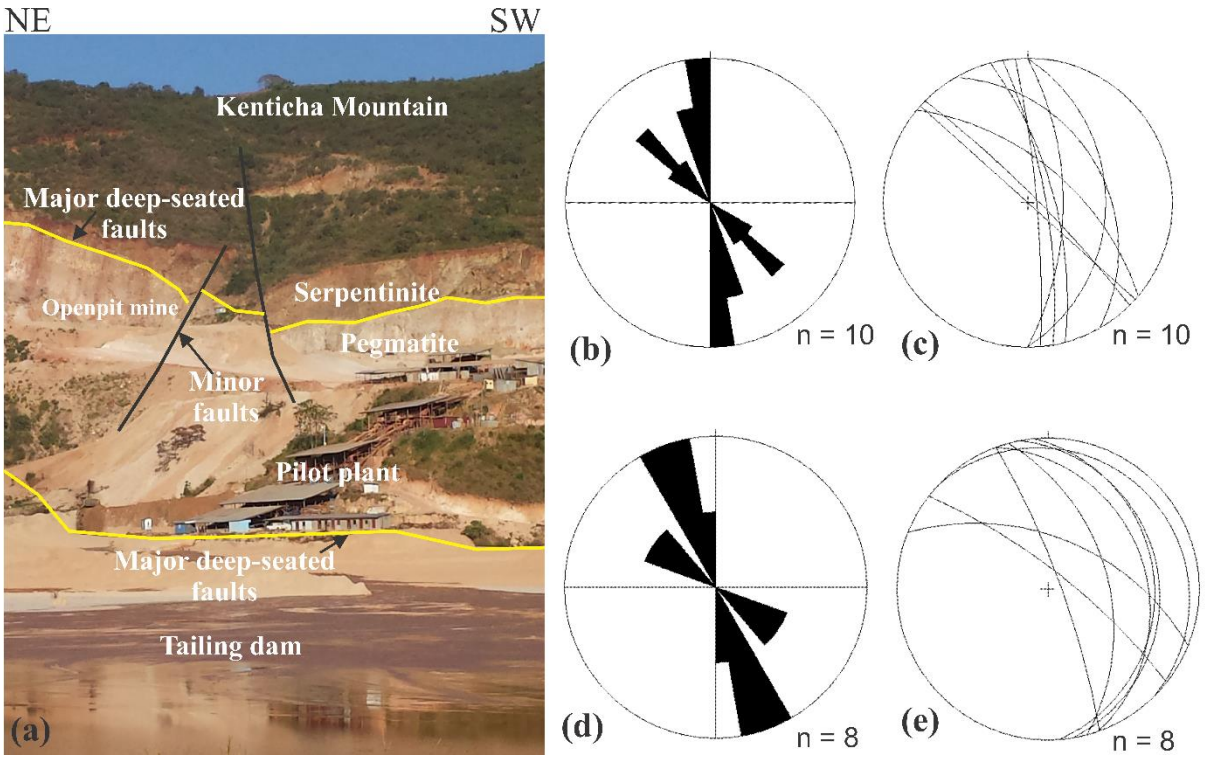

Figure 3.10: Geologic structures. (a) The Kenticha rare metal field viewed from the southwest-northeast direction from the tailing dame, pilot plant and pegmatite and serpentinite. The faults clearly observing juxtaposing the serpentinite rock and separating localities. The serpentinite is exposed in the open-pit mine which cover further to the Kenticha mountain chain. The open-pit estimated 40km to >100km. The attitude of faults and joint sets (replotted from Tadesse, 1998); (b & d) rose diagram and (c & e) equal area stereographic projection of the minor normal faults and joint sets, respectively. The faults and joints have similar strike and dip directions.

Numerous joints also observed in the area though currently they are obstructed by the mining activity. Tadesse (1998) grouped these joints into eight joint sets where their average strike varies from 30 to 60 relatively with higher dip amount and 170 to 277 relatively with lower dip amount.

3.2 Geochemistry of the Kenticha tantalite deposit

3.2.1 Whole-rock composition

The whole-rock composition of the pegmatite from the primary ore zone shows high concentration (wt.%) of SiO_2, Al_2O_3 and Na_2O. The concentration of BaO and SrO is very low, below the detection limitof the method (Table 3.2). However, the elemental composition of boron and strontium is relatively higher. This indicates that these elements are not compatible to form their own oxides at this stage. The silica content ranges from 70 -83 wt.% and 66.8 wt.% for pegmatite and granite samples, respectively (Table 3.2). The silica content also increases from the border to core zones, quartz core unit. The Na_2O on the other hand increase in a reverse way, increases from the core to border zones. The Cr_2O_5 and Ti_2O wt.% is relatively low and constant through all the samples.

Noticeable differences in minor and trace elements in the border, intermediate and core zones also recognized. The tantalum content increases towards the core zone and in reverse the niobium content increases towards the border zone. The content of V, Hf, W, Th, U and Y is relatively very low (all are approximately below 5 wt.%; see Table 3.3).

The sample plots lies on the SiO_2 vs $Na_2O + K_2O$ classification diagram plotted on the granite field (Figure 3.11a). This indicates that the Kenticha pegmatite field is dominantly of originated from a tholeiitic magma (Figure 3.11b). The ratio of $Al_2O_3/Na_2O + K_2O$ and $Al_2O_3/CaO + Na_2O + K_2O$ is greater than one indicating a peraluminous granitic pegmatite (Figure 3.11c & 3.11d).

Table 3.2: Major oxides (wt.%) of the Kenticha pegmatiteof deep borehole drill core samples using ICP-AES. The samples are mainly enriched in SiO_2, Al_2O_3 and Na_2O. Note: BaO and SrO are below the detection limit (bdl) of the method.

Rock	Pegmatite										Talc	Granite
Zone	Border				Intemediate			Core				
Sample	K-1-249-59	K-1-28A-28	K-1-225-28	K-1-245-50	K-1-219-36	K-1-27-42	K-1-69A-32	K-1-32A-25	K-1-24B-41	K-1-245-42	K-1-85A-2	K-1-224-31
SiO_2	74.5	73.9	74.6	75.7	75.4	70.5	74.1	73.9	83.8	78.9	56.4	66.8
TiO_2	0.01	0.01	0.01	0.01	0.01	0.01	0.01	0.01	0.01	0.02	0.01	0.01
Al_2O_3	16	16.65	15.05	15	14.75	22	15.25	15.4	9.87	12.75	12.1	18.7
Fe_2O_3	0.69	0.66	0.81	0.95	0.9	1.41	1.03	0.99	1.14	1.29	2.41	0.51
MnO	0.09	0.12	0.17	0.12	0.09	0.13	0.08	0.11	0.08	0.07	0.11	0.05
MgO	0.12	0.19	0.21	0.18	0.65	0.52	0.25	0.76	0.31	0.4	16.15	0.86
CaO	0.26	0.32	0.24	0.33	0.62	0.11	0.3	0.22	0.24	0.15	0.82	0.46
Na_2O	8.08	6.88	7.69	6.74	5.37	0.66	7.18	3.69	1.31	2.53	1.23	9.02
K_2O	0.71	1.47	0.59	0.73	0.91	1.18	0.7	0.82	1.78	2.82	1.45	0.64
P_2O_5	0.2	0.28	0.2	0.23	0.5	0.1	0.2	0.22	0.2	0.13	0.16	0.33
Cr_2O_3	0.04	0.03	0.02	0.03	0.02	0.04	0.03	0.03	0.04	0.03	0.13	0.01
LOI	0.58	1.12	0.73	0.65	2.18	1.86	0.79	2.66	1.16	1.61	7.16	2.82
Total	101.28	101.63	100.32	100.67	101.4	98.52	99.92	98.81	99.94	100.7	98.14	100.21

Table 3.3: Trace element composition (ppm) of the Kenticha pegmatite from deep drilled boreholes using ICP-MS. The result shows high concentration of Rb, Cr, Be, Nb, Ta and Cs in their decreasing order. Note: V is below the detection (bdl) limit of the method in all the samples.

Element	K-1-249-59	K-1-28A-28	K-1-225-28	K-1-245-50	K-1-219-36	K-1-27-42	K-1-69A-32	K-1-245-42	K-1-32A-25	K-1-24B-41	K-1-85A-2	K-1-224-31
Ta	64.9	91.9	86	51.2	92.2	30.5	55.1	132	93.7	222	108	65
Nb	160	167	168	137	157	23.8	146	152.5	62	110.5	39.9	147
Be	191	203	212	236	265	16	223	116	404	92	54	83
Sn	9	16	6	10	10	29	7	42	23	16	28	8
Cr	230	260	200	230	210	340	260	250	270	320	930	90
Ga	45	67.3	44.1	45.6	47.3	90.1	44.2	73	58.2	45	44.7	53
Hf	2.9	2.8	2.7	2.7	3	0.8	2.3	6	1.7	4.1	2.9	2.1
Zr	18	17	18	22	22	3	20	35	8	46	15	14
Sr	5.2	5.5	5.6	7	12	42.6	6.7	18.2	12.3	36.1	25.1	16.3
Rb	332	800	261	285	497	763	297	1915	501	1235	2290	406
Cs	75.2	70.9	63.3	65.1	162.5	154	86.5	292	257	274	2480	150.5
Y	0.8	1.1	1.2	1.3	4.2	bdl	0.7	3.2	0.6	5.7	bdl	1.5
Ba	8.5	11.5	8.1	9.5	8.9	15.4	8.7	12.1	20.5	18.9	67.6	5.8
Th	4.98	7.95	6.74	4.84	4.97	1.52	6.76	3.61	5.12	3.77	2.47	6.53
U	3.53	3.33	2.77	7.88	5.22	1.56	6.85	6.32	5.55	5.66	2.89	1.92
W	4	4	3	4	4	3	3	7	2	4	3	3
Nb/Ta	2.47	1.82	1.95	2.68	1.70	0.78	2.65	1.16	0.66	0.50	0.37	2.26
Zr/Hf	8.15	7.33	6.67	5.83	4.71	8.70	6.67	6.07	11.22	6.21	3.75	5.17
Ta/(Ta + Nb)	0.29	0.35	0.34	0.27	0.37	0.56	0.27	0.46	0.60	0.67	0.73	0.31
Mn/(Mn + Fe)	0.13	0.74	0.68	0.73	0.93	0.91	0.97	0.88	0.92	0.87	0.99	0.97

Table 3.4: REE concertation analysed by using ICP-MS (in ppm). The concentration of Eu is very low (below the detection limit = 0.3 for Eu).

Element	K-1-249-59	K-1-28A-28	K-1-225-28	K-1-245-50	K-1-219-36	K-1-27-42	K-1-69A-32	K-1-32A-25	K-1-24B-41	K-1-245-42	K-1-85A-2	K-1-224-31
La	0.7	0.7	0.5	0.7	1.1	bdl	0.9	bdl	1.7	bdl	0.6	0.5
Ce	2	2	1.8	1.8	3.2	bdl	1.9	0.7	4.4	1.3	0.9	1.5
Pr	0.24	0.27	0.21	0.22	0.41	bdl	0.17	0.07	0.47	0.16	0.07	0.17
Nd	0.8	1.1	0.9	0.9	1.5	0.1	0.6	0.3	1.7	0.9	0.3	0.8
Sm	0.47	0.66	0.46	0.59	1.67	bdl	0.55	0.04	0.47	0.69	0.06	0.51
Eu	bdl	0.03	0.06	0.04	bdl	bdl	bdl	bdl	0.04	0.08	bdl	0.04
Gd	0.47	0.63	0.49	0.77	2.1	0.05	0.5	0.06	0.66	0.78	0.12	0.49
Tb	0.09	0.1	0.1	0.1	0.46	bdl	0.09	0.02	0.13	0.12	0.02	0.11
Dy	0.23	0.28	0.29	0.36	1.28	bdl	0.29	0.09	0.8	0.5	0.06	0.26
Ho	0.01	0.02	0.02	0.02	0.08	0.01	0.02	0.01	0.18	0.07	bdl	0.03
Er	bdl	0.03	bdl	0.05	0.12	bdl	0.04	0.12	0.78	0.11	bdl	0.03
Tm	0.01	bdl	0.03	0.03	0.04	bdl	bdl	0.01	0.08	0.02	0.02	0.02
Yb	0.06	bdl	0.04	bdl	0.07	0.04	0.07	0.08	0.56	0.1	bdl	0.1
Lu	0.01	0.01	bdl	0.01	0.02	0.01	0.01	0.01	0.06	0.01	0.01	0.02
Eu/Eu*	0.19	0.14	0.38	0.18	0.05	0.78	0.17	0.62	0.22	0.78	1.06	0.24
$(La/Yb)_N$	7.86	15.73	8.43	15.73	10.59	8.43	8.67	4.21	2.05	3.37	13.48	3.37
LREE/HREE	13.76	12.53	10.05	8.96	5.04	15.00	10.50	4.68	4.79	4.77	20.50	8.91
totREE	5.15	5.87	4.94	5.62	12.08	1.38	5.18	2.02	12.03	5.34	2.26	4.58

3.2.2 Tectonic setting

The data point falls on the field of granite using TAS (SiO_2 vs $K_2O + Na_2O$) diagram (Figure 3.11a). It comprises peraluminous pegmatites (Figure 3.11c) with SiO_2contents varying between 70 to 83 wt. %. The Al_2O_3 is abundant in the samples next to SiO_2 and its contents varying between 12 to 22 wt.%. Most of the samples shows theoleitic magma which has high concentration of silca and low-K values. However, the K/Rb is very high in most of the samples. Using geotectonic diagrams such as Yb + Ta x Rb and Y +Nb x Rb (Pearce et al., 1984), samples plot in the "Within Plate Granites (WPG)"or in the limit of WPG and "syn-Collisional Granites (syn-COLG)" fields (Figure 3.11e & 3.11f).

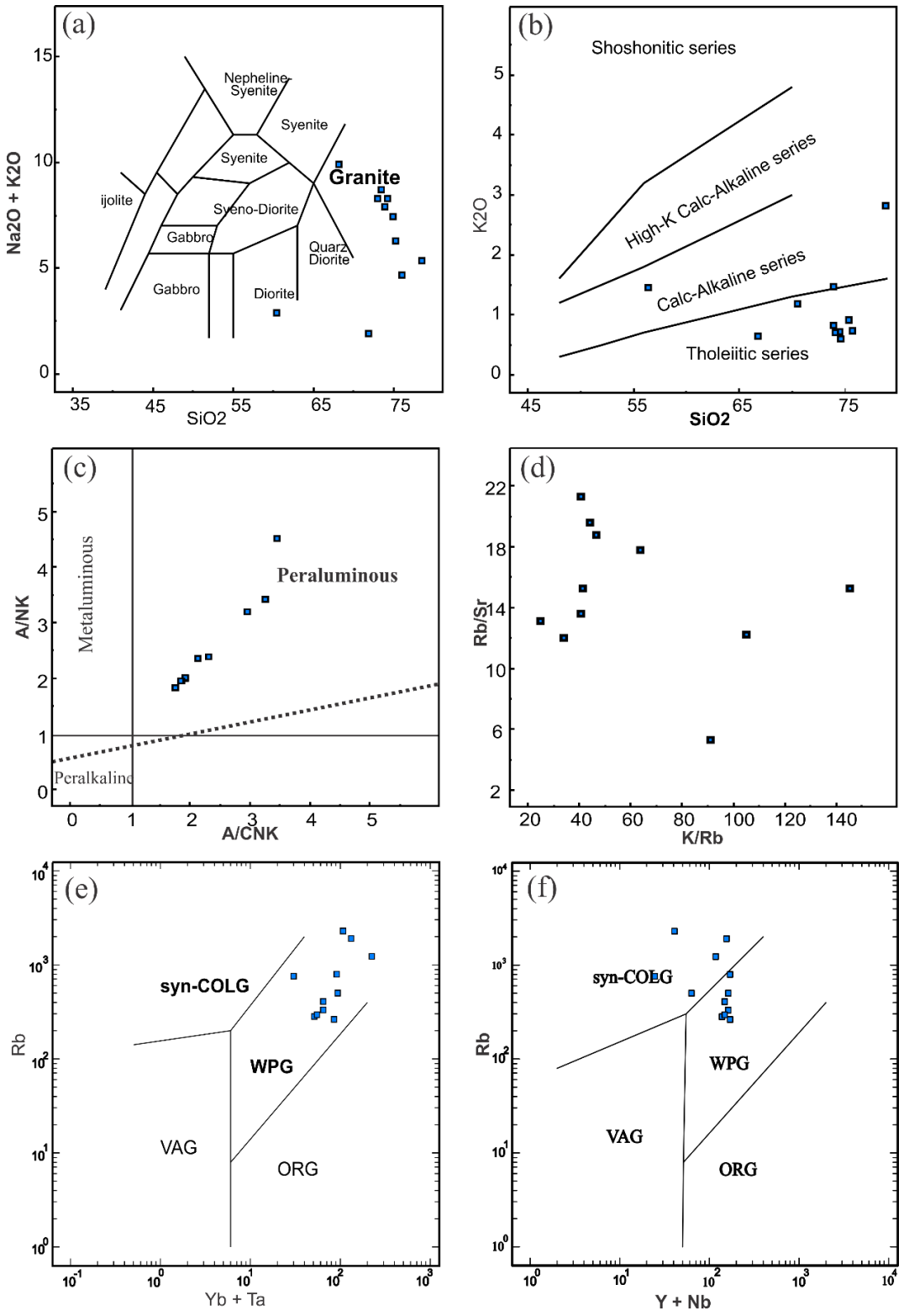

Figure 3.11: Classification diagrams for analyses on whole-rock samples. (a) TAS (Cox et al., 1979), (b) K_2O vs. SiO_2(Peccerillo and Taylor, 1976), (c) A/NK (A = Al_2O_3, N = Na_2O) vs. A/CNK (K= K_2O) diagram (Shand, 1943), (d) K/Rb vs. Rb/Sr ratios (ppm), and (e) and (f) geotectonic discrimination diagrams (Yb + Ta x Rb and Y +Nb x Rb; Pearce et al., 1984). Where, VAG: Volcanic Arc Granites, ORG: Orogenic Granites, WPG: Within Plate Granites, syn-COLG: syn-Collisional Granites.

3.2.3 Minor and trace elements

Rb, Nb, Ta and Cs comprise the highest trace element values (in ppm) in the samples (Table 3.3). Ta and Nb are higher in the pegmatite samples and beryllium (Be) is very high in the granite samples (K-1-69-32 and K-1-245-50). The concentration of large ion lithophile elements of Rb, Cs and Th are comparatively very high as they are incompatible to the mineral phase of this suit during the late stage magma differentiation (Figure 3.14). The high field strength elements (HFSE) of Hf, Zr, Ta and Nb on the other hand show significantly high enrichment (Figure 3.13). The consistency of the sample plots indicate that they are sourced from the same magma.Rb concentration also has inverse relationship with K/Rb concentration, plotting negative slope (Figure 3.12). The concentration of Rb increases with the decrease in the K/Rb ratio.

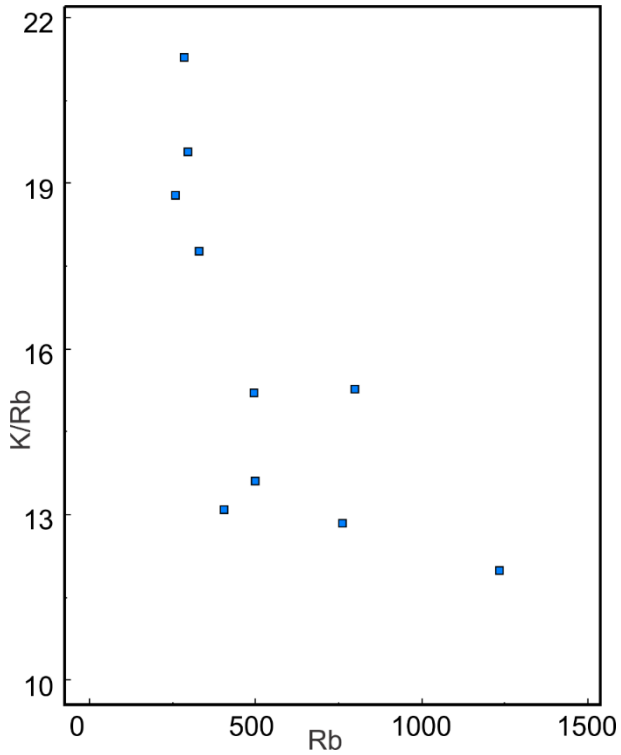

Figure 3.12: Variations of K/Rb ratio relative to Rb (ppm) of the Kenticha pegmatite. Primordial mantle normalized diagrams show similar trends i.e., enrichment in CS, Ta and depletion of Ba and some other elements like Nd, Pr, Ti and Yb.

Zirconium also follow similar trend with Hf, Ta and Na, and Nb/Ta contrasting with Rb concentration (Figure 3.13). Hence, the concentration of Zr increases as Ta, Rb, Nb, and Hf, and ratios of Nb/Ta and Zr/Hf concentration increases. Similar fractionation trend has been observed in these elements during magma fractionation. The fractionation increases from the

border zone to the core zones (Figure 3.13). The tantalum concentration is high in the core zone where as the niobium concentration is high in the border zone (Figure 3.13b and 3.13d).

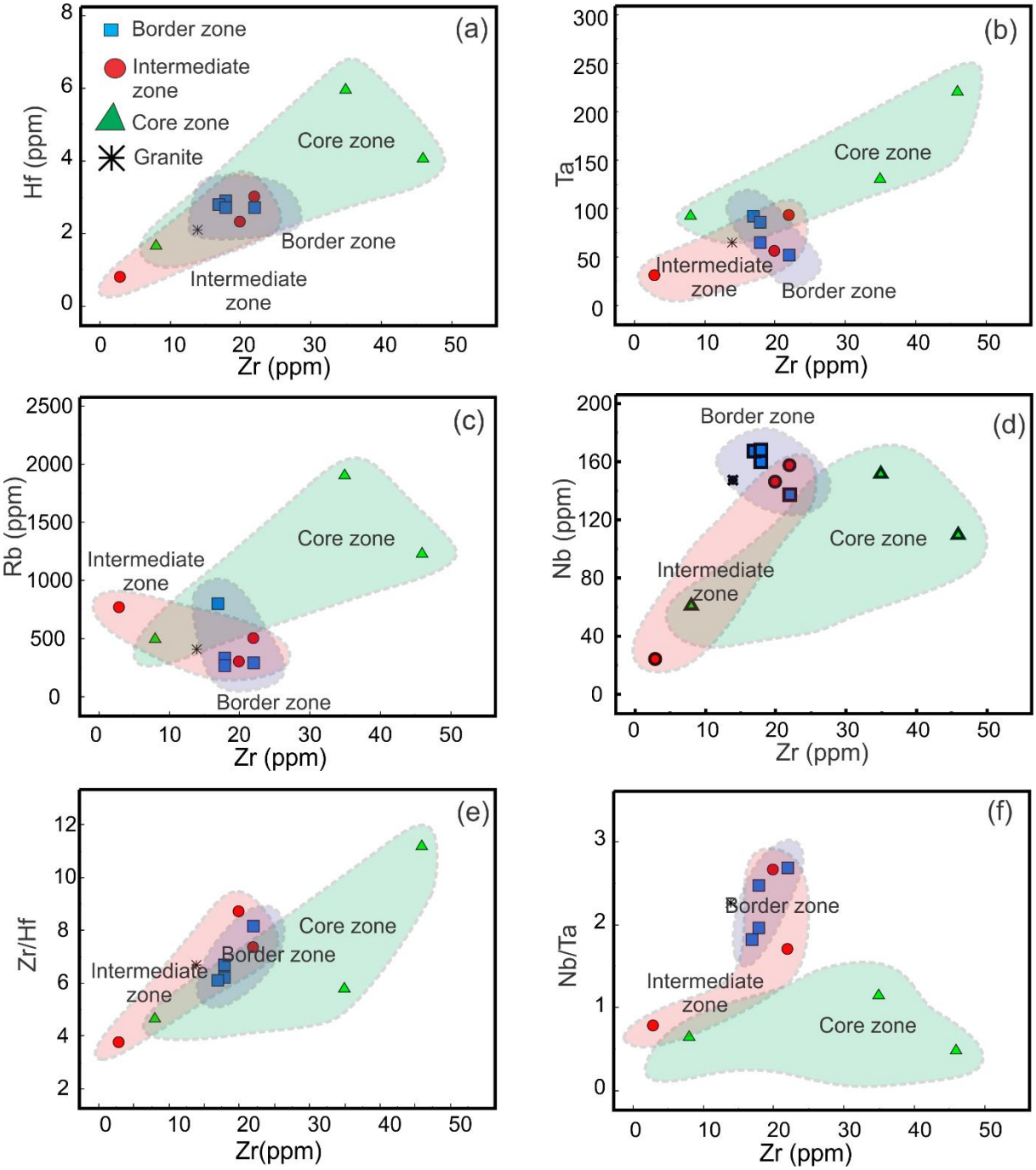

Figure 3.13: The variation diagrams of (a) Zr vs Hf, (b) Zr vs Ta, (c) Zr vs Rb, (d) Zr vs Nb, (e) Zr vs Zr/Hf and (f)Zr vs Nb/Ta. Except with Rb, Zr shows similar fractionation trend with Hf, Ta and Nb.

The concentration of Ba, Nd, and Ti is very low and the concentration of Cs, Rb and Ta is very high in the whole-rock samples (Figure 3.14).

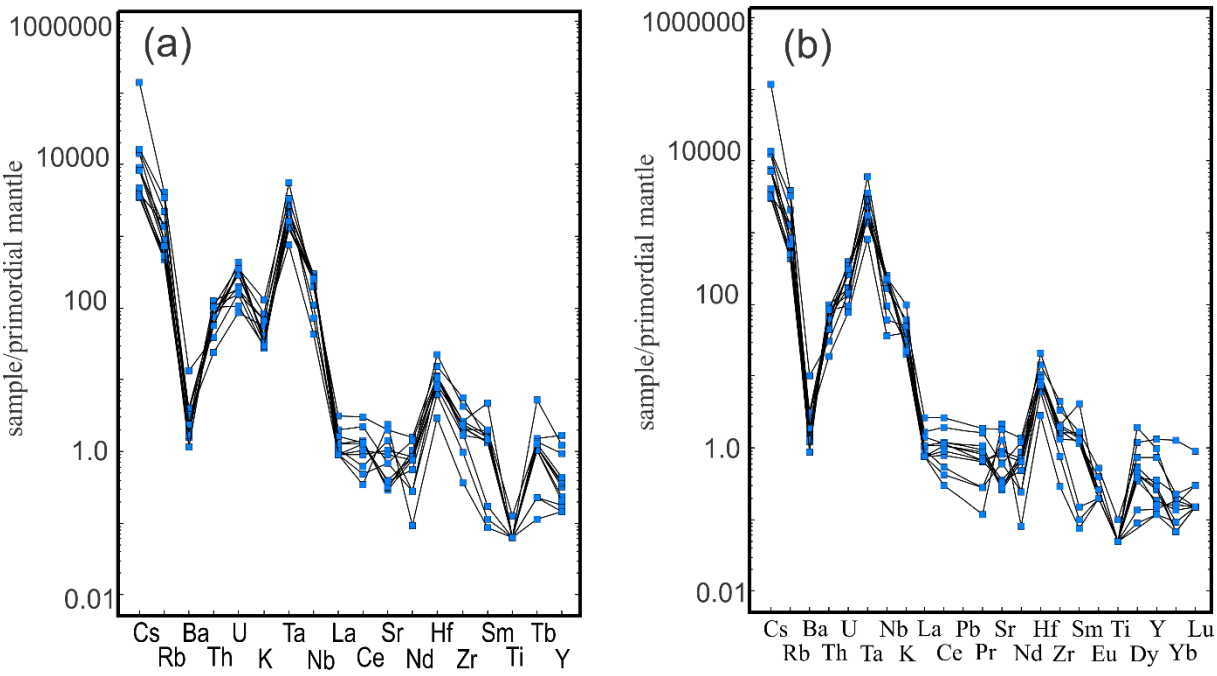

Figure 3.14:Multi-element spider diagram(a) Taylor and McLennan (1985) and (b) McDonough and Sun (1995).

3.2.4 REE composition of the weathered and primary ore zones

The REE pattern of the whole-rock samples in the weathered zone and primary zones are show enrichment in REE (Figure 3.15). Most of the weathered zone samples does not show negative Eu-anomaly. This positive anomaly could be related to later hydrothermal-metasomatic processes. Except the granite samples almost all of the pegmatite samples in the primary zone shows REE enrichment with pronounced negative Eu-anomaly. Besides majority of the primary ore zone whole-rock samples show negative anomalies at dysprosium (Dy), erbium (Er) and ytterbium (Yb) (Figure 3.15). The REE pattern in Figure 3.15b is separated into five V-shape, (10 separate individual) sectors (La-Sm, Sm-Gd, Gd-Ho, Ho-Tm and Tm-Lu) corresponding four minima positions at Nb, Eu, Dy, Er and Yb. This forms “double M-type” shape neglecting the first and the last sectors.

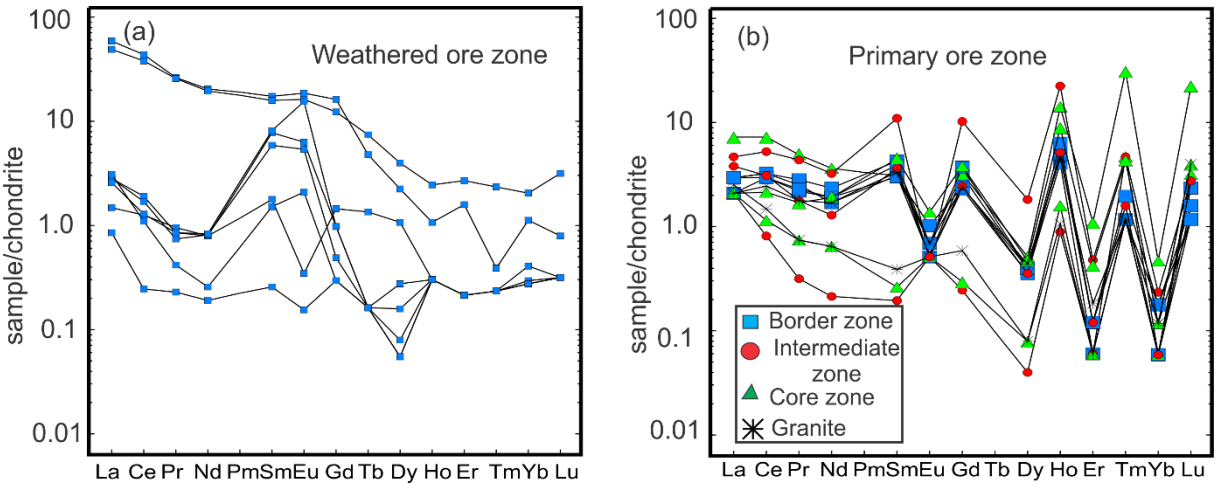

Figure 3.15: Chondrite normalizedREE pattern (Sun and McDonough, 1989) of (a) the weathered zone and (b) primary ore zone of Kenticha pegmatite. Most of the samples show tetrad effect from the weathered and primary ore zones.

Chapter 4 Discussion

4.1 Whole-rock geochemistry

4.1.1 Major elements

Different evolutionary trends can be identified from Mn/(Mn + Fe) versus Ta/(Ta + Nb) CGM diagram conventionally used for these purposes. From this diagram discrete fields of the different CGM generations, zonings and trends of magma fractionation were identified. The variation is much in Ta/(Ta + Nb) while Mn/(Mn +Fe) relatively constant in all of the generations. Compositional zonation can be also outlined from the variation of Mn* vs Ta* diagram (Figure 4.1). Three zones can be broadly identified form this diagram: core, intermediate and border zones. The core zone is dominated by manganotantalite whereas the border zone is dominated by manganocolumbite. This trend can be related to the primary magma fractionation. Ferrotantalite (tapiolite) and ferrocolumbite enrichment indicates hydrothermal-metasomatism replacement processes (Desta, 1996; Küster et al., 2009; Tadesse and Desta, 1996). This is observed in one of the granite sample plot enriched with ferrocolumbite. The trend shows the mineralization is evolved from ferrocolumbite to manganotantalite, in agreement with the interpretation of Küster et al. (2009) and Tadesse and Desta (1996).

The compositional zoning of the Kenticha rare metal pegmatite corresponds to the major trends recognized by Černý (1989) and Černý et al. (1992) for the lepidolite and spodumene subtypes of rare metal pegmatite worldwide. A concomitant increase in Ta and Mn in columbite minerals is a common trend with progressive pegmatite fractionation. With progressive fractionation the pegmatite is enriched in Nb and then Ta. An increase in Ta/(Ta+Nb) ratio during crystallization of the pegmatite with fractionation could be explained by the lower solubility of columbite-(Mn) in peraluminous granite/pegmatite melts as compared to the tantalite-(Mn) (Linnen and Keppler, 1997). Besides, the solubilities of columbite and tantalite increase with increasing temperature and Li content of the melt (Fiege et al., 2011). Accordingly, Li-bearing minerals such as spodumene are dominant in the intermediate zone of the study area and further Ta enrichment is occurred in the core zone. The increase in Mn/(Mn + Fe) ratio on the other hand depends on the fact that higher solubility of columbite-(Fe) as compared to columbite-(Mn). This could suggest that the Fe-Mn balance is controlled by Fe-Mn-bearing minerals such as micas, tourmaline,or garnet during the pegmatite evolution (Van Lichtervelde et al., 2007). The concentration of Mn/(Mn+Fe) is controlled by the crystallization of tourmaline at the early

fractionation and laterthe control of micas become more dominant.So, Fe-Mn-, Nb-Ta- and Ta-Nb-fractionation trends have been observed from the border zone to intermediate and core zones, respectively.An increase in the Mn during the post-magmatic and hydrothermal-metasomatic stages increases tantalite-(Mn). This reflects an increase of Mn in the mineral forming environment with extreme fractionation in Li-Fe-rich melt (Černý and Ercit, 1989).

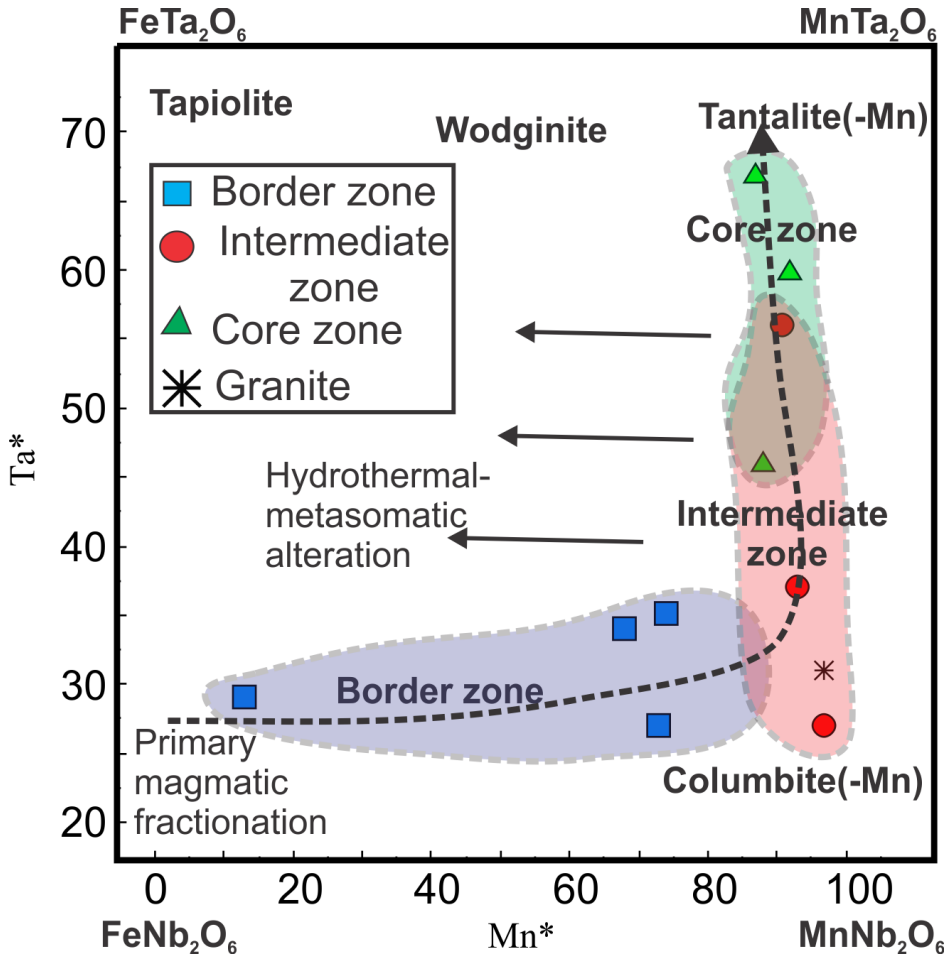

Figure 4.1: CGM Variation diagramof Mn* (Mn/(Mn + Fe)*100) and Ta* (Ta/(Ta + Nb)*100) in CGM of the main Kenticha pegmatite rare-metal field. Black dotted arrow indicates primary magmatic fractionation trend whereas the black arrow is the trend for metasomatic alteration.

4.1.2 Trace elements

The Rb-Ba-Sr triangular plot indicates a granitic trend (Figure 4.2 and Table 3.2) typical of strongly differentiated graniteswith Rb enrichment and low Ba and Sr contents. This is related to the magma differentiation, feldspar normative and their Rb, Ba and Sr affinities (Larsen,

2002). Most of the Kenticha whole-rock samples show Cs-enrichment (upto 565 ppm; Küster et al., 2009).

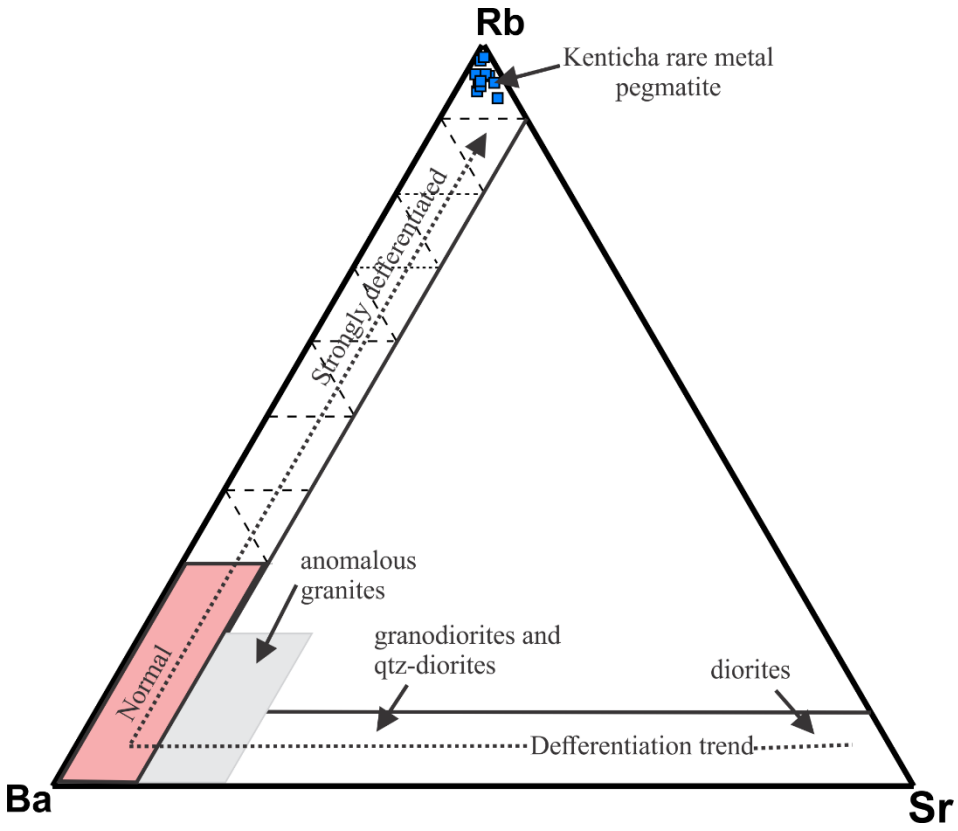

Figure 4.2: Rb-Ba-Sr plot of El Bouseily and El Sokkary, 1975 for granitic rocks. It indicates a granitic trend typical of strongly differentiated granites with Rb enrichment and low Ba and Sr contents for whole–rock analyses of the Kenticha drill core samples.

Fractional crystallization cannot be only simply characterized bysome aspects of Kenticha granite pegmatite. The K/Rb ratio (11-21) of the Kenticha pegmatiteis very low as compared to crustal average which is approximately 230 (Taylor and McLennan, 1985) and is signify a hydrothermal evolution of pegmatites(Černý et al., 1985; Shaw, 1968). The K/Rb vs Rb/Sr and K/Rb vs Rb/Sr shows the evolution of the pegmatite from its primitive to the most evolved stages (Figure 4.3a). The plots in Figure 4.3 generally show similar fractionation trend, fractionation of those elements through the magma differentiation. The concentration of Ga, incompatible in K-feldspar, shows a negative slope when compared to K/Rb and Sr/Rb. The melt composition in granitic pegmatites is a function of K, Sr and Rb distribution in K-feldspar which depend on the extent of fractional crystallization and the degree of differentiation of the parent magma before the emplacement of the pegmatite-forming melt (Larsen, 2002). So, these elements are sensitive to igneous processes.

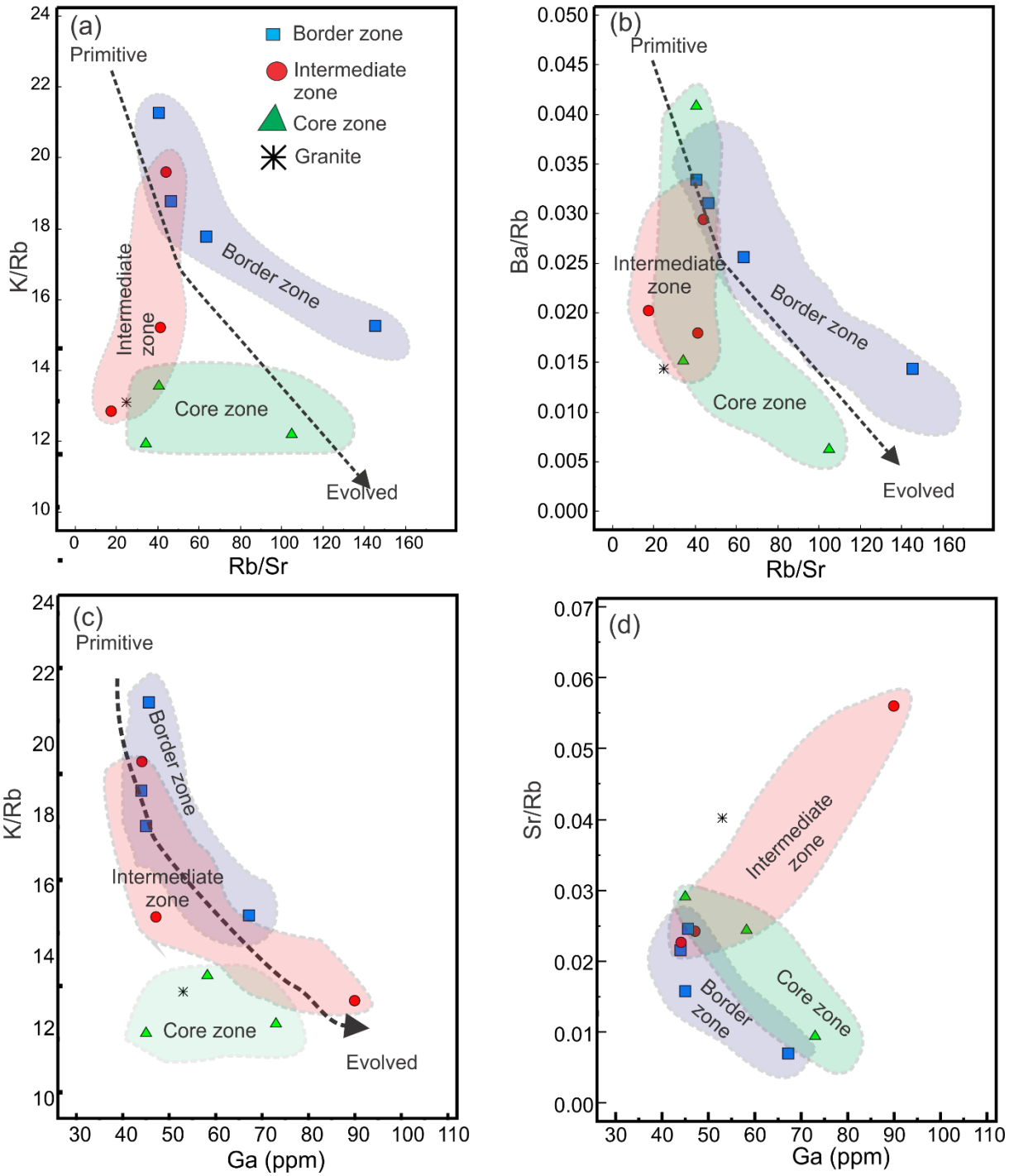

Figure 4.3: Plots of some sensitive elements for igneous processes. (a) Rb/Sr vs K/Rb, (b) Rb/Sr vs Ba/Rb, (c) Ga vs K/Rb, and (d) Ga vs Sr/Rb. These plots help to infer the evolution of the granitic pegmatites as the pegmatite-forming liquid become more evolved. The dotted arrow indicates the general increase in fractionation from the border to the core zones.

The K/Rb, Sr/Rb and Ba/Rb ratios are higher in the border zone and continued fractionation increases the content of Ga and ratio of Rb/Sr. The ratio of Rb/Sr and content of Ga show enrichment during the fractionation, as indicated from the border to the core zones of Kenticha

whole-rock samples. Syn-collisional veins and pegmatite dikes indicate highly peraluminous magmas with Ga enrichment (Bongiolo et al., 2016).

Generally, the ratio of Nb/Ta decrease during magmatic fractionation of a granitic melt. The temperature is the main factor for the concentration of Ta more or less than the source rock, high temperature anatexis results high Ta fractionate due to residual biotite (Stepanov et al., 2014). Biotite in the early stage partial melting produce Ta-rich melt, progressively muscovite with less biotite and then muscovite become dominant in the melt. At the most evolved stage of the pegmatite Ti-bearingoxides (e.g., illimenite, rutile and garnet) become the host for the Ta and Nb. In contrast to concentration of Nb, Ta concentration increases from the border to core zones during magmatic fractionation since the Nb/Ta concentration decreases. This generally agree with the fact that the quartz core zone has more tantalite concertation, large crystals are visible with naked eyes. Similarly, the Cs concertation and the ratio of Zr/Hf also increases towards the core zone (Figure 4.4). The lower solubility of manganocolumbite compared to manganotantalite in most evolved peraluminous pegmatite such as Kenticha pegmatite also enhance the decrease of the Nb/Ta ratio in the melt (Linnen and Keppler, 1997).

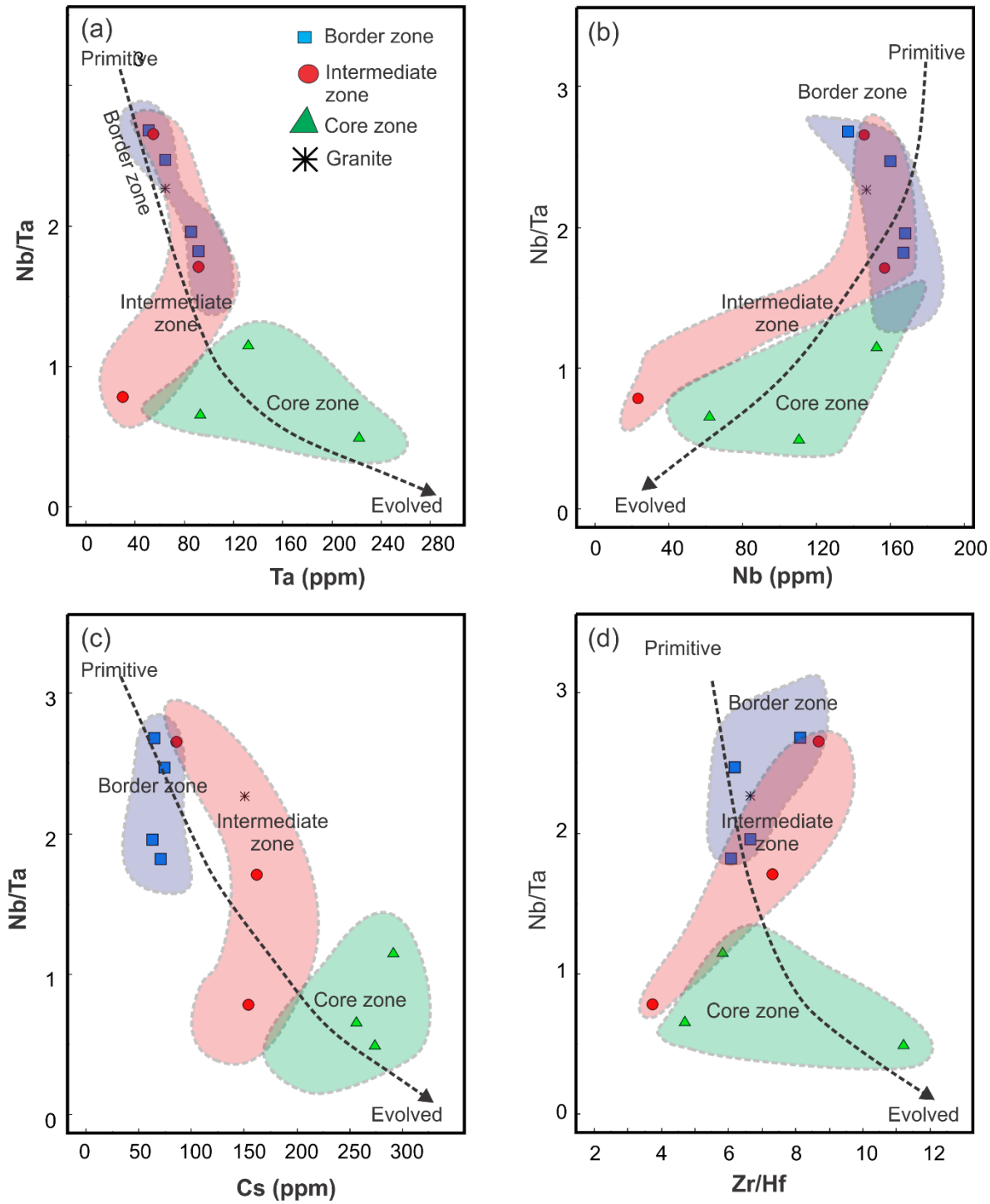

Figure 4.4: Ratio of Nb/Ta during magmatic fractionation. Ta (ppm) vs Nb/Ta, (b) Nb (ppm) vs Nb/Ta, (c) Cs (ppm) vs Nb/Ta and (d) Zr/Hf vs Nb/Ta. In contrast to Nb, the concertation of Ta and Cs, and the ratio of Zr/Hf increase during magmatic fractionation when the Nb/Ta decreases. Note: the dotted arrow indicates the evolution of the pegmatite prom the border zone (primitive) to core zone (evolved).

Ballouard et al.(2016) proposed (1) the ratio of Nb/Ta (~5), (2) secondary muscovitization and greisenization, (3) anti-correlation of Sn with ratio of Nb/Ta, and (4) Sn-W-U and rare-metal

mineralization as markers of the transition between primary magmatic fractionation and secondary hydrothermal-metasomatic replacement processes. During interaction between crystallized granites and acidic late magmatic fluids secondary muscovitization and greisenization become prominent under sub-solidus conditions(Pirajno, 2013). On this basis, the hydrothermal-metasomatic processes are significant in the Kenticha rare metal granite pegmatite. The contrasting trends of Sn vs Nb/Ta and K/Rb vs Nb/Ta show a decrease in Nb/Ta ratio and enrichment in Sn to the core zone (Figure 4.5). Tin (Sn) is highly mobile at the magmatic-hydrothermal transition which is a good marker for magmatic fractionation and hydrothermal-metasomatic alteration. The ratios of K/Rb are correlate with very low Nb/Ta ratioswhich is typical of the secondary metasomatic-hydrothermal processes. Most granites with low Nb/Ta which characterized by pegmatite-hydrothermal evolution mostly display K/Rb values less than 150 (Shaw, 1968). The ratios Zr/Hf (<~25) (corresponding to the lower limit of the charge and radius control range) and Nb/Ta has been proposed as a marker of either magmatic-hydrothermal interactions (Bau, 1996)or fractional crystallization (Claiborne et al., 2006; Linnen and Keppler, 2002) with the corresponding low content ofNb/Ta (< 5), and lower Zr/Hf ratios (<18) for rare metal granite. This is evident in the Kenticha rare metal granite pegmatite (Figure 4.4).

The above mineralogical, geochemical and metallogenic markers are evidence of a fluid interaction recorded in the Kenticha whole-rock samples. The ratio of Nb/Ta (~5) is a good marker of the magmatic-hydrothermal transition in peraluminous granites. The decrease in the ratio of Nb/Ta in peraluminous granite pegmatites is also associated with an increase in secondary muscovitization and a subsolidus alteration involved in the fractionationof Nb-Ta. So, the ratio of Nb/Ta (~5) is a good geochemical indicator to differentiate the barren from rare metal peraluminous granite pegmatites(Ballouard et al., 2016). This used as an exploration criteria for rare metal granite pegmatites, especially for tantalite and columbite exploration. The ratio of Nb/Ta of the whole-rock samples of the Kenticha rare metal pegmatites is well below (<~3) the value proposed as marker for exploration criteria (Figure 4.5).

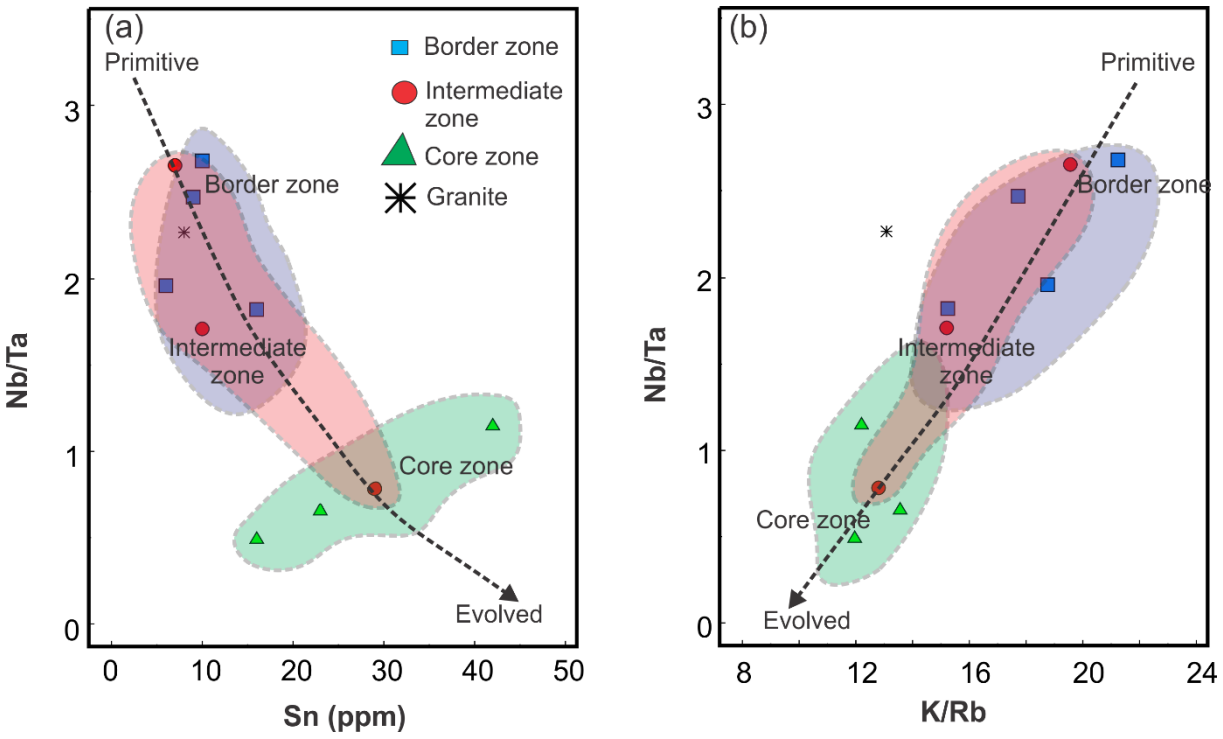

Figure 4.5: Evolution of Nb/Ta ratios of Kenticha rare metal pegmatite to infer magmatic-hydrothermal alteration. (a) Sn vs Nb/Ta and K/Rb vs Nb/Ta showing metasomatic-hydrothermal alteration.

4.1.3 REE pattern

From the REE plots four different patterns are identified generally showing REE enrichment (Figure 4.6). They shows contrasting characteristic of enrichment (Figure 4.6a) and negative to no (Figure 4.6b and 5.6d) Eu anomalies. Most of the samples show negative Eu anomaly caused by feldspar fractionation, which does not affect significantly the other REE (Rushmer and Knesel, 2011). The rare earth elements (REE) on the other hand shows slight enrichment of LREE (Figure 4.6a). In most of the samples of the primary ore zone, negative Eu-anomaly, higher REE towards LREE and lower to HREE, enrichment of REE is shown. The Kenticha pegmatite possess slightly lower total REE (totREE = 2.02-12.08 ppm) abundance, strong Eu depletion (Eu/Eu* = 0.05-1.06; average Eu/Eu* = 0.4) and moderate REE enrichment ($(La/Yb)_N$ = 2.05-15.73; average of 8.5 and LREE/HREE = 4.77-20.5; average of 9.96). This shows moderate enrichment in REE during magmatic fractionation, implying high fractionation in the Kenticha pegmatite. The REE pattern revealed similar fractionation trend as of Küster et al. (2009) and Melcher et al. (2015).

The dominant REE pattern form a tetrad effect (M-type) by having the lowest concentration at Eu (Figure 4.6 and Table 3.4). Pegmatite and granite commonly show convex tetrad effects and pronounced negative Eu anomaly without much notable Y/Ho fractionation (Takahashi et al., 2007). Most of the Kenticha rare metal pegmatite whole-rock samples have Y/Ho values ranging 50-80, this suggests that the complexation with fluorine as major cause for values >28 (Bau and Dulski, 1995). This suggests the original tetrad effect in the original magma before crystallization. Few of the primary ore zone samples attain the lowest REE concentration at Tb, Dy and Ho or no anomaly. This REE pattern is also shown on the weathered ore samples (re-plotted from Desta et al., 1995). The tetrad effect in the samples were calculated according to Irber (1999). The lanthanide tetrad effect of peraluminous Kenticha granite pegmatite is very high, indicating it is a highly fractionated granite pegmatite suite (Figure 4.7).

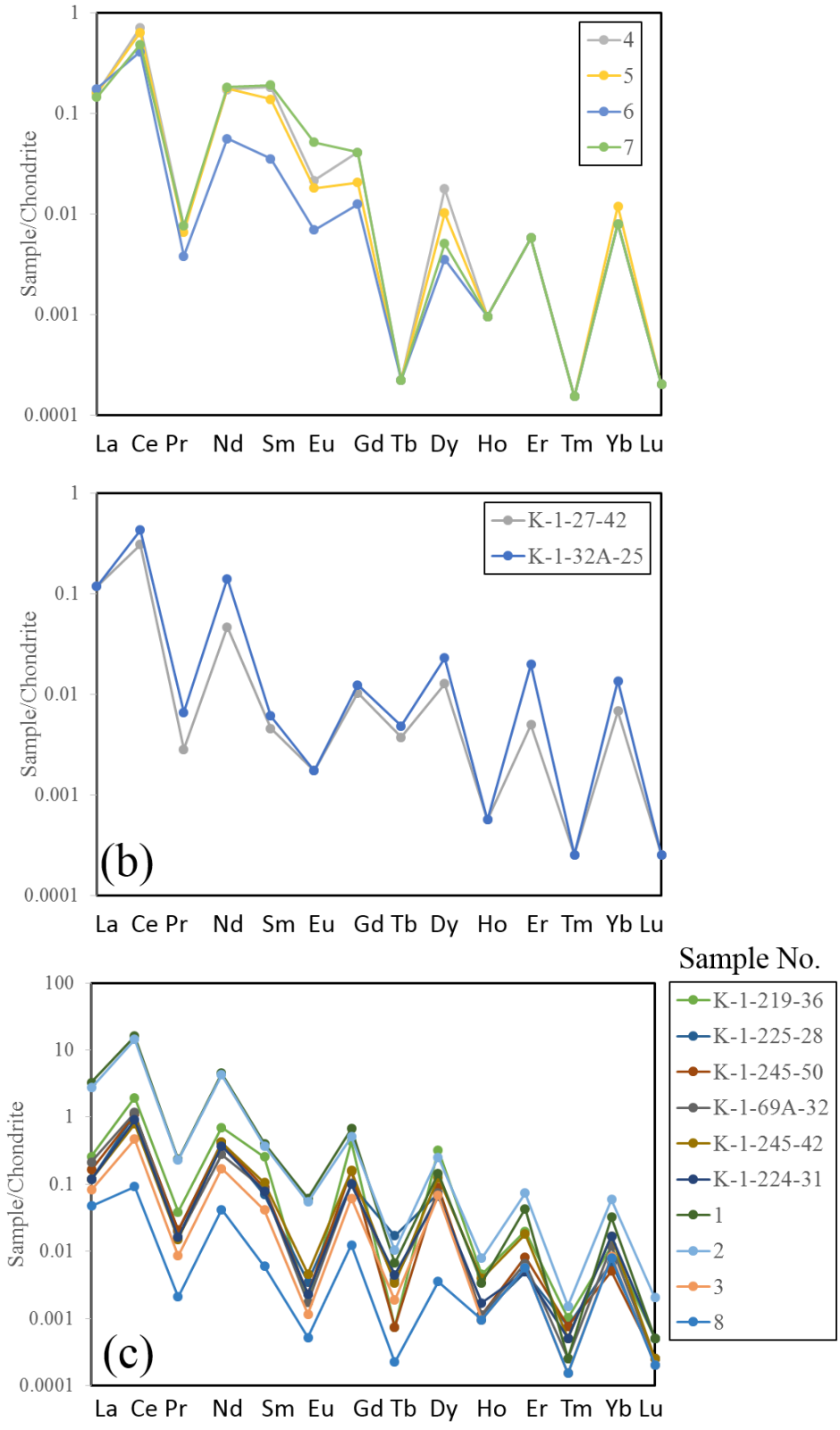

Figure 4.6: Different REE patterns showing internal differentiation and paragenesis. (a) Slight enrichment towards LREE (average LREE/HREE = 34.2), (b) enriched in samarium (Sm) and depletion of Dy (Dysprosium) (average LREE/HREE = 21.4) and

(c) Eu (Europium) anomaly (average LREE/HREE = 8.8). Note: the samples 1 to 8 are the weathred ore zone while the others are primary ore zone samples.

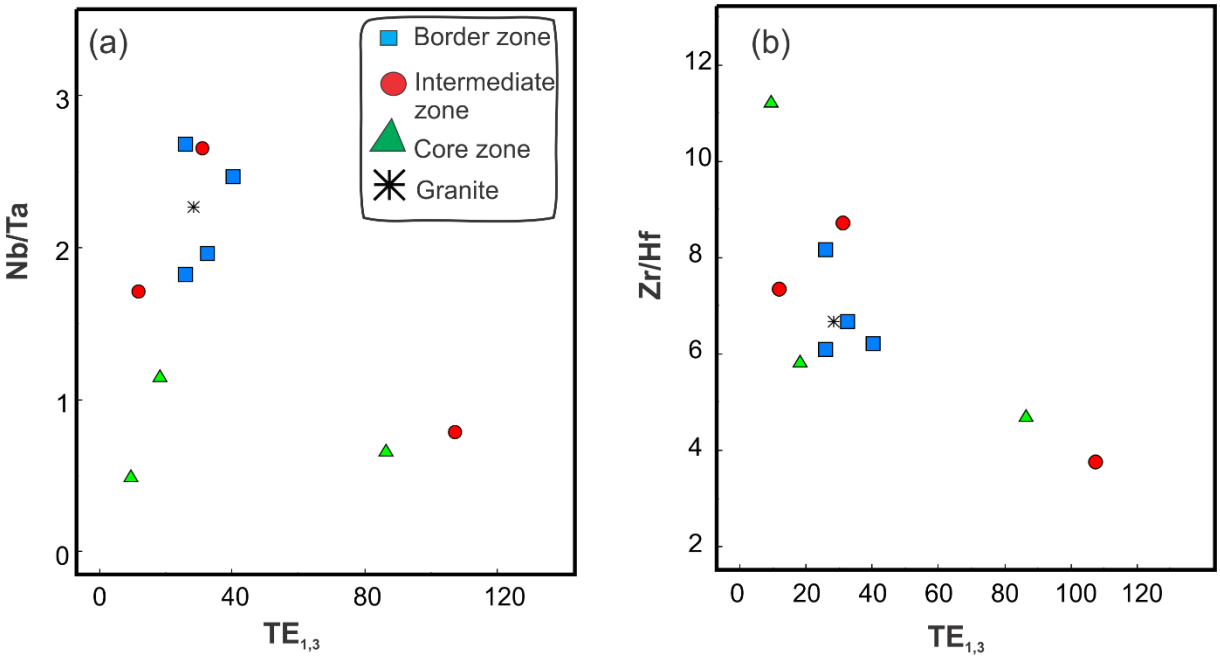

Figure 4.7: Lanthanide tetrad effect ($TE_{1,3}$) calculated according to the method of Irber (1999). (a) The tetrad effect is correlated to the low Nb/Ta ratio (< 5) which is used decide the economic cut-off during exploration. The samples plotted incomparably well below to the average chondrite value (~39). Note: see Appendix.1 for $TE_{1,3}$ calculation.

4.2 Zoning

Petrographic characterization of rock forming minerals highlight the zonal variation in mineral assemblage. Tadesse and Desta (1996) described three types of compositional zoning in CGM: oscillatory, patchy, and mixed oscillatory and patchy using samples from the main Kenticha granite pegmatite. The oscillatory zoning is the most common in the area. It can be caused by mixing of different magmas, rapid cooling, or degassing/decompression of the system (Holten et al., 1997; Shore and Fowler, 1996). The former case could be the most plausible for the origin of Kenticha granite pegmatite. Vertical compositional zoning can be inferred from the different mineralogical assemblages which was noted during the field observation. The CGM variation diagrams also show the different zones of the rare metal bearing pegmatite deposit. Detailed zonal description for the Kenticha rare metal pegmatite have given by Desta (1996) and Küster et al. (2009). For simplicity, three zones: core, intermediate and border zones, were identified

from CGM variation diagram and the different binary diagrams (Figure 4.1, 4.3 and 4.4). The trend shows enrichment from ferrocolumbite to manganotantalite which indicates the magmatic fractionation (Küster et al., 2009). The data plots out of this trend are showing more to ferrocolumbite to ferrotantalite which suggests late stage hydrothermal-metasomatic replacement processes. Additionally, the fractionation trend of sensitive elements for igneous processes at different zones revealed the compositional zoning. The core zone is characterized by high Ga, Sn, Rb/Sr, Zr/Hf and low content of Nb/Ta and K/Rb (Figure 4.3, 4.4 and 4.5).

4.3 Mineral alteration and paragenesis

Mineralogical characterization shows mineral alterations. Some of the important alteration processes of the deposit are muscovitization, sericitization, greisenization, albitization, and kaolinization processes. The orthopyroxene in the serpentinite rocks shows alteration at the rims to iron oxides. Secondary muscovitization has been observed from thin section analysis of the Kenticha rare metal pegmatite samples. Muscovite, microcline and tourmaline are altered to chlorite, sericite, and muscovite, respectively (Table 3.1). Spodumene can be altered into eucryptite + albite, muscovite + albite, and finally to muscovite (London and Burt, 1982). Metasomatic alteration of these minerals occurred along cleavages, fractures, and crystal borders/rime zones of the host primary phases. Towards the border and wall zones albitization is a dominant process that is manifested by replacement of potassium by sodium rich solution leads to the formation of an albite rich zone.

The zonal variations in mineral assemblage and the different trends shown from REE patterns of the whole-rock samples from the primary ore zone can be attributed to the different phases of paragenesis. Badanina et al. (2015) demonstrate the different stages of paragenesis using REE patterns. Similarly, three paragenetic stages can be outlined in the Kenticha rare metal pegmatite as inferred from the REE patterns. The enrichment and depletion of the different elements are also attributed to the different mineral assemblages and(or) paragenetic effects. The first stage (CGM1) of paragenesis is characterized by no Eu-anomaly which can be caused by the mineral assemblage which is not enriched in K-feldspar (Figure 4.6a). In contrast to this, the second stage (CGM2) of paragenesis shows some relative depletion of Europium without showing significant tetrad effect (Figure 4.6b). The third stage (CGM4) of paragenesis shows clear negative Eu-anomaly suggesting that K-feldspar become dominant at this stage causing

Eu-depletion (Figure 4.6d). So, the REE pattern start with positive or no anomaly (Figure 4.6a) and end up with positive anomaly during these stages (Figure 4.6c).

4.4 Comparison of pegmatites in the Adola Belt

Besides the Kenticha pegmatite there are also rare metal bearing pegmatite fields in the Adola Belt. These includes Bupo (I & II), Kilkele (I, II & III), Dermi Dama and Shuni Hill granite pegmatite fields. U-Pb dating of Mn-tantalite from Bupo pegmatite, 9 km north of Kenticha, gave 529 ±4.2 Ma which is comparable to the Mn-tantalite age of Kenticha (530.2±1.3). This indicates the coeval emplacement of the two pegmatites is temporally related to the postorogenic granite magmatism. The Bupo pegmatite is highly weathered and relatively show simple zoning than the complex spodumene-type main Kenticha pegmatite,and is classified as Albite-Spodumene type (Desta et al., 1995; Tadesse and Desta, 1996). The Li content of muscovite in spodumene unit (is lower than the K-feldspar unit) of Kenticha and Bupo pegmatite is low besides of Cs and Rb in the border zonewhich become enrichedto the core zone (Küster et al., 2009). Regionally, the fractionation trend, from the rare alkali and whole-rock data, increases from slightly fractionated Shuni Hill pegmatite (Zone C) which is slightly less or similarly evolved as border zone muscovite from Kenticha to the core zone muscovite from Kenticha pegmatite (zone D) with further fractionation to the Bupo pegmatite (zone E) (see Figure 2.2). The coherent Rb/Tl ratio in muscovite from Kenticha, Shuni Hill, and Killkile II pegmatites could indicate their cogenetic formation, with each of them representing a separate batch of fractionated melt (Figure 4.8).

However, the Kenticha, Bupo and Shuni Hill pegmatites show distinct difference in REE patterns in CGM (Figure 4.9). This could be arise as result of (1) formation of CGM in different zones and at different stages of fractionation within the pegmatite(s), (2) abundance and nature of coexisting REE-incorporating minerals, or (3) different sources of the pegmatite melts. The trend also shows enrichment from manganotantalite to manganotantalite and manganocolumbite in Kenticha and Bupopegmatites (Figure 4.1and 5.9; Küster et al., 2009), respectively.In Shuni Hill, ferrocolumbite become more dominant fractionate (Figure 4.8). Dermi Dama pegmatite shows similar trend as of the Kenticha pegmatite in CGM composition showing progressive manganotantalite enrichment (Tadesse and Desta, 1996). CGM composition field were also deduced by Tadesse and Desta (1996) in which fractionation trend outlined from ferrocolumbite at Kilkele II & III and Bupo II pegmatites towards progressive

enrichment in manganotantalite at Kilkele I and Dermi Dama pegmatites. Bupo I is highly fractionated and enriched in manganotantalite.

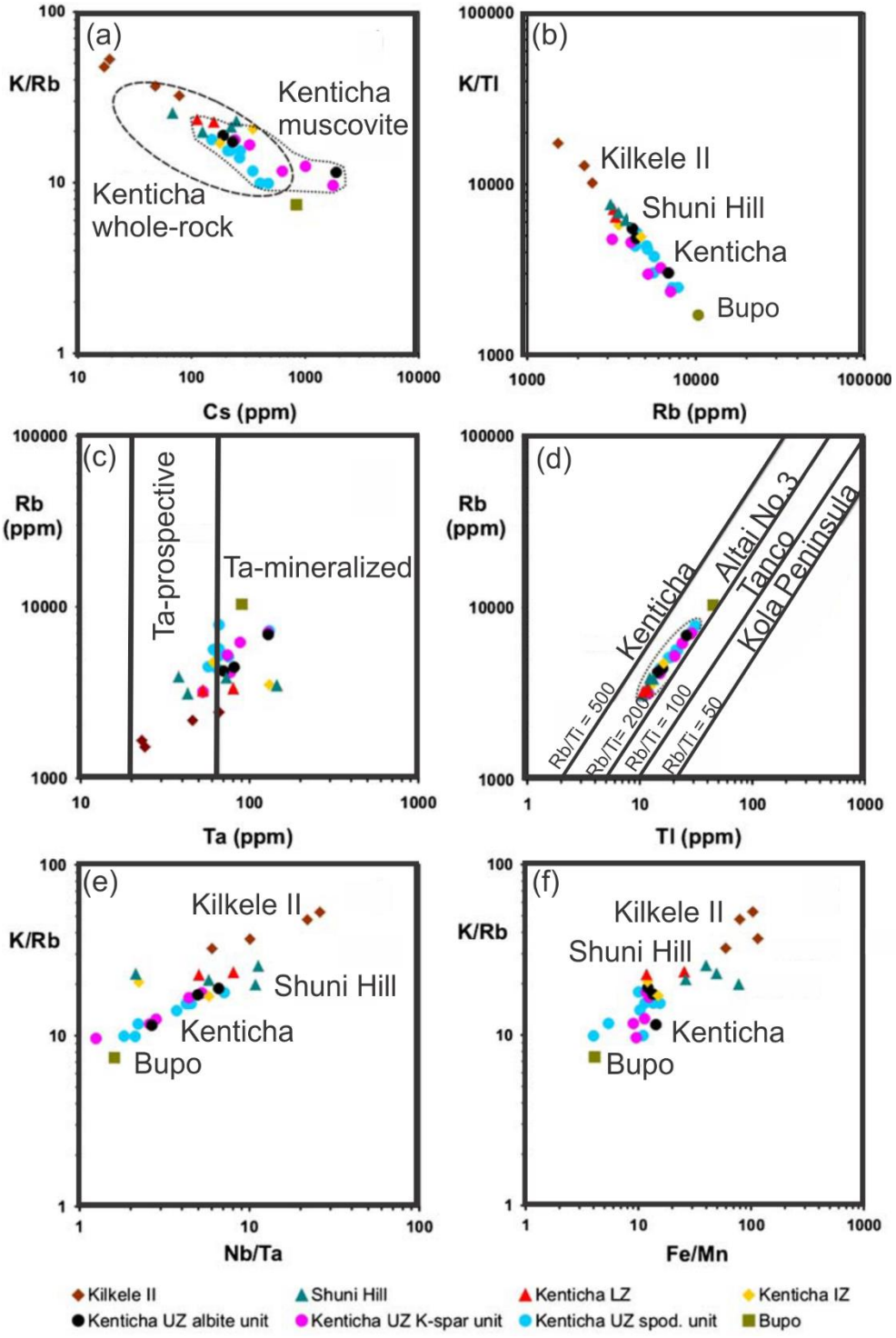

Figure 4.8: Bivariate logarithmic diagrams showing chemical variation in muscovite from Kenticha, Bupo, Shuni Hill, and Kilkele II pegmatites: (a) K/Rb vs Cs, (b) K/Tl vs Rb, (c) Rb vs Ta (minimum Ta contents for Ta prospective and Ta-mineralizedpegmatites are from Beus, 1966; Gordiyenko, 1971); (d) Rb vs Tl (data for other pegmatite fields are from Černý et al., 1985), (e) K/Rb vs Nb/Ta, and (f) K/Rb vs Fe/Mn(adapted from Küster et al., 2009).

Furthermore, The Rb/Tlratio of the Kentichais higher than the Tanco, Altai/Keketuohai No.3, or Kola Peninsula pegmatites (Figure 4.8d). The upward fractionation of the Kenticha pegmatite hassimilarities with the internal differentiation of the Tancopegmatite at Bernic Lake (Canada) that represents asubhorizontal sheet-like intrusion of similar size to Kenticha.In contrast to concentric downward directed solidification at Tanco, bottom-to-top differentiation and asymmetric zonation is evident in the Kenticha pegmatite thus be a general characteristic of flat-lying sheet-like pegmatiteintrusions (London, 2008).

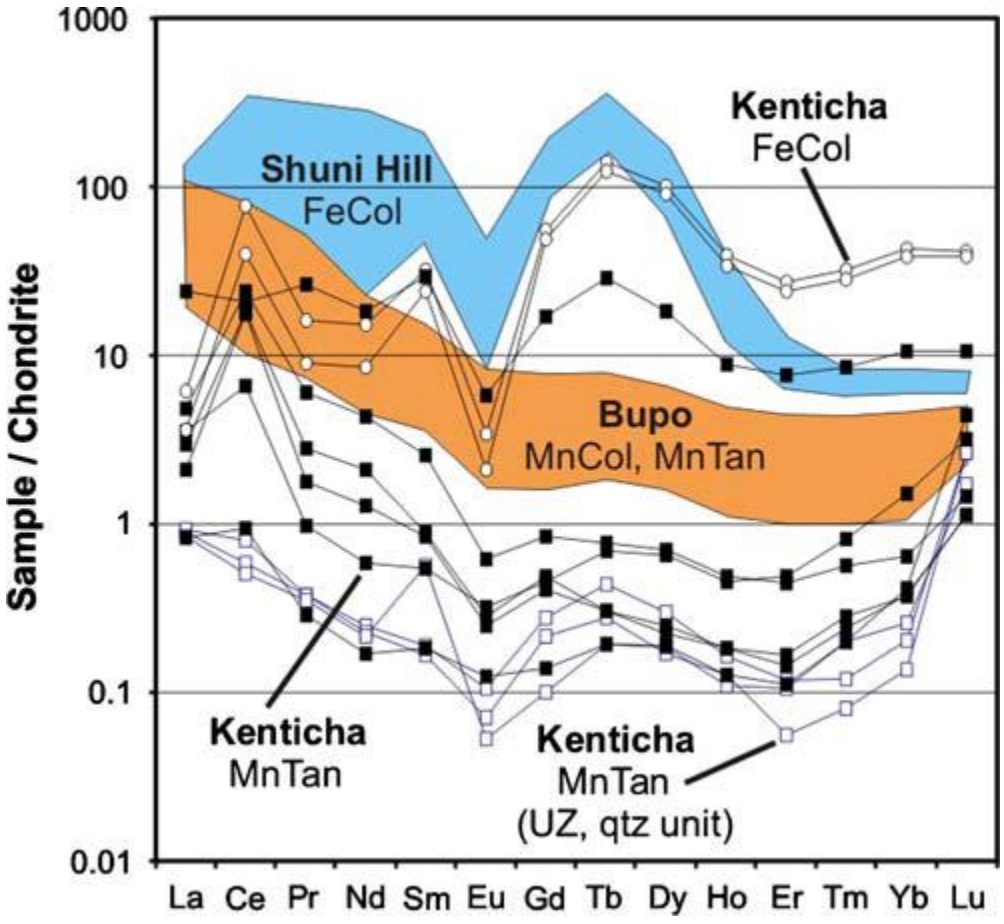

Figure 4.9: Chondrite normalized REE concentrations incolumbite-tantalite from the Kenticha, Bupo, and Shuni Hill pegmatites (McDonough and Sus, 2005). Note: the Kenticha samples here are not drill core samples rather were collected from the processing plant and from the outcropping orebody (core zone). FeCol: ferrocolumbite, MnCol: manganocolumbite, MnTan: manganotantalite (adapted from Küster et al., 2009).

4.5 Genesis of Kenticha tantalite deposit

The formation of rare-element granitic pegmatites is of mainly by fractional crystallization of a granitic melt (Černý, 1991; Černý et al., 1992; Neiva et al., 2008). Partial melting of appropriate composition (e.g., Shearer et al., 1992) such as metasedimentary Mn-bearing exhalites also proposed for the formation of these pegmatites (Bongiolo et al., 2016). The data plot on the tectonic discrimination diagrams show WPG and Syn-COLG (Figure 3.11). This probably indicate that the Kenticha pegmatite is formed in narrow synclinal shear zone(Emelyanov et al., 1986). This is however contrasting withTadesse (2001) which showed that the Kenticha granite pegmatite is Volcanic Arc Granite (VAG) and interpreted as subduction related magmatic source. However, this work in the contrary argue that the Kenticha granite pegmatite is mainly a "Within Plate Granite (WPG)" and the granite pegmatite probably sourced from (1) extreme fractionation syn- to late tectonic granites (e.g.,Černý, 1990)or (2) anatexis process or in-situ partial melting of the metasedimentary rocks in the area(Bongiolo et al., 2016; Simmons, 2007). The genesis of the Kenticha pegmatite is similar with the Harney Peak and Tin Mountain granite pegmatites, Black Hills (South Dakota) and Ponta Negra, Brazil which is by partial melting of metasedimentary rocks with further strong fractional crystallization (Bongiolo et al., 2016; Shearer et al., 1992, 1987). Besides, their tectonic setting is similar and related to post stage Gondwana assembly. Some of the data point also plotted in the limit and to the syn-collisional granite. This further indicates the formation of granite pegmatite can be also partly related to post-collisional processes during the post Gondwana assembly.

The relict textures in minerals such as relict of garnet in the studied samples can suggest for anatectic origin of granitic pegmatite (Simmons et al., 1995). The other evidence is the age of the Kenticha pegmatite (ca. 530 Ma; Küster et al., 2007) which is bracketing with the time interval of Gondwana assembly and related to thecollapsemagmatism in the region (ca. 580 to 520 Ma; Heilbron et al., 2008). Heilbron et al., 2008 pointed out the heat that triggered this magmatic event could still be a consequence of the collisional orogeny. Küster et al.(2007) also pointed out that the Kenticha pegmatites are temporally related to the post-collisional phase of granitic magmatism (570 to 520 Ma). Uranium-Lead dating for the Kenticha tantalite in the spodumene zone gave an age of ca. 520 Ma. Based on the age the Kenticha pegmatite is formed after the cease of East African Orogeny (~550 Ma; Johnson et al., 2011). This further implies the origin of the granite and granite pegmatite is from an attenuated continental crust, not from

an oceanic island granite. So, they probably derived from A-type granites(SiO2 = ~ 73.2 wt.%; F = 0.12 wt.%), which intern formed by partial melting of metasedimentary rocks, rather than previously interpreted as S- and I-type granites as stated by Küster et al. (2009). A-type granites are emplaced within plate anorogenic setting or in the final stages of an orogenic events, during the amalgamation of tectonostratigraphic terrains (Collins and Pisarevsky, 2005; Seer and Moraes, 2013). They are characterized by high SiO2 (~ 73.84 wt.%), high F contents (6000 to 8000 ppm) and typical of presence of fluorite.S-type granites are derived by partial melting of sedimentary and metasedimentary rock. They are peraluminous granites characterized by the presence of typical minerals such as muscovite, biotite and marginally elevated SiO_2 contents. I-type granites also derived by partial melting of igneous protolith or metaigneous rock from the lower continental crust. They are metaluminous granites characterized by the presence of hornblende/alkali amphiboles and biotite (Farahat et al., 2007).

The Zr/Hf ratio (ranges from ~10 to 3) is far lower than the values of Zr/Hf ratio of those of the mantle and chondrites (~39) (Dostalal and Chatterjee, 2000). This ratio ranges from 39 to 9 (~ 39) and are mostly close to the chondritic ratio. The average Zr/Hf (ranging from 28 to 4; average ~ 25) for pegmatites is lower with depending on the increasing evolution of the silicate melt(Moller and Dulski, 1983). Hafnium in felsic rocks are usually incompatible until zircon saturation occurs (Watson and Harrison, 1984) and inhibits a strong magmatic enrichment of Zr and Hf. The significant depletion in Eu, Ba and Sr, and enrichment in Rb, Nb, Ta, Hf and Cs, and strong negative Eu anomaly on the REE patterns show that the fractional crystallization must occur within the crust, or that the magma must originate from partial melting of the continental crust (Li et al., 2015; Mi et al., 2015; Figure 4.10). Hence, the formation of the Kenticha tantalite deposit is after the closure of the ocean.

Nb/Ta ratio is very low (below ~3) for the Kenticha pegmatite in the primary ore where Ta concentration increases and Nb concentration decreases from the border to the core zones. The Nb/Ta ratio in the continental crust (~11-12; which can vary from 2 to 14) is lower than those of mantle and chondrites ranges 13-20 in most pegmatites (~17.5) suggesting hydrothermal-metasomatic processes during the evolution of the crust (Green, 1995). The Na/Ta ratio of Kenticha pegmatite (0.5-2.7) is even far less than that of the crustal average value.The REE pattern of the weathered and primary ore zones shows some variations. Most of the primary ore zone samples show slight enrichment from light to heavy REE and negative Eu anomaly; which is not common in the weathered zone whole-rock samples (Figure 4.6).

The petrogenic processes that form the parental liquids can be by (1) single-stage anatexis of high grade (amphibolite to granulite grade) and Li-rich low grade metamorhic rocks (Cerny, 1982) and/or (2) fractionation of less evolved granite produce more complex type granitic pegmatites. Both of the process could be involved in the Kenicha granite pegmatite. The collision orogeny can cause a single-phase anatexis of prexisting metasedimentary rocks. The three different types of granites in the area also shows chemical evolution which can be asource of complex granitic pegmaite in the area during fractionation as a result of the collision orogeny. Though these all granites are formed by partial melting of pre-existing metasedimentary rocks.

The increase in basal heat flow by ascending magmatic intrusion or collision causes partial melting of the pre-existing metasedimentary rocks. The later case is more reseanable for the Kenticha pegmatites since they are sturcurally located at shear zone. During the ascent of the magma fractional crystalization and assimilation with the country rocks results different zonal mineral assemblages, geochemical variations and tantalite mineralization (Figure 4.10). The parent rock for granite and pegmaite is probably the metasedimentary rocks which form felsic magma during the increase in temperature triggered by the collision orogeny. This forms its own mineral and melt phases. Magma assimilation changes the composion of the rising magma. The ascent of the magma further allows to melt the country rock which modify the compoion of the magma. The incompatible elements such as Ta and Nb concequentely separate in the late stage of fractonal crystalization. Fractionated compositions of pegmatite magmas and their final aqueous fluids are highly reactive with less-evolved to wall zone and host-rocks (e.g., Morgan and London, 1987; Novák et al., 2012). Local contamination is occurred during the emplacement of the pegmatites along dike margins (metasomatic zone), and at the transition into sub-solidus conditions (Figure 4.10).

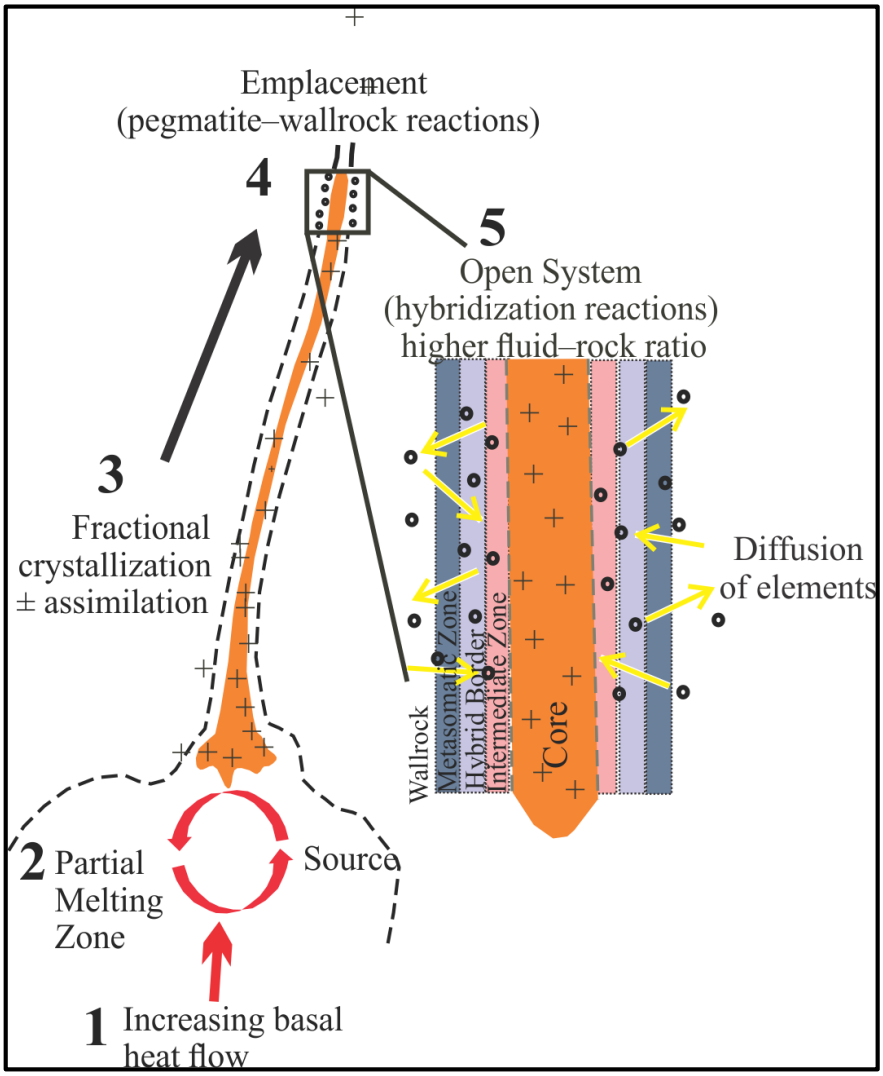

Figure 4.10: Conceptual diagram to illustrate the genesis of the Kenticha pegmatite(modified from McKeough et al., 2013).

Chapter 5 Conclusions and Recommendations

5.1 Conclusions

- The different zones show typical differences in mineral assemblages, texture and tantalite mineralization. Six main mineral assemblages: (1) alaskitic granite (quartz + microcline + albite with subordinate muscovite), (2) aplitic layer (quartz + albite), (3) muscovite–quartz–microcline–albite pegmatite, (4) spodumene–microcline–albite pegmatite partly albitized or greisenized, (5) microcline–albite–green and pink spodumene pegmatite with quartz-microcline block which is partly albitized and greisenized, and (6) quartz core were identified. The tantalum concentration increases from the border to the core zones.
- The whole-rock data on the tectonic discrimination diagrams was plotted on WPG and Syn-COLG and is interpreted the Kenticha pegmatite is formed by collision and felsic magmatism during post-Gondwana assembly.
- The Kenticha granite pegmatite shows mineralogical zonation with different concentration of major oxides, trace elements and REE.
- CGM fractionation with an increase in Ta/(Ta+Nb) ratio during crystallization of the pegmatite result enrichment in manganotantalite during primary magmatic fractionation.
- The Kenticha granite pegmatite is highly fractionated peraluminous pegmatite with high concentration of Rb,Be, Nb, Ta and Cs and depleted in Ba, Sr and V.Elemental fractionation of indicators in minerals such as Rb, Sr, Ga, K and their ratios indicate typical trend of magma fractionation of evolved pegmatite.
- The Kenticha pegmatite (Rb-Ba-Sr plot) shows a granitic trend typical of strongly differentiated granites with Rb enrichment and low Ba and Sr contents for whole–rock analyses of the Kenticha drill core samples.
- The REE chondrite normalized diagram on the other hand shows strong Eu-anomaly and slight enrichment from LREE towards the HREE which is typical character of evolved LCT-type granitic pegmatites.
- The mineralogical assemblage, tectonic setting, and geochemical signatures showed the genesis of Kenticha tantalite is by partial melting of metasedimentary rocks predated the granite and pegmatite with later hydrothermal-metasomatic enrichment of tantalite deposit in the area.

5.2 Recommendations

Modern state-of-the art microbeam analysis using instruments such as LA-ICP-MS/OES and EMPA (electron microprobe analysis) with proper number of samples is crucial to characterize the geochemical evolution of the Kenticha tantalite deposit. Microthermometric, age, and fluid inclusion (FI) and melt inclusion (MI) studies should combine to understand the origin the tantalite deposit and interplay processes from primary melt crystallization to secondary hydrothermal-metasomatic processes that form the deposit. Specifically full understanding of the genesis of the ore deposit and relating with the tectonic setting and parent magma is very difficult. Further work on these aspects using the above techniques is need to fully understand the chemical evolution and genesis of the Kenticha tantalite deposit. Integrated studyof trace element and REE analysis with FI and MI studies are recommended to understand the nature of pegmatite and ore forming melt. Trace element modelling is highly recommended to identify the type of petrogenetic processes and explain the origin of the parental liquids for a complex type granite pegmatite.

References

Abdalla, H.M., Helba, H.A., Mohamed, F.H., 1998. Chemistry of columbite-tantalite minerals in rare metal granitoids, Eastern Desert, Egypt. Mineral. Mag. 62, 821–836.

Abdelsalam, M.G., Stern, R.J., 1996. Sutures and shear zones in the Arabian-Nubian Shield. J. African Earth Sci. 23, 289–310.

Abdelsalam, M.G., Tsige, L., Yihunie, T., Hussien, B., 2008. Terrane rotation during the East African Orogeny: evidence from the Bulbul Shear Zone, south Ethiopia. Gondwana Res. 14, 497–508.

Acosta-Vigil, A., London, D., VI, G.B.M., Dewers, T.A., 2003. Solubility of excess alumina in hydrous granitic melts in equilibrium with peraluminous minerals at 700–800 C and 200 MPa, and applications of the aluminum saturation index. Contrib. to Mineral. Petrol. 146, 100–119.

ALS, 2016. Analytical methodes about ICP-MS/ICP-AES [WWW Document]. ALS geochemistry. URL http://www.alsglobal.com (accessed 3.17.16).

Aster, G.M., Getachew, T., Hack, M., Schmerold, R., Tesfaye, T., 1988. Types of gold mineralization in the Adola thrust belt, Sidamo Province, southern Ethiopia. Internal report (unpubl), Ethiopian Institute of Geological Surveys, Addis Ababa.

Ayalew, T., Bell, K., Moore, J.M., Parrish, R.R., 1990. U-Pb and Rb-Sr geochronology of the western Ethiopian shield. Geol. Soc. Am. Bull. 102, 1309–1316.

Badanina, E. V, Sitnikova, M.A., Gordienko, V. V, Melcher, F., Gäbler, H.-E., Lodziak, J., Syritso, L.F., 2015. Mineral chemistry of columbite–tantalite from spodumene pegmatites of Kolmozero, Kola Peninsula (Russia). Ore Geol. Rev. 64, 720–735.

Ballouard, C., Poujol, M., Boulvais, P., Branquet, Y., Tartèse, R., Vigneresse, J.L., 2016. Nb-Ta fractionation in peraluminous granites: A marker of the magmatic-hydrothermal transition. Geology 44, 231–234.

Bau, M., 1996. Controls on the fractionation of isova lent trace elements in magmatic and aqueous systems: Evidence from Y/Ho, Zr/Hf, and lanthanide tetrad effect. Contrib. to Mineral. Petrol. 123, 323–333.

Bau, M., Dulski, P., 1995. Comparative study of yttrium and rare-earth element behaviours in fluorine-rich hydrothermal fluids. Contrib. to Mineral. Petrol. 119, 213–223.

Baumgartner, R., Romer, R.L., Moritz, R., Sallet, R., Chiaradia, M., 2006. Columbite–tantalite-bearing granitic pegmatites from the Seridó Belt, northeastern Brazil: genetic constraints from U–Pb dating and Pb isotopes. Can. Mineral. 44, 69–86.

Belkasmi, M., Cuney, M., Pollard, P.J., Bastoul, A., 2000. Chemistry of the Ta-Nb-Sn-W oxide minerals from the Yichun rare metal granite (SE China): genetic implications and comparison with Moroccan and French Hercynian examples. Mineral. Mag. 64, 507–523.

Beus, A., 1966. Distribution of tantalum and niobium in muscovites from granitic pegmatites. Geokhimiya 10, 1216–1220, In Russian.

Bilay, A.Y., Kisters, A.F.M., Meyer, F.M., Schneider, J., 1997. The geology of the Lega Dembi gold deposit, southern Ethiopia: implications for Pan-African gold exploration. Miner. Depos. 32, 491– 504.

Bongiolo, E.M., Renac, C., de Toledo Piza, P. d'Almeida, da Silva Schmitt, R., Mexias, A.S.,

2016. Origin of pegmatites and fluids at Ponta Negra (RJ, Brazil) during late-to post-collisional stages of the Gondwana Assembly. Lithos 240, 259–275.

Cameron, E.N., 1949. Internal structure of granitic pegmatites. Economic Geology Pub. Co.

Cerny, P., 1982. Anatomy and classification of granitic pegmatites. Min Soc Can Short Course Handb 8, 1–39.

Černý, P., 1989. Characteristics of pegmatite deposits of tantalum. In: Lanthanides, Tantalum and Niobium. Springer, pp. 195–239.

Černý, P., 1990. Distribution, affiliation and derivation of rare-element granitic pegmatites in the Canadian Shield. Geol. Rundschau 79, 183–226.

Černý, P., 1991. Rare-element granitic pegmatites. part I: Anatomy and internal evolution of pegmatitic deposits. Geosci. Canada 18.

Černý, P., 1997. REE trends in rare-element granitic pegmatites: enrichment vs. depletion in granite-to-pegmatite sequences. J. Czech Geol. Soc. 42, 34.

Černý, P., 2005. The Tanco rare-element pegmatite deposit, Manitoba: regional context, internal anatomy, and global comparisons. Rare-Element Geochemistry Miner. Depos. (RL Linnen IM Samson, eds.). Geol. Assoc. Canada. Short Course Notes 17, 127–158.

Cèrny, P., Ercit, T., 1985. Some recent advances in the mineralogy and geochemistry of Nb and Ta in rare-element granitic pegmatites. Bull. Minerai 108, 499–532.

Černý, P., Ercit, T.S., 1989. Mineralogy of niobium and tantalum: crystal chemical relationships, paragenetic aspects and their economic implications. In: Lanthanides, Tantalum and Niobium. Springer, pp. 27–79.

Černý, P., Ercit, T.S., 2005. The classification of granitic pegmatites revisited. Can. Mineral. 43.

Černý, P., London, D., Novák, M., 2012. Granitic pegmatites as reflections of their sources. Elements 8, 289–294.

Černý, P., Meintzer, R.., Andorson, A.., 1985. Extreme fractionation in rare-element granitic pegmatites: selected examples of data and mechanisms. Can. Mineral. 23.

Černý, P., Novak, M., Chapman, R., 1992. Effects of Sillimanite-grade metamorphism and shearing on Nb-Ta oxide minerals in granitic pegmatites: Marsikov, Northern Moravia, Czechoslovakia. Can. Mineral. 30, 699–718.

Chappell, B.W., White, A.J.R., 2001. Two contrasting granite types: 25 years later. Aust. J. Earth Sci. 48, 489–499.

Chater, A., 1971. The geology of the Megado region of southern Ethiopia. University of Leeds,UK.

Chevychelov, V., Zaraisky, C., Borisovsky, S., Borkov, D., 2004. Partitioning of Ta and Nb between magmatic melt and aqueous (K, Na, H) F-containing fluid: Effects of temperature and chemical composition of the melt. Abstract Volume. Lithos 73.

Chevychelov, V.Y., Borodulin, G.P., Zaraisky, G.P., 2010. Solubility of columbite,(Mn, Fe)(Nb, Ta) 2O6, in granitoid and alkaline melts at 650–850 C and 30–400 MPa: an experimental investigation. Geochemistry Int. 48, 456–464.

Claiborne, L.L., Miller, C.F., Walker, B.A., Wooden, J.L., Mazdab, F.K., Bea, F., 2006. Tracking magmatic processes through Zr/Hf ratios in rocks and Hf and Ti zoning in zircons: An example from the Spirit Mountain batholith, Nevada. Mineral. Mag. 70, 517–

54.
Collins, A.S., Pisarevsky, S.A., 2005. Amalgamating eastern Gondwana: the evolution of the Circum-Indian Orogens. Earth-Science Rev. 71, 229–270.
Cox, K.G., Bell, J.D., Pankhurst, R.J., 1979. The Interpretation of Igneous Rocks. George Allen & Unwin.
Desta, Z., 1991. Le mineralizzazioni a Ta-Nb: classificazione, prospezione, valutazione. Il caso di Kenticha (area di Adola, Sidamo, Ethiopia).—unpubl PhD.
Desta, Z., 1996. Mineralogical, geochemical, internal structure and metallogenetic relationship of granitite-pegmatite units in Kenticha area (Adola, Ethiopia). Ethiop. Geosci. Miner. Eng. Assoc. 251 – 280.
Desta, Z., Abdella, K., Admasse, A., Tsegaye, G., Solomon, T., Nuri, M., 2003. Results of deep level primary ore exploration for Tantalum and Niobium deposit at Kenticha area. Ethiop. Miner. Dev. Share Co. 1–60.
Desta, Z., Garbarino, C., Valera, R., 1995. Granite pegmatite system in Kenticha (Adola, Sidamo, Ethiopia) rare metal pegmatite belt: petrochemistry, regional pegmatite zoning and classification. SINET Ethiop. J Sci 18, 119–148.
Dill, H.G., 2015. Pegmatites and aplites: Their genetic and applied ore geology. Ore Geol. Rev. 69, 417–561.
Dostalal, J., Chatterjee, A.K., 2000. Contrasting behaviour of Nb/Ta and Zr/Hf ratios in a peraluminous granitic pluton (Nova Scotia, Canada). Chem. Geol. 163, 207–218.
El Bouseily, A.M., El Sokkary, A.A., 1975. The relation between Rb, Ba and Sr in granitic rocks. Chem. Geol. 16, 207–219.
EMA, (Ethiopian Meteorological Agency), 2015. Annual Rainfall and Temperature Records.
Emelyanov, E.L., Abebaw, T., Tesfaye, T., Teweldemedhin, T., 1986. Preliminary report on prospecting results of the Kenticha rare metal deposit.—Internal report (unpubl) Ethiopian Mineral Resource Development Corp, Ministry of Mines and Energy, Addis Ababa.
Ethiopian Mineral Development Enterprise, 1997. Background information on Kenticha Tantalum development, Volum I—Internal report (unpubl).
Farahat, E.S., Mohamed, H.A., Ahmed, A.F., El Mahallawi, M.M., 2007. Origin of I-and A-type granitoids from the Eastern Desert of Egypt: implications for crustal growth in the northern Arabian–Nubian Shield. J. African Earth Sci. 49, 43–58.
Fiege, A., Kirchner, C., Holtz, F., Linnen, R.L., Dziony, W., 2011. Influence of fluorine on the solubility of manganotantalite (MnTa2O6) and manganocolumbite (MnNb2O6) in granitic melts — an experimental study. Lithos 122, 165–174.
Galliski, M.A., Černý, P., 2006. Geochemistry and structural state of columbite-group minerals in granitic pegmatites of the Pampean Ranges, Argentina. Can. Mineral. 44, 645–666.
Gerra, S., 2000. A short introduction to the geology of Ethiopia. Chron. Rech. Min 540, 3–10.
Ghebreab, W., Greiling, R.O., Solomon, S., 2009. Structural setting of Neoproterozoic mineralization, Asmara district, Eritrea. J. African Earth Sci. 55, 219–235.
Gichile, S., 1992. Granulites in the Precambrian basement of southern Ethiopia: geochemistry, PT conditions of metamorphism and tectonic setting. J. African Earth Sci. (and Middle East) 15, 251–263.
Gilboy, C.F., 1970. The geology of the Gariboro region of southern Ethiopia. University of

Leeds, UK.

Ginsburg, A.I., Timofeyev, I.N., Feldman, L.G., 1979. Principles of geology of the granitic pegmatites. Nedra, Moscow 296.

Gordiyenko, V., 1971. Concentration of Li, Rb and Cs in potash feldspar and muscovite as criteria for assessing the rare metal mineralization in granitic pegmatites. Int. Geol. Rev. 13, 134–142.

Green, T.H., 1995. Significance of Nb/Ta as an indicator of geochemical processes in the crust-mantle system. Chem. Geol. 120, 347–359.

Hargrove, U.S., Stern, R.J., Kimura, J.I., Manton, W.I., Johnson, P.R., 2006. How juvenile is the Arabian–Nubian Shield? Evidence from Nd isotopes and pre-Neoproterozoic inherited zircon in the Bi'r Umq suture zone, Saudi Arabia. Earth Planet. Sci. Lett. 252, 308–326.

Heilbron, M., Valeriano, C.M., Tassinari, C.C.G., Almeida, J.C.H. Tupinambá, M., Siga Junior, O., Trouw, R.A.J., 2008. Correlation of Neoproterozoic terranes between Ribeira Belt, SE Brazil and its African counterpart: comparative tectonic evolution and open questions. In: Pankhurst, R.J.; Trouw, R.A.J.; de Brito Neves, B.B.; de Wit, M.J. (Eds.), West Gondwana: Pre–Cenozo. Geol. Soc. London Spec. Publ. 295, 211–237.

Holten, T., Jamtveit, B., Meakin, P., Cortini, M., Blundy, J., Austrheim, H., 1997. Statistical characteristics and origin of oscillatory zoning in crystal. Am. Mineral. 82, 596–606.

Irber, W., 1999. The lanthanide tetrad effect and its correlation with K/Rb, Eu/Eu*, Sr/Eu, Y/Ho, and Zr/Hf of evolving peraluminous granite suites. Geochim. Cosmochim. Acta 63, 489–508.

Jahns, R., 1982. Internal evolution of pegmatite bodies. In: ˇCerný P (ed) Granitic Pegmatites in Science and Industry. Mineral. Assoc. Canada Short Course Handb. 8 293–327.

Jahns, R.H., Burnham, C.W., 1969. Experimental studies of pegmatite genesis; l, A model for the derivation and crystallization of granitic pegmatites. Econ. Geol. 64, 843–864.

Johnson, P.R., Andresen, A., Collins, A.S., Fowler, A.R., Fritz, H., Ghebreab, W., Kusky, T., Stern, R.J., 2011. Late Cryogenian–Ediacaran history of the Arabian–Nubian Shield: a review of depositional, plutonic, structural, and tectonic events in the closing stages of the northern East African Orogen. J. African Earth Sci. 61, 167–232.

Johnson, P.R., Woldehaimanot, B., 2003. Development of the Arabian-Nubian Shield: perspectives on accretion and deformation in the northern East African Orogen and the assembly of Gondwana. Geol. Soc. London, Spec. Publ. 206, 289–325.

Kazmin, V., 1972. The Precambrian geology of Ethiopia and some aspects of the geology of the Mozambique belt. Bull. Geoph. Obs 15, 27–43.

Kazmin, V., Shifferaw, A., Balcha, T., 1978. The Ethiopian basement: stratigraphy and possible manner of evolution. Geol. Rundschau 67, 531–546.

Kozyrev, V., Girma, K., Safonov, J., Bekele, W., Teweldemedhin, T., 1982. Regional geological and exploration work for gold and other minerals in the Adola gold fields. Internal report (unpubl) Ethiopian Mineral Resource Development Corp, Adddis Ababa.

Kozyrev, V., Girma, K., Safonov, J., Tuliankin, V., Bekele, W., Bestujev, A., Darijapov, A., Teweldemedhin, T., Gurbanivich, G., Kaitukov, M., Arijapov, A., 1988. Geological map of the Adola Region, 1:100000. Ethiop. Mapp. Agency, Addis Ababa.

Kusky, 2003. Evolution of the East African and related orogens, and the assembly of

Gondwana. Precambrian Res. 123, 81–85.

Küster, D., 2009. Granitoid-hosted Ta mineralization in the Arabian–Nubian Shield: ore deposit types, tectono-metallogenetic setting and petrogenetic framework. Ore Geol. Rev. 35, 68–86.

Küster, D., Romer, R.L., Tolessa, D., Bheemalingeswara, Zerihun, D.K.B., Melcher, F., Oberthür, T., 2009. The Kenticha rare-element pegmatite, Ethiopia: internal differentiation, U–Pb age and Ta mineralization. Min. Depos. 44, 723–750.

Küster, D., Romer, R.L., Tolessa, D., Zerihun, D., Bheemalingeswara, K., 2007. Geochemical evolution and age of the Kenticha tantalum pegmatite, southern Ethiopia. In: International Symposium on Granitic Pegmatites: The State of the Art. pp. 50–51.

Larsen, R.B., 2002. The distribution of rare-earth elements in K-feldspar as indicator of petrogenetic processes in granitic pegmatites: Examples from two pegmatite fields in southern Norway. Can. Mineral. 40, 137–151.

Li, N., Chen, Y.J., Santosh, M., Pirajno, F., 2015. Compositional polarity of Triassic granitoids in the Qinling Orogen, China: implication for termination of the northernmost paleoTethys. Gondwana Res. 27, 244–257.

Linnen, R.L., Keppler, H., 1997. Columbite solubility in granitic melts: consequences for the enrichment and fractionation of Nb and Ta in the Earth's crust. Contrib. to Mineral. Petrol. 128, 213–227.

Linnen, R.L., Keppler, H., 2002. Melt composition control of Zr/Hf fractionation in magmatic processes. Geochim. Cosmochim. Acta 66, 3293–3301.

Linnen, R.L., Lichtervelde, M. Van, Cˇerný, P., 2012. Granitic Pegmatites as Sources of Strategic Metals. Elements 8, 275–280.

London, D., 1984. Experimental phase equilibria in the system LiAlSiO4-SiO2-H2O: a petrogenetic grid for lithium-rich pegmatites. Am Miner. 69, 995–1004.

London, D., 2008. Pegmatites. Can. Mineral. Spec. Publ. 10, 374.

London, D., Burt, D.M., 1982. Alteration of spodumene, montebrasite and lithiophilite in pegmatites of the White Picacho district, Arizona. Am. Mineral. 67, 97–113.

London, D., Morgan, G.B., 2012. The pegmatite puzzle. Elements 8, 263–268.

McDonough, W., Sun, S., 1995. The composition of the Earth. Chem. Geol. 120, 223–253.

McDonough, W., Sus, S., 2005. The composition of the earth. Chem Geol 120:223–253. Chem. Geol. 120, 223–253.

McKeough, M.A., Lentz, D.R., McFarlane, C.R.M., Jarrod, B., 2013. Geology and evolution of pegmatite-hosted U–Th ± REE–Y–Nb mineralization, Kulyk, Eagle, and Karin Lakes region, Wollaston Domain, northern Saskatchewan, Canada: examples of the dual role of extreme fractionation and hybridization processes. J. Geosci. 58, 321–346.

Mechessa, A., 1996. Geochemistry, Geochronology and Genesis of the Lega Dembi Gold Deposit in the Adola Gold field of southern Ethiopia. Ph.D. Thesis (unpubl). University of Vienna. 168pp.

Melcher, F., Graupner, T., Gäbler, H.-E., Sitnikova, M., Henjes-Kunst, F., Oberthür, T., Gerdes, A., Dewaele, S., 2015. Tantalum–(niobium–tin) mineralisation in African pegmatites and rare metal granites: constraints from Ta–Nb oxide mineralogy, geochemistry and U–Pb geochronology. Ore Geol. Rev. 64, 667–719.

Mi, M., Chen, Y.J., Yang, Y.F., Wang, P., Li, F.L., Wan, S.Q., Xu, Y.L., 2015. Geochronology and geochemistry of the giant Qian'echong Mo deposit, Dabie Shan, eastern China: implications for ore genesis and tectonic setting. Gondwana Res. 27, 1217–1235.

Moller, P., Dulski, P., 1983. Fractionation of Zr and Hf in cassiterite. Chem. Geol. 40, 1–12.

Morgan, G.B., London, D., 1987. Alteration of amphibolitic wallrocks around the Tanco rare-element pegmatite, Bernic Lake, Manitoba. Am. Mineral. 72, 1097–1121.

Neiva, A.M.R., Gomes, M.E.P., Ramos, J.M.F., Silva, P.B., 2008. Geochemistry of granitic aplite-pegmatite sills and their minerals from Arcozelo da Serra area (Gouveia, central Portugal). Eur. J. Mineral. 20, 465–485.

Novák, M., Škoda, R., Gadas, P., Krmíček, L., Černý, P., 2012. Contrasting origins of the mixed (NYF+ LCT) signature in granitic pegmatites, with examples from the Moldanubian Zone, Czech Republic. Can. Mineral. 50, 1077–1094.

Partington, G.A., McNaughton, N.J., Williams, I.S., 1995. A review of the geology, mineralization, and geochronology of the Greenbushes pegmatite, Western Australia. Econ. Geol. 90, 616–635.

Pearce, J.A., Harris, N.B.W., Tindle, A.G., 1984. Trace element discrimination diagrams for the tectonic interpretation of granitic rocks. J. Petrol. 25, 956–983.

Peccerillo, A., Taylor, S.R., 1976. Geochemistry of Eocene calc-alkaline volcanic rocks from the Kastamonu area, northern Turkey. Contrib. to Mineral. Petrol. 58, 63–81.

Pirajno, F., 2013. Effects of metasomatism on mineral systems and their host rocks: alkali metasomatism, skarns, greisens, tourmalinites, rodingites, black-wall alteration and listvenites. In: In Metasomatism and the Chemical Transformation of Rock. pp. 203–251.

Robie, R.A., Hemingway, B.S., 1984. Entropies of kyanite, andalusite, and sillimanite: additional constraints on the pressure and temperature of the Al2SiO5 triple point. Am. Mineral. 69, 298–306.

Rushmer, T., Knesel, K., 2011. Defining geochemical signatures and timescales of melting processes in the crust: an experimental tale of melt segregation, migration and emplacement. In: Dosseto, A., Turner, S., Van Orman, J. (Eds.), In: Dosseto, A., Turner, S., Van Orman, J. (Eds.), Ti. Blackwell, Oxford, UK 181–211.

Seer, H., Moraes, L., 2013. Within plate, arc, and collisional Neoproterozoic granitic magmatism in the Araxá Group, Southern Brasília belt, Minas Gerais, Brazil. Brazilian J. Geol. 43, 333–354.

Shand, S.J., 1943. Eruptive rocks: Their genesis, composition, and classification, with a chapter on meteorites. J. Wiley & sons, Incorporated.

Shaw, D.M., 1968. A review of K–Rb fractionation trends by covariance analysis. Geochim. Cosmochim. Acta 32, 573–601.

Shearer, C.K., Papike, J.J., Jolliff, B.L., 1992. Petrogenetic links among granites and pegmatites in the Harney Peak rare-element granite-pegmatite system, Black Hills, South Dakota. Can. Mineral. 30, 785.

Shearer, C.K., Papike, J.J., Laul, J.C., 1987. Mineralogical and chemical evolution of a rare-element granite-pegmatite system: Harney Peak Granite, Black Hills, South Dakota. Geochim. Cosmochim. Acta 51, 473–486.

Shore, M., Fowler, A.D., 1996. Oscillatory zoning in minerals: a common phenomenon. Can.

Mineral. 34, 1111–1126.

Simmons, S., 2007. Pegmatite genesis: Recent advances and area for future research. In: Granitic Pegmatites: The State of the Art-International Symposium. 06th – 12th May 2007, Porto, Portugal. p. 4.

Simmons, W.., Foord, E.., Falster, A.., King, V.., 1995. 1995. Evidence for an anatectic origin of granitic pegmatites, western Maine, USA. Geologigical Society of America Annual Meeting, New Orleans, Abstract Volume 27. p. A411.

Simmons, W.B., Pezzotta, F., Shigley, J.E., Beurlen, H., 2012. Granitic pegmatites as sources of colored gemstones. Elements 8, 281–287.

Stepanov, A., Mavrogenes, J.A., Meffre, S., David son, P., 2014. The key role of mica during igneous concentration of tantalum. Contrib. to Mineral. Petrol. 167, 1009–1016.

Stern, R.., Ali, K.., Abdelsalam, M.., Wilde, S.A., Zhou, Q., 2010. U-Pb Zircon geochronology of the eastern part of the Southern Ethiopian Shield. Precambrian Res. 159–167.

Stern, R.J., 1994. Arc-assembly and continental collision in the Neoproterozoic African orogen: implications for the consolidation of Gondwanaland. Annu. Rev. Earth Planet. Sci. 22, 319–351.

Stoeser, D.B., Camp, V.E., 1985. Pan-African microplate accretion of the Arabian Shield. Geol. Soc. Am. Bull. 96, 817–826.

Sun, S.-S., McDonough, W.F., 1989. Chemical and isotopic systematics of oceanic basalts: implications for mantle composition and processes. Geol. Soc. London, Spec. Publ. 42, 313–345.

Tadesse, G., Allen, A., 2002. Geology and geochemistry of the Neoproterozoic Tuludimtu Orogenic belt, western Ethiopia. In: 19th Colloquium of African Geology-El Jadida, Morocco, Abstract Volume. pp. 173–174.

Tadesse, S., 1998. Structure of pegmatitic bodies of the Kenticha deposit, Adola gold field (southern Ethiopia). Africa Geosci. Rev. 5, 527–535.

Tadesse, S., 2001. Geochemistry of the pegmatitic rocks and minerals in the Kenticha Belt, Southern Ethiopia: Implication to geological setting. Gondwana Res. 4, 97–104.

Tadesse, S., 2004. Genesis of the Shear Zone-related Gold Vein Mineralization of the Lega Dembi Gold Deposit, Adola Gold Field, Southern Ethiopia. Gondwana Res. 7, 481–488.

Tadesse, S., Desta, Z., 1996. Composition, fractionation trend and zoning accretion of the columbite-tantalite group of minerals in the Kenticha rare-metal field (Adola, southern Ethiopia). J. African Earth Sci. 23, 411–431.

Tadesse, T., 1990. Geochemistry of the vein gold mineralization at Lega Dembi, Ethiopia. M.Phil. Thesis, University of Leeds, England.

Takahashi, T., Tanaka, K., Kawabe, I., 2007. Lanthanide tetrad effect of Naegi granite-pegmatite suite, central Japan: Convex tetrad effect by fractional loss of fluid from hydrous felsic melt. Earth Planet. Sci. Lett. 54, 13–35.

Taylor, S.R., McLennan, S.M., 1985. The Continental Crust; Its Composition and Evolution. Blackwell, Oxford, UK.

Teklay, M., Kröner, A., Mezger, K., Oberhänsli, R., 1998. Geochemistry, Pb-Pb single zircon ages and Nd-Sr isotope composition of Precambrian rocks from southern and eastern Ethiopia: implications for crustal evolution in East Africa. J. African Earth Sci. 26, 207–

227.

Tsige, L., 2006. Metamorphism and gold mineralization of the Kenticha–Katawicha area: Adola belt, southern Ethiopia. J. African Earth Sci. 45, 16–32.

Van Lichtervelde, M., Salvi, S., Beziat, D., Linnen, R.L., 2007. Textural features and chemical evolution in tantalum oxides: magmatic versus hydrothermal origins for Ta mineralization in the Tanco Lower pegmatite, Manitoba, Canada. Econ. Geol. 102, 257–276.

Watson, E.B., Harrison, T.M., 1984. Zircon saturation revisited: temperature and composition effects in a variety of crustal magma types systems: a summary and prospectus of experimental approaches. Phys. Earth Planet. Inter. Earth Planet. Inter. 35, 19–30.

Wondafrash, M., 2010. Opportunities for Tantalum resources development in Ethiopia, Geological Survey of Ethiopia.

Worku, H., Schandelmeier, H., 1996. Tectonic evolution of the Neoproterozoic Adola Belt of southern Ethiopia: evidence for a Wilson Cycle process and implications for oblique plate collision. Precambrian Res. 77, 179–210.

Worku, H., Yifa, K., 1992. The tectonic evolution of the Precambrian metamorphic rocks of the Adola Belt (southern Ethiopia). J. African Earth Sci. (and Middle East) 14, 37–55.

Yibas, B., Reimold, W.U., Armstrong, R., Koeberl, C., Anhaeusser, C.R., Phillips, D., 2002. The tectonostratigraphy, granitoid geochronology and geological evolution of the Precambrian of southern Ethiopia. J. African Earth Sci. 34, 57–84.

Yihunie, T., Adachi, M., Takeuchi, M., 2004. PT conditions of metamorphism in the Neoproterozoic rocks of the Negele area, southern Ethiopia. Gondwana Res. 7, 489–500.

Appendix

Appendix.1: The tetrad effect for the whole-rock samples of the Kenticha rare metal pegmatite. The tetrad effect is calculated according to Irber (1999).The lanthanide tetrad effect of peraluminous Kenticha granite pegmatite is very high, indicating it is a highly fractionated granite pegmatite suite. Note: the chondrite normalized REE were calculated by Sun and McDonough (1989) REE normalizing values.

Samples	Ce/Ce^t	Pr/Pr^t	Tb/Tb^t	Dy/Dy^t	t1	t3	$TE_{1,3}$
K-1-249-59	2.86	2.98	75.82	4124.22	2.92	559.19	40.40
K-1-28A-28	2.44	2.30	42.16	1965.20	2.37	287.84	26.11
K-1-27-42	9.56	9.96	237.57	5895.59	9.76	1183.48	107.46
K-1-24B-41	1.26	1.26	15.30	360.60	1.26	74.28	9.67
K-1-32A-25	5.52	5.07	279.98	7220.59	5.29	1421.84	86.73
K-1-219-36	1.66	1.66	13.56	575.35	1.66	88.33	12.11
K-1-225-28	3.19	2.93	54.21	2267.77	3.06	350.62	32.74
K-1-85A-2	5.04	4.63	139.99	4168.81	4.83	763.93	60.75
K-1-245-50	2.69	2.53	34.49	2015.59	2.61	263.66	26.23
K-1-69A-32	2.91	2.95	50.40	2244.97	2.93	336.37	31.39
K-1-245-42	3.19	2.56	19.94	674.32	2.86	115.96	18.20
K-1-224-31	3.38	2.96	46.42	1431.51	3.16	257.78	28.55

The tetrad effect has been calculated based on the method of Irber (1999). The first (t1) and the third (t3) tetrad effects are the most important to understand mineral fractionation which are calculated as follows:

$t1 = (Ce/Ce^t \times Pr/Pr^t)^{0.5}$ .....(1)

$t3 = (Tb/Tb^t \times Dy/Dyt)^{0.5}$ ..... (2)

where,

$Ce/Ce^t = Ce_{cn}/(La_{cn}^{2/3} \times Nd_{cn}^{1/3})$

$Pr/Pr^t = Pr_{cn}/(La_{cn}^{1/3} \times Nd_{cn}^{2/3})$

$Tb/Tb^t = Tb_{cn}/(Gd_{cn}^{2/3} \times Ho_{cn}^{1/3})$

$Dy/Dy^t = Dy_{cn}/(Gd_{cn}^{1/3} \times Ho_{cn}^{2/3})$

Ln_{cn}= chondrite-normalized lanthanide concentration

Degree of the tetrad effect = $TE_{1,3} = (t1 \times t3)^{0.5}$ .....(3)

Appendix.2: Ratios of different elements used for different plots.

Sample	Nb/Ta	Zr/Hf	K/Rb	Rb/Sr	Sr/Rb	Ba/Rb
K-1-249-59	2.47	6.21	17.75	0.03	37.5	35.42
K-1-28A-28	1.82	6.07	15.25	0.02	59.26	42.59
K-1-27-42	0.78	3.75	12.84	0	966.67	513.33
K-1-24B-41	0.5	11.22	11.97	0.03	34.04	40.21
K-1-32A-25	0.66	4.71	13.59	0	328.57	292.86
K-1-219-36	1.7	7.33	15.2	0.04	24.39	21.71
K-1-225-28	1.95	6.67	18.77	0.04	28.57	38.57
K-1-245-50	2.68	8.15	21.26	0.02	45.45	43.18
K-1-69A-32	2.65	8.7	19.57	0.02	41.18	51.18
K-1-245-42	1.16	5.83	12.23	0	262.5	75.63
K-1-224-31	2.26	6.67	13.09	0.02	47.06	34.12